A STUDY OF THE CYTOCHROME c_3 FROM *SHEWANELLA* NCIMB400 AND THE FLAVOCYTOCHROME b_2 FROM *SACCHAROMYCES CEREVISIAE*

ANDREW PIKE

THESIS PRESENTED FOR THE DEGREE OF DOCTOR OF PHILOSOPHY
THE UNIVERSITY OF EDINBURGH
FEBRUARY 1998

EX BIBL. UNIV. EDINBURGEN

Dedication

For Mum and Dad

'...the British plan everything in retrospect, so it always looks as though everything occured as they intended.'

- Louis de Bernières 'Captain Corelli's Mandolin'

Acknowledgements

I would like to thank Steve Chapman and Graeme Reid for their expertise, guidance and encouragement during the last three years.

Special thanks to Euan Gordon for all his help with molecular biology, Simon Daff for inspirational help with kinetics and electrochemistry and to Forbes Manson for making the b_2 mutants.

I have enjoyed (almost) every moment I spent in Steve's and Graeme's labs and this was due to the fantastic people who I shared the time with. I couldn't have asked for a better team of people to work with.

Many thanks go to Neil, Al, Zander and Craig for some of the most eventful Friday nights out I've ever had. Cheers to Ali for the meals and for being an excellent pub guide.

Finally, thanks to Fi, without whom I definitely wouldn't have got through it.

Abstract

PART 1

The tetrahaem cytochromes c_3 are a group of proteins which were originally purified from the strictly anaerobic, sulphate-reducing bacteria. The proteins are small (84-117 residues), soluble and contain four covalently bound, bis-histidine ligated mesohaem IX prosthetic groups.

A cytochrome c_3 has been purified from the bacterium *Shewanella* sp. NCIMB400 and the gene encoding it, *cycA* has been cloned and sequenced along with some flanking sequence. The mature protein is 86 amino acids in length and contains four covalently bound haem groups, with a molecular weight of 11780 Da, which has been confirmed by electrospray mass spectrometry. The electronic absorption spectrum is characteristic of a low-spin c-type cytochrome with an α-peak at 551nm. A redox titration of the four haems, yielded a pair of values at -60 mV and -200 mV, within the range observed for cytochromes c_3. Resonance Raman spectra of the protein contain bands characteristic of low-spin haems, consistent with bis-histidine ligation for all haems. Electron paramagnetic resonance spectroscopy on the protein gave a single set of g-values at g_x=1.53, g_y=2.22 and g_z=2.83. The values are within the region observed for low spin, six coordinate, bis-histidine ligated haemoproteins. The one dimensional nuclear magnetic resonance spectrum of the protein contains well resolved haem methyl peaks, shifted to low field region by the paramagnetic iron centres.

The deduced amino acid sequence from the *cycA* gene is 86 residues long for mature cytochrome c_3 and has an additional 25 amino acid, periplasm directing presequence. The predicted sequence contains four, CXXCH haem binding motifs. This is consistent with the presence of four *c*-type haems in the mature protein. A total of eight histidines in the amino acid sequence is consistent with four bis-histidine ligated haems. Two additional reading frames, in the same orientation lie on either side of the *cycA* gene. The reading frames show sequence similarity with two cytoplasmic proteins and are clearly unrelated to cytochrome c_3. Hence, no information about the physiological function of cytochrome c_3 can be inferred.

PART 2

Flavocytochrome b_2 (L-lactate : cytochrome *c* oxidoreductase (E. C. 1.1.2.3.)) is a homotetrameric enzyme from the mitochondria of the yeast *Saccharomyces cerevisiae*. Each monomer consists of an N-terminal cytochrome domain and a C-terminal flavin domain, joined by a short flexible peptide. The haem domain has been identified as being mobile from the crystal structure of the *Saccharomyces cerevisiae* enzyme and a nuclear magnetic resonance study of *Hansenula anomala* flavocytochrome b_2. The rate of flavin to haem electron transfer observed in the wild-type enzyme is ~1500 s^{-1}. This rate is lower than expected considering the distance between the cofactors is ~10Å. It has been postulated that mobility accounts for the lowered rate. A number of interdomain interactions are observed in the crystal structure of flavocytochrome b_2 which may influence domain mobility. In order to

probe the importance of two such interactions the mutants K296M and R289K were characterised.

Lysine 296 forms an interdomain salt bridge by binding to a haem propionate in the crystal structure. The mutant enzyme has kinetic characteristics which are, within error, identical to the wild type enzyme. It appears that lysine 296 has no influence on the rate of interdomain electron transfer.

Arginine 289 hydrogen bonds to a haem propionate via a water molecule. Steady-state data for lactate oxidation by R289K, with ferricyanide as the terminal electron acceptor show a ten-fold fall in k_{cat} to 33 s^{-1} (400 s^{-1} for wild-type). The K_M for lactate oxidation by R289K is increased to 3.2 mM (0.5 mM for wild type). Stopped-flow data indicate lowering of the microscopic rate constants for flavin and haem reduction. The R289K flavin rate constant was 20 s^{-1} compared to 600 s^{-1} for wild-type, and 15 s^{-1} for haem reduction compared to 445 s^{-1} for wild-type. Stopped-flow kinetic isotope effects for [2-^{2}H]L-lactate flavin and haem reduction were the same as wild type. This indicates cleavage of α-H bond is rate limiting in the flavin reduction step. The haem value indicates no significant effect on flavin to haem electron-transfer rate. This was confirmed by haem re-reduction in fully reduced flavocytochrome b_2, after abstraction of a single electron by cytochrome *c*. The R289K steady-state kinetic isotope effect of 4.5±1.5 is the same as wild-type and indicates a similar transition state in both enzymes.

Index

PART 1: Cytochrome c_3

PART 2: Flavocytochrome b_2

CHAPTER 6. : *Results & Discussion*

Part 1-Cytochrome c_3

Chapter 1 : *INTRODUCTION*

1.1. BACTERIAL ENERGY TRANSDUCTION

1.1.1. Introduction

A problem faced by all living systems is the need to obtain cellular energy from their environment. Bacterial metabolic flexibility allows utilisation of an array of chemical species for growth. It is this flexibility which allows bacteria to flourish in seemingly hostile environments. Chemotrophic bacteria employ one of two mechanisms to derive cellular energy; fermentation or respiration. Each process requires an array of specialised enzymes and other proteins to regulate and facilitate energy transduction.

Fermentation is the simplest process of bacterial energy generation, both evolutionarily and metabolically. Fermentative processes generally occur in the absence of oxygen. The substrates and products of bacterial fermentations are extremely diverse. The components of the respiratory chain play no part in fermentation. The first stage of fermentation involves splitting energy-rich molecules, such as sugars, into two or more fragments, including CO_2. These fragments are phosphorylated during the breakdown process. The formation of ATP is achieved by reaction of ADP with the phosphorlylated intermediates of metabolic pathways. As a method of ATP generation, it is an inefficient process and has a low net yield. One example, homolactic fermentation, converts 1 mole of glucose into 2 moles of pyruvate and yields only 2 moles of ATP. This is in sharp contrast with the 28 moles of ATP formed from the same substrate by aerobic respiration. The main disadvantages of fermentation are the requirement for large masses of substrate and the accumulation of toxic end products such as ethanol.

Obligate respiratory bacteria cannot ferment to fulfil their energy requirements and must instead respire. Respiration is an inherently more efficient process than fermentation. Generally speaking, respiration is oxidation of a substrate molecule and reduction of an inorganic electron acceptor, coupled to generation of a protonmotive force. Aerobic respiration uses molecular oxygen as the terminal acceptor, whereas anaerobic respiration uses a number of oxidised compounds, such as SO_4^{2-}, NO_3^-, Fe^{3+} *etc*. Anaerobes can again be subdivided into; obligate anaerobes which only grow in

the absence of oxygen and facultative anaerobes which can grow with or without oxygen.

1.1.2. Bacterial electron transport chains and chemiosmosis

As has already been stated, respiration consists of a series of biological electron transfer reactions. Transfer of electrons from substrate to acceptor requires a net redox potential difference (r.p.d.) between the two components. The r.p.d. is spanned in small steps by an electron transport chain consisting of a number of proteins (Anraku, 1988). The cofactor of each protein in the chain has a redox potential higher than its predecessor. As electrons pass through the electron transport chain, they lose energy. The energy is conserved by coupled transport of "energised protons" across a proton-impermeable membrane (Nicholls & Ferguson, 1992). In gram-negative bacteria, such as *S. putrefaciens*, this impermeable barrier to protons is formed by the cytoplasmic membrane. This postulated coupling is the basis of the "chemiosmotic theory" (Mitchell, 1961, Williams, 1978). The coupling allows conversion of electronic energy into a form which is more directly useful to the cell. A schematic of this circuit is shown in Figure 1.1.

The primary proton pumping, from the cytoplasm to the periplasm, is achieved by large, membrane-spanning protein complexes. An expression relating to the magnitude of proton motive force (pmf) generated is:

$$pmf = \Delta\Psi - 2.303\ (RT / F)\ \Delta pH$$

The two components of the protonmotive force are ; firstly, the ΔpH term, relating to the imbalance in $[H^+]$ across the membrane and secondly, the $\Delta\Psi$ term relating to the electrical potential difference across the membrane. The large, membrane anchored F_1F_0 ATPase complex utilises the protonmotive force to synthesise ATP from ADP and P_i. The ATPase is a secondary pump, passing protons back into cytoplasm and thus completing the proton pumping circuit. The protonmotive force can also be used to drive other cellular processes, including import of substrates and ions, turning of flagella, maintenance of cell turgor *etc.*

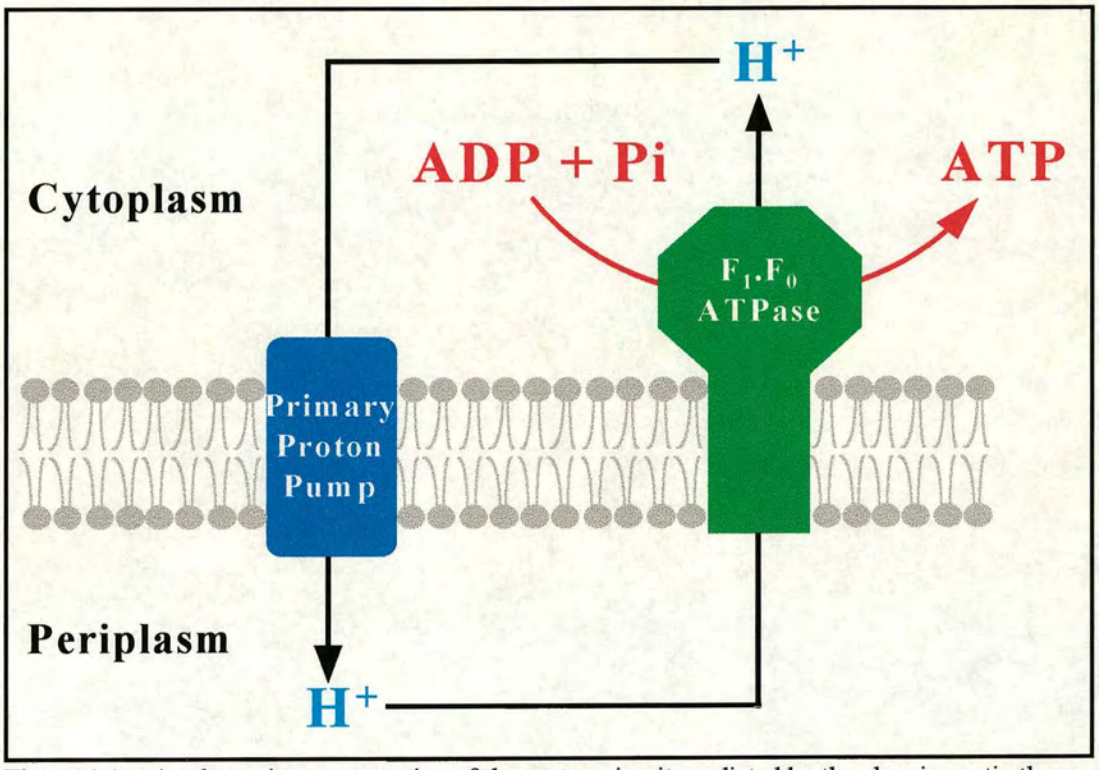

Figure 1.1. : A schematic representation of the proton circuit predicted by the chemiosmotic theory. The primary pump is a component of a respiratory chain which uses electron transfer to expel protons from the cell. This sets up a proton concentration gradient across the cell which is utilised by the ATPase. (After Nicholls and Ferguson, 1991)

The components of the electron transport chain are mostly located in the cytoplasmic membrane, although some reside in the periplasm. Generally, bacterial electron transport chains consist of; a primary dehydrogenase, a quinone and a terminal oxidase (Figure 1.2.). The elements of the chain are variable, depending on the potential of the donor and terminal acceptor. Quinones link the primary donor and the terminal acceptor. These are hydrophobic and limited to the lipid bilayer of membranes. They undergo a $2e^- + 2H^+$ reduction to quinols, the charge balancing of this reduction is important, as an ionic species would be unstable in the membrane. They are also able to translocate protons from one side of the membrane to the other. Different quinones are used according to their suitability. Ubiquinone (E_M +70 mV) is predominantly used in aerobic respiration whereas menaquinone (E_M -74 mV) has a potential more suited to anaerobic couples. Likewise, the primary electron donor will require a specific enzyme, for example lactate dehydrogenase and succinate dehydrogenase are found in *E. coli*. Where a selection of terminal acceptors is present, the one with highest redox potential is, in most bacteria, used preferentially. In *E. coli* a hierarchy exists, whereby; O_2 (+820 mV) > NO_3^- (+420 mV) > trimethyl amine N-oxide (+130 mV) > fumarate (+30 mV). The values in brackets denote the midpoint potential for each acceptor. Respiratory chain regulation ensures maximum energy yield from the available substrates. Reduction of chemical species by growing bacteria does not conclusively prove the existence of a specific reductase however. In many cases the reduction can be facilitated by chemical reaction of bacterially generated species. For example, reduced sulphur species generated from reduction of thiosulphate by *S.putrefaciens* MR-1 enhance rates of manganese reduction (Myers & Nealson, 1988a).

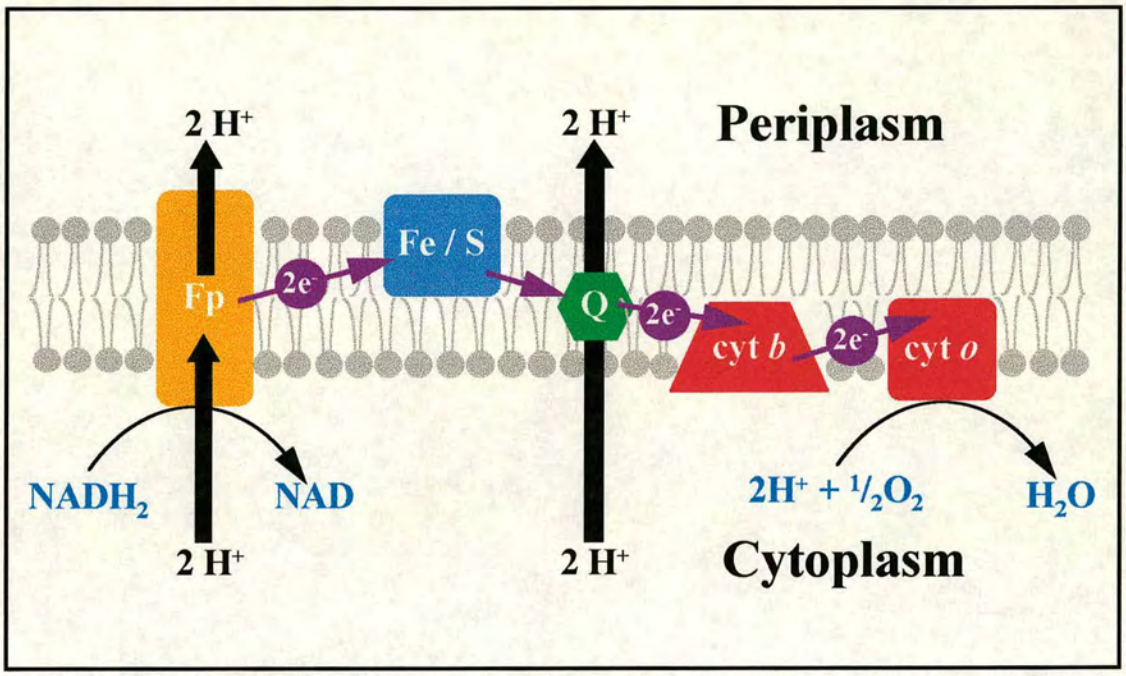

FIGURE 1.2. : Organisation of one electron transport chain from *E. coli*. This chain functions in environments of high pO_2 and contains two proton translocating centres / electron carriers; **Fp**-flavoprotein and **Q**-ubiquinone; and the electron carriers **Fe / S**-iron sulphur protein, **cyt *b***-cytochrome *b*, **cyt *o***-cytochrome *o*. Cytochrome *o* transfers electrons to the terminal acceptor which is oxygen in this case. (After Neidhardt *et al.*, 1990)

1.2. *SHEWANELLA PUTREFACIENS*

1.2.1. A brief history of *Shewanella putrefaciens*

Shewanella putrefaciens is a gram-negative, non-fermenting, facultative aerobe. The bacteria are rod shaped with a single polar flagellum. The first isolates were classified as a member of the genus *Achromobacter* (Derby & Hammer, 1931). In 1941 it was transferred to the genus *Pseudomonas* on the basis of morphology (Long & Hammer, 1941). The classification *Shewanella* finally arose after analysis of 5S ribosomal RNA sequence data (MacDonall & Colwell, 1985). Another classification, which was in use until recently, is *Alteromonas putrefaciens*. The genus was confirmed after analysis of the complete 16S ribosomal DNA for several *Shewanella* strains (Gauthier, 1995).

Two *Shewanella* strains have been extensively used; NCIMB 400 with which our lab is concerned and MR-1. Several respiratory enzymes have been isolated from each strain. *Shewanella* NCIMB400 is a marine organism which was isolated from the North Sea, near Aberdeen (Lee *et al.*, 1977) whereas MR-1 was isolated from freshwater sediment near Oneida Lake, New York (Myers & Nealson, 1988a). It has become apparent that significant sequence differences exist between homologous proteins from these strains. A 16S rRNA analysis and comparison has been carried out for a number of *Shewanella* strains. It is apparent that NCIMB400 is more closely related to the newly identified *S. frigidimarina*, isolated from Antarctic sea ice (Bowman *et al.*, 1997), than to the *S. putrfaciens* MR-1 type strain. It has therefore been proposed that NCIMB400 be reclassified as *S. frigidimarina* (Reid & Gordon 1998). The G+C content of *S. frigidimarina* is 40-43 mol% (Bowman *et al.*, 1997) whereas *S. putrefaciens* DNA has a value of 44-47 %. The value for NCIMB400 is 41.7 % which falls well within the range for *S. frigidimarina*. Hereafter *Shewanella* strain NCIMB400 will be specifically referred to as NCIMB400. *S. putrefaciens* or *Shewanella putrefaciens* refers to strain MR-1 or its close relatives.

1.2.2. Electron donor and acceptor usage in *Shewanella*

Shewanella putrefaciens can utilise a variety of terminal electron acceptors to support growth. The proliferation of *S. putrefaciens* in a number of habitats is a reflection of this capability. To date *Shewanella* sp. have been isolated from; marine and lacustrine waters (Myers & Nealson, 1988a; Perry *et al.*, 1993; Bowman *et al.*,1997; Lee *et al.*, 1977), oil field fluids and anaerobic sediments (Semple & Westlake, 1987), dairy products (Long & Hammer, 1941) and even clinical specimens (Nozue, 1992). Although *S. putrefaciens* is an obligate respiratory organism, the species, *S. frigidimarina*, closely related to *Shewanella* NCIMB400 can ferment (Bowman, 1997). *S. putrefaciens* is able to use H_2, lactate, formate and pyruvate as electron donors. The ability to respire with H_2 is shared with sulphate reducing bacteria, but *S. putrefaciens* can grow at H_2 partial pressures some 25 fold lower than them (Lovely *et al.*, 1989). *Shewanella putrefaciens* exhibits an unparalleled respiratory versatility when it comes to choice of terminal acceptor. To date, the known species, to which it can couple respiratory electron transfer are:

O_2, Mn^{IV}, Fe^{III}, $S_2O_4^{2-}$, SO_3^{2-}, S, DMSO, TMAO, NO_3^-, NO_2^-, Fumarate.

The respiratory versatility predicts a potentially complex electron transport system with some potentially unique components. At present it is not clear whether individual reductases exist for each of the terminal electron acceptors. Many of the species are of environmental importance, especially in chemical cycling between oxic and anoxic regions. The dissimilatory bacterial action on iron and manganese species in anaerobic sediments is thought to account for the banding observed in many rocks (Nealson & Myers, 1990). Anaerobic sediments show zoning, characterised by reductive processes occurring at different depths. *S. putrefaciens* is implicated in Mn^{IV} reduction in such environments, a process previously thought to be predominantly chemical, not microbial (Myers & Nealson, 1988a,b; Nealson & Saffarini, 1994). The mechanism of Fe^{III} and Mn^{IV} reduction is of great interest. The ability to reduce ferric iron is shared with some of the sulphate reducing bacteria, notably *Desulfuromonas acetoxidans* and *Desulfovibrio desulfuricans* (Nealson & Saffarini, 1994). Both

metals exist as a number of insoluble oxide forms at pH 7.0. Despite the insoluble nature of the terminal acceptor, it is not thought that siderophores are implicated in the reduction process (cf. assimilatory iron reduction). Particulate oxide reduction may require direct bacterial cell contact with the insoluble oxide, possibly through exopolysaccharide adhesion (Obuekwe, 1981). One postulated reduction mechanism, is a link from the cytoplasmic-membrane respiratory chain across the periplasm and outer membrane to the metal oxide particles (Myers & Myers, 1993a). Cytochromes located in the outer-membrane have been implicated in this process (Myers & Myers, 1992; Myers & Myers, 1997b).

The siderophore putrebactin from *S. putrefaciens* was recently identified (Ledyard, 1997) and could be involved in dissimilatory iron reduction. Siderophores are organic molecules which chelate ferric iron allowing it to be taken up by the bacterium. Once inside the cell, the complex is reduced and ferrous iron is released into solution. This mechanism is most commonly associated with assimilatory iron reduction however. Iron oxide reduction by *S. putrefaciens* is a problem in oil fields, where removal of the protective oxide coat from steel pipes accelerates their corrosion. Reduction of iron by *S. putrefaciens* is strongly inhibited by oxygen, whilst nitrate, or a nitrate reduction product, has a partial inhibitory effect on metal reduction (Arnold, 1990; DiChristina, 1992; Myers & Nealson, 1988b).

1.2.3. Genes involved in anaerobic respiration

The genetic control of anaerobic respiration in *Shewanella* sp. is still poorly understood. When grown anaerobically on fumarate or nitrate *Shewanella putrefaciens* is able to respond to a number of electron acceptors. This response suggests some co-ordinate control over anaerobic genes similar to that of *E. coli*. The fumarate nitrate respiration (Fnr) control protein of *E. coli* is a monomer in the presence of O_2. The protein is converted to an active dimer under anaerobic conditions. The sensing of O_2 is thought to use an Fe-S cluster bound to four cysteines (Lazzazera, 1996). This acts as a conformational switch under conditions of O_2 deprivation. A gene encoding EtrA, an analogue of Fnr, has been identified in *S. putrefaciens* (Saffarini & Nealson, 1993). EtrA contains the conserved active

cysteines of Fnr and the amino acid sequence of the DNA binding domain in both proteins is identical. Mutants deficient in *etrA* are unable to grow on; NO_2^-, $S_2O_4^{2-}$, SO_3^{2-}, TMAO, DMSO, Fe^{III} and fumarate, suggesting that EtrA is involved in regulation of the corresponding reductase genes. However, the mutants were still able to grow using NO_3^- and Mn^{IV} suggesting that it is not involved in the regulation of these two systems. The presence of a further *etrA* analogue has also been predicted from Southern blots of *S. putrefaciens* DNA with *etrA* as the hybridisation probe. Further genes which are strictly essential for anaerobic respiration have also been identified, yet in a southern blot, the genes did not hybridise to *etrA* or *fnr* (Saffarini *et al.*, 1994).

Recently, a gene which encodes a 21 kDa tetrahaem, *c*-type cytochrome (*cymA*) has been implicated in anaerobic respiration of a number of substrates (Myers & Myers, 1997a). Mutants lacking the gene show little respiratory reduction of Fe^{III}, NO_3^- and fumarate and they also have a deficiency of Mn^{IV} reduction. The gene is not necessary for TMAO usage. Biochemical and genetic evidence implies unique terminal reductases for Fe^{III}, NO_3^- and Mn^{IV}. The fumarate reductase in NCIMB400 (Gordon, 1996; Gordon *et al.*, 1998) and MR-1 (Myers & Myers, 1997c) has also been identified The phenotype of the *cymA* removal indicates that the CymA protein functions at a step in the electron transport chain that is common to reduction of the four species. This pathway appears to be the most efficient, but not the only pathway to Mn^{IV} reduction. A menaquinone deficient *S. putrefaciens* mutant which lacks electron transfer to the same species as the CymA deficient mutant (Myers & Myers, 1993b) is in fact also deficient in *cymA* (Myers & Myers 1997a). It has been suggested that CymA could be one of the proteins reported to be located on the outer face of the cytoplasmic membrane (Myers and Myers, 1992; 1993a; 1997b). This could allow the organism to pass electrons from the periplasm to membrane localised components, in order to reduce extracellular electron acceptors.

1.2.4. **Cytochromes from *Shewanella***

When grown anaerobically, *Shewanella* is known to produce a large number of cytochromes (Morris, 1990). CymA is one of several multiple-haem containing

cytochromes *c* which have been identified. One of the best studied of these, is the periplasmic fumarate reductase flavocytochrome c_3 (Pealing, 1992; Morris, 1994; Gordon, 1998). The enzyme has an M_r value of 63800 and contains FAD and four *c*-type haems as cofactors. It contains a large flavin binding domain, similar to that of the membrane bound fumarate reductases and a small cytochrome domain, similar to the low molecular weight cytochromes c_3 of the sulphur reducing bacteria. The enzyme has a number of novel properties which distinguish it from other fumarate reductases. Firstly, flavocytochrome c_3 is soluble, not membrane bound. Secondly, it consists of a single polypeptide chain as opposed to multiple subunits. Thirdly, it contains the four *c*-type haems instead of an Fe-S cluster. The analogous cytochromes c_3 from the sulphur reducing bacteria have been widely studied.

1.3. THE SULPHUR-REDUCING BACTERIA

The dissimilatory reduction of sulphur species features in the metabolism of a large number of different bacteria. The terms sulphate-reducing and sulphur-reducing bacteria are rather broad. Here, the terms describe bacteria which use the processes of energy conservation through oxidation of a substrate and concomitant reduction of sulphur compounds. The process of assimilatory sulphur reduction uses many similar enzymes but is limited to the building of molecules such as amino acids and cofactors. In assimilatory processes, there is no appreciable build up of sulphide associated with the reduction of sulphur species. Dissimilatory sulphur reduction is a true respiration, performed by specialised bacteria and, under appropriate conditions, can lead to large accumulations of sulphide.

The cytochromes c_3 (tetrahaem) are generally associated with the sulphate and sulphur-reducing bacteria and are found in all the *Desulfovibrio* spp. (Postgate, 1984). The first observation of cytochrome c_3 was made by Postgate in 1954. He described a pigment obtained from the sulphate-reducing bacterium *Desulfovibrio desulphuricans* (Hildenborough) as "in several ways resembling the cytochrome *c* of yeast and muscle". The *Desulfovibrio* are ecologically versatile. In the absence of sulphate they can grow by fermentation on lactate, pyruvate or ethanol in association

with a methanogen, which uses the hydrogen produced. Lactate and pyruvate can also be used as substrates in the presence of sulphate, probably involving the release of hydrogen as an intermediate. They are also able to grow chemolithotrophically in the presence of hydrogen and sulphate. The hydrogen may be supplied from association with a fermentative bacterium. The reduction of sulphate has little in common with other modes of bacterial respiration (Figure 1.3.). Sulphite reductase contains siroheme and is named desulfiviridin or desulforubidin depending on the spectral properties. The enzyme produces sulphide or trithionite under different conditions.

The electron transport processes involved in sulphate reduction have been confused in the past for a number of reasons. The first reason is, the multiplicity of terminal acceptors which appear to be present. Secondly, physiological roles were ascribed on the basis of *in vitro* stimulation of a reaction. For example, cytochrome c_3 is an oxygen scavenger which may stimulate oxygen-sensitive processes non-specifically (LeGall & Postgate, 1973). Thirdly, the segregation of redox processes to the cytoplasm and periplasm was only realised relatively recently. The *in vitro* reactions between cytochrome c_3 and ferredoxin, flavodoxin or rubredoxin are well characterised (Guerlesquin *et al.*, 1984; Cambillau *et al.*, 1988; Stewart *et al.*, 1988; Dolla *et al.*, 1991; Stewart & Wampler., 1991). These provide insights into theoretical aspects of protein complex formation. However, *in vivo* these reactions would not occur due to the cellular location of the components. Cytochrome c_3 has a periplasm directing leader sequence, yet all the other proteins are located on the other side of the cytoplasmic membrane. It is likely then, that the proposed models are invalid. The interaction of the proteins is probably due to non-specific complementarity between the numerous charged resides
present. It has been suggested that *in vivo*, the interaction could be with a membrane spanning cytochrome, similar to tetrahaem cytochrome c_3 (LeGall & Fauque, 1988).

Cytochrome c_3 most likely accepts electrons from periplasmic hydrogenase, which oxidises molecular hydrogen. In the hydrogen cycling model, the cytoplasmic membrane separates the hydrogen generating system from the periplasmic hydrogen utilising system (Odom & Peck, 1981). The hydrogenase in the cytoplasm is thought to obtain electrons from fermentation of pyruvate or lactate. The hydrogen then

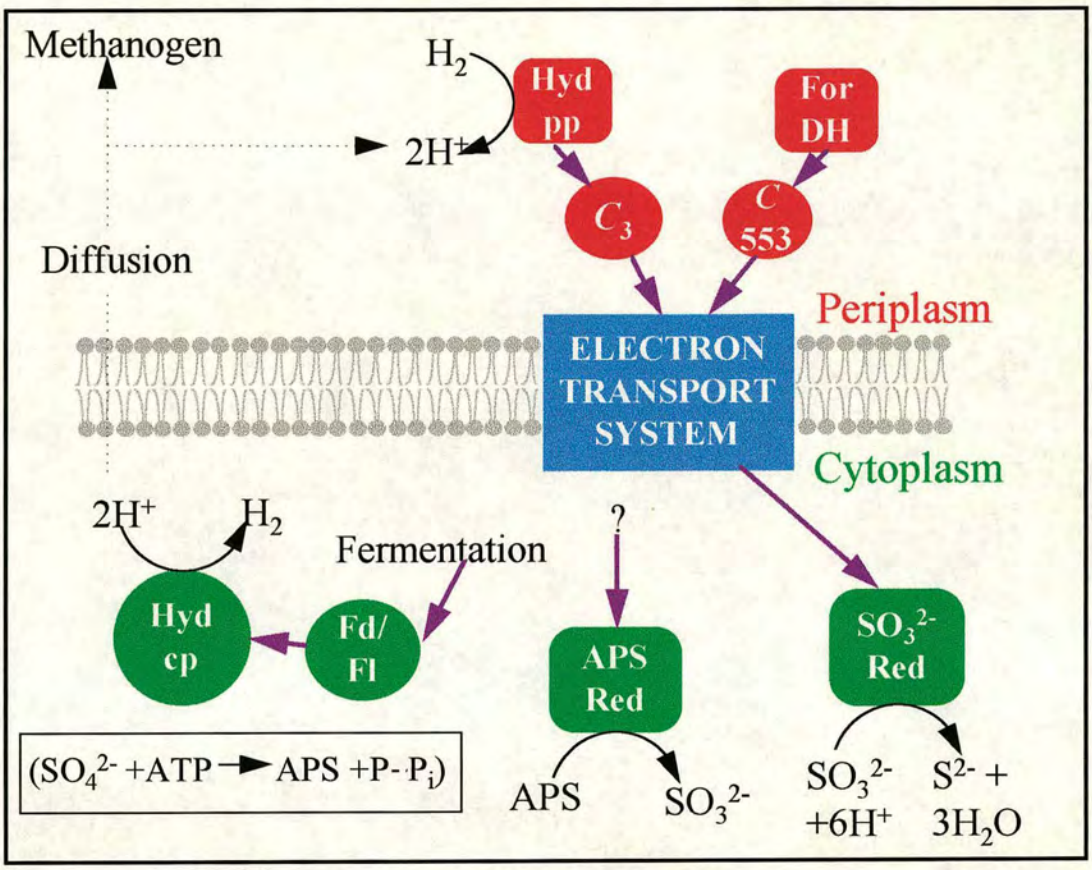

Figure 1.3. : Postulated electron transport and energy conversion pathways from *Desulfovibrio*. Purple arrows indicate electron-transfer reactions. The abbreviations are: **APS** adenosine phosphosulphate, **Hyd pp** periplasmic hydrogenase, C_3 cytochrome c_3, **ForH** formate hydrogenase, **C553** cytochrome *c*553, **Hyd cp** cytoplasmic hydrogenase, **Fd** ferredoxin, **Fl** flavodoxin, **APS red** adenosine phosphosulphate reductase, **$S0_3^{2-}$ red** sulphate reductase. The donor to APS reductase is unknown. (After Pettigrew & Moore, 1987).

diffuses across the membrane and is utilised in the periplasm. Electrons are donated to the membrane electron transport chain, from where they are passed to the sulphite reductase. This forms a central step in the metabolism of *Desulfovibrio* spp.. The physiological partnership of the two enzymes was proposed as early as 1968 (Yagi *et al.*, 1968).

1.4. CYTOCHROMES c_3

1.4.1. Introduction

Cytochromes *c* all contain mesohaem IX as the redox active cofactor. Cytochromes c_3 as they will be referred to hereafter, contain multiple haem groups with bis-histidine ligation (Ambler, 1980). Thus far cytochromes c_3 have only been identified form prokaryotic organisms. Two extensive reviews have recently been published about tetrahaem cytochrome c_3 (Coutinho & Xavier, 1994; Cusanovich *et al.*, 1994). Little sequence similarity with class I and class II cytochrome *c* has been observed. The motif CXXCH or occasionally CXXXXCH, forms the usual binding site for haem (where Xaa is any amino acid). Thioether linkages are formed by reaction between the two haem vinyls and the two cysteine thiols. The sixth histidine lies in a part of the sequence remote from the thioether forming motif. The axial ligation of the haem iron in class III cytochromes *c* is different from class I and II. Cytochromes c_3 all contain six co-ordinate iron, with the imidazole nitrogen of histidine as the fifth and sixth ligands. As a result the haem irons are low-spin and the redox potentials are low and nonidentical. This discussion will be concerned with low molecular weight (11-15 kDa), tetrahaem cytochromes c_3, but cytochromes c_3 with 3, 8 and 16 haems have been identified. The accommodation of four haems in such a short peptide chain is remarkable among redox proteins. The array of linkages and interactions between the haems and the protein backbone also lead to a very stable structure. The small size of the protein, leads to short edge-to-edge haem distances. In the structures completed so far, there are none greater than 2 nm.

The physiological mechanisms of intra-molecular and inter-molecular electron transfers by cytochrome c_3 are still not fully understood. The physiological donor is

most likely periplasmic hydrogenase, which catalyses the oxidation of hydrogen to two protons. The hydrogenase contains an acidic patch of residues which can complement the lysine rich patch on cytochrome c_3. Some possible models for the intra- and inter-protein electron transfer mechanisms are detailed in Figure 1.4. A variety of spectroscopic techniques and genetic methods have been used to probe the properties of cytochrome c_3.

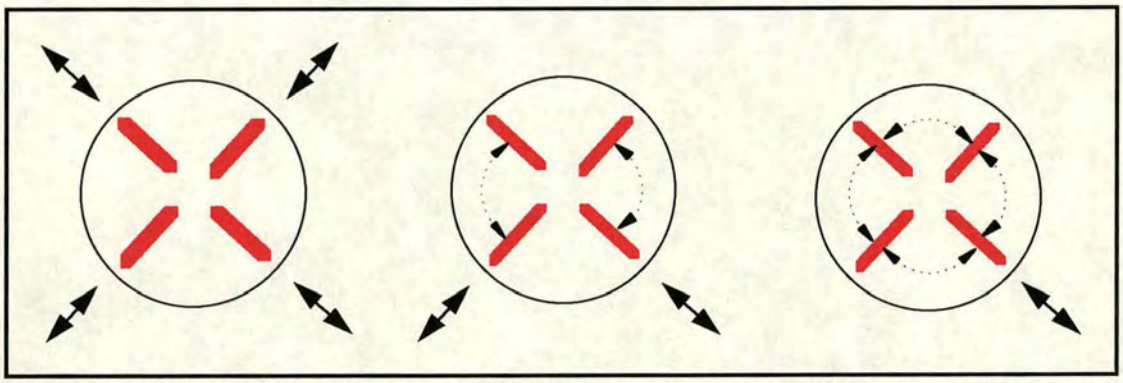

Figure 1.4. : Some possible models for electron transfer in cytochrome c_3, the haems are shown in red. Bold arrows represent intermolecular electron exchange, dotted arrows represent intramolecular electron exchange. The first figure denotes intermolecular electron exchange only. The second shows pairwire intramolecular and intermolecular electron exchange. The third shows intramolecular exchange between haems and intermolecular exchange with only one centre (After Pettigrew & Moore, 1987)

1.4.2. X-ray crystal structures

To date crystal structures have been obtained for five cytochromes c_3 from the sulphate reducing bacteria:

1)*Desulfomicrobium baculatum* Norway 4, [formerly *Desulfovibrio baculatum* and *Desulfovibrio desulfuricans*] (Haser *et al.*, 1979; Pierrot *et al.*, 1982; Czjzek *et al.*, 1994) - DbN

2)*Desulfovibrio desulfuricans* ATCC 27774 (Morais *et al.*, 1995) - Dd

3)*Desulfovibrio vulgaris* Hildenborough (Matias *et al.*, 1993) - DvH

4)*Desulfovibrio vulgaris* Miyazaki (Higuchi *et al.*, 1981; Higuchi *et al.*, 1984) - DvM

5)*Desulfovibrio gigas* (Matias *et al.*, 1996) - Dg

It is immediately apparent from the structures that the haem core architecture is highly conserved. The position of the four haems, and their binding regions, show little variation between proteins despite the low sequence homology as can be seen in Figure .1.6. The variations in the sequence tend to occur as peptide inserts in the surface loop regions of the protein . The proteins have very similar iron-to-iron distances and present the same haem plane orientations. The haems are numbered H_I to H_{IV}, according to the position of the cysteine residues which form the thioether linkage, in the amino acid sequence (Coutinho & Xavier, 1994). The inter-haem distances vary between 1.1 and 1.8 nm and the planes defined by the haems H_I and H_{IV} are roughly parallel and both approximately perpendicular to haems H_{II} and H_{III} which are mutually perpendicular. The haem edges are much more accessible to the solvent than in mitochondrial cytochrome *c*. The cytochromes also show a highly charged, high lysine content region near haem H_{IV} at the C-terminus of the protein. This patch has been proposed as a recognition site for a redox partner of cytochrome c_3 is absent in the protein from *Dsm. baculatum* (Stewart al., 1988).

1.4.3. Sequence alignment

The amino acid sequences for a number of cytochromes c_3 have been determined (Haser *et al.*, 1979; Bruschi *et al.*, 1981; Shinkai *et al.*, 1980; Voordouw & Brenner, 1986) and six are aligned in Figure 1.7. Even within the cytochrome c_3 group only 25-45% pairwise identity is observed (Pettigrew & Moore, 1987) and can be as low as 20% (Morais *et al.*, 1995). The smallest homology is observed between *Dsm. baculatum* and *D. vulgaris* which are the least phylogenetically related organisms (Devereaux *et al.*, 1990). Most of the invariant residues in the sequence are involved in binding and co-ordinating the haems, no role for the other invariant residues has been proposed yet.

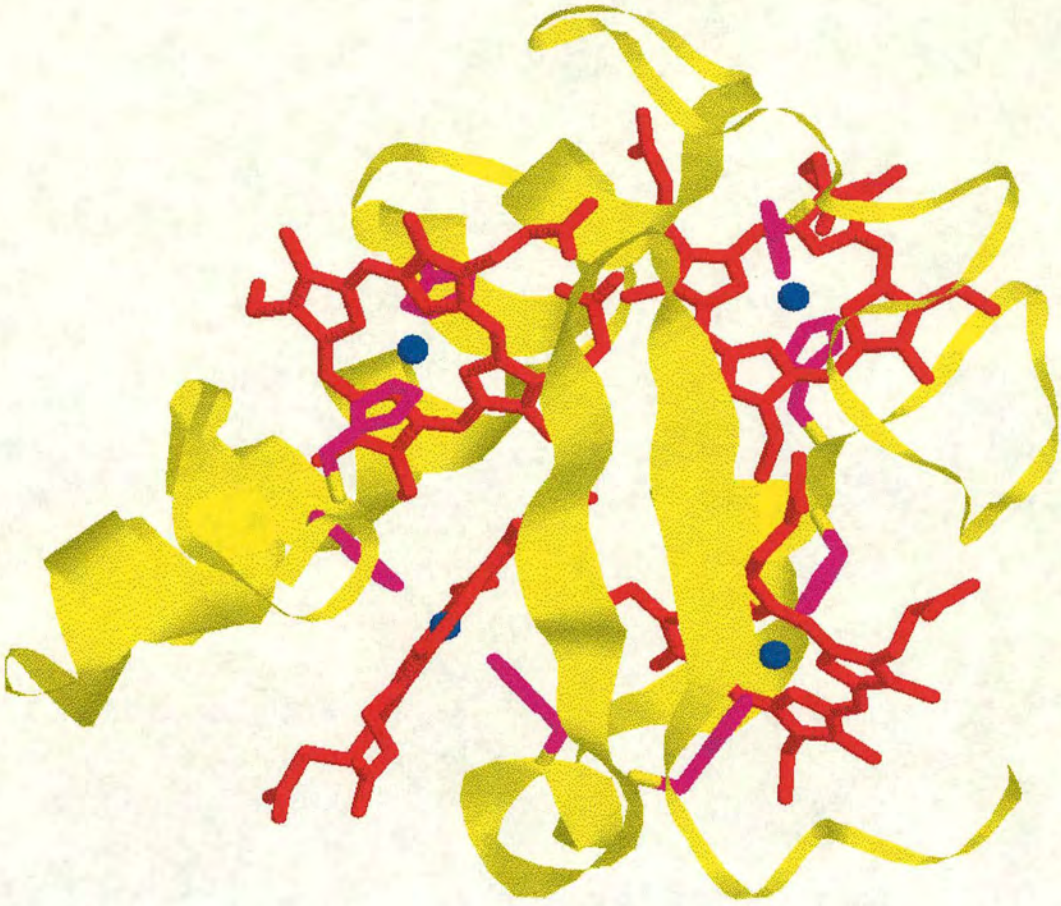

Figure 1.5. : The three dimensional structure of the cytochrome c_3 from *D. vulgaris*. The bis histidine ligation of the haem irons can be clearly seen.

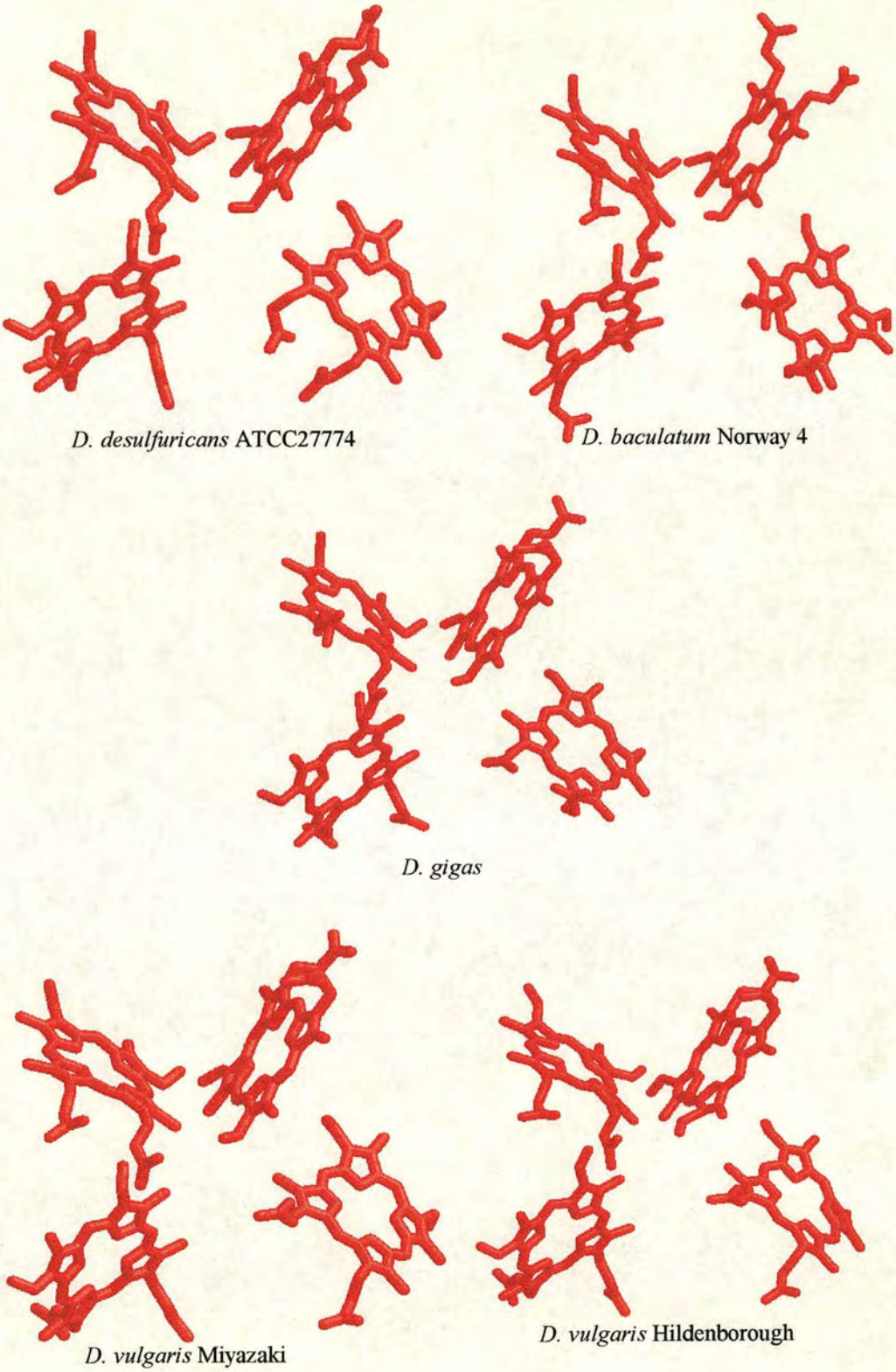

Figure 1.6. : The conservation of the haem core architecture between cytochromes c_3 obtained from different sources

1.4.4. Redox potentials

The short haem-haem distances in cytochrome c_3 greatly complicate the redox behaviour of the protein. There is evidence for interactions between the four haems. A full consideration of thermodynamic and kinetic relationships is required to describe the function of the protein. The redox potential of the molecule is referred to as the macroscopic potential. The redox potential of an individual haem is referred to as the microscopic potential or micropotential. There are five possible oxidation states for the molecule (Figure 1.8.), which give rise to four macroscopic potentials. One can measure the macroscopic reduction potentials through techniques such as cyclic voltammetry or uv / visible redox potentiometry. This indicates nothing of the complexity of the protein but gives useful insights into the apparent midpoints of the haems.

A more complex study will assign microscopic redox potentials (Figure 1.8.) to each haem (micropotentials). The reduction (or oxidation) of the protein takes the form of five different stages (or steps) (Moura *et al.*, 1982; Moura *et al.*, 1988; Gayda *et al.*, 1988; Benosman *et al.*, 1989; Park *et al.*, 1995). Each stage corresponds to the addition (or removal) of one equivalent of electrons to the protein. The presence of four non-equivalent haems leads to an equilibrium between the 16 possible microstates (Figure 1.8). The microstates within one reduction stage will be in equilibrium with each other by intramolecular electron exchange. There will be yet another equilibrium between molecules of different redox stage, these can exchange electrons via intermolecular collisions. The situation is complicated even further by a network of homotropic (e^- / e^-) interactions between the haems (Park *et al.*, 1996a). This leads to modification of the potential of adjacent haems upon reduction (or oxidation). Both positive and negative cooperativities have been observed for cytochrome c_3. Heterotropic cooperativity (e^- / H^+ referred to as redox Bohr effect) has also been observed for cytochromes c_3 and the related parameters were determined (Turner *et al.*, 1994; Park & Kang, 1996b; Turner *et al.*, 1996). EPR and NMR techniques have proved particularly suitable for studying the interactions between haems and the individual microstates.

ORGANISM	**1**					**5**					**10**						**15**					**20**		
1)*Dsm.b*	A	D	A	P	G	D	D	Y	V	I	S	A	P	E	-	G	M	K	A	K	P	K	G
2)*D.d*(EA)	V	D	A	P	A	D	M	-	V	I	K	A	P	A	-	G	A	K	V	-	T	K	-
3)*D.s*	V	D	A	P	G	D	M	-	V	L	K	A	P	A	-	G	A	K	M	-	T	K	-
4)*D.v*(H)	A	P	K	A	P	A	D	G	L	K	M	E	-	-	-	-	-	-	-	-	A	T	K	-
5)*D.v*(M)	A	P	K	A	P	A	D	G	L	K	M	D	-	-	-	-	-	-	-	-	K	T	K	-
6)*D.g*	V	D	V	P	A	D	G	A	K	I	D	F	I	A	G	G	E	K	-	-	-	-	-	

	25						**30**					**35**					**40**					**45**			
1)	D	K	P	G	A	L	Q	K	T	V	P	F	P	H	T	K	H	A	T	-	V	E	C	V	Q	C	H	H
2)	-	-	-	-	-	-	A	P	-	V	A	F	S	H	K	G	H	A	S	-	M	D	C	K	T	C	H	H
3)	-	-	-	-	-	-	A	P	-	V	D	F	S	H	K	G	H	A	A	-	L	D	C	T	K	C	H	H
4)	-	-	-	-	-	-	Q	P	-	V	V	F	N	H	S	T	H	K	S	-	V	K	C	G	D	C	H	H
5)	-	-	-	-	-	-	Q	P	-	V	V	F	N	H	S	T	H	K	A	-	V	K	C	G	D	C	H	H
6)	-	-	-	-	-	-	N	L	-	V	V	F	N	H	S	T	H	K	D	-	V	K	C	B	B	C	H	H

	50					**55**					**60**					**65**					**70**				**75**		
1)	T	L	E	A	D	G	-	G	A	V	K	K	C	T	T	S	G	C	H	D	S	L	E	F	R	D	K	A
2)	K	-	-	W	D	G	A	G	A	I	Q	P	C	Q	A	S	G	C	H	A	N	T	E	S	K	-	K	G
3)	K	-	-	W	D	G	K	A	E	V	K	K	C	S	A	E	G	C	H	V	B	T	S	K	K	G	K	K
4)	P	-	-	V	N	G	K	E	D	Y	R	K	C	G	T	A	G	C	H	D	S	M	D	K	K	D	K	-
5)	P	-	-	V	N	G	K	E	N	Y	Q	K	C	A	T	A	G	C	H	D	N	M	D	K	K	D	K	-
6)	Z	-	-	-	P	G	B	K	Q	Y	A	G	C	T	T	D	G	C	H	N	I	L	D	K	A	D	K	-

	80						**85**					**90**										**95**			
1)	N	A	K	D	I	K	L	V	E	S	A	F	H	T	-	-	-	-	-	-	-	Q	C	I	D	C	H	A
2)	-	D	D	S	F	Y	-	-	-	M	A	F	H	E	R	K	S	E	-	K	-	S	C	V	G	C	H	K
3)	S	T	P	K	F	Y	-	-	-	S	A	F	H	S	K	S	D	I	-	-	-	S	C	V	G	C	H	K
4)	S	A	K	G	Y	Y	-	-	-	H	V	M	H	D	K	N	T	K	F	K	-	S	C	V	G	C	H	V
5)	S	A	K	G	Y	Y	-	-	-	H	A	M	H	D	K	G	T	K	F	K	-	S	C	V	G	C	H	L
6)	S	V	N	S	W	Y	-	-	-	K	V	V	H	D	A	K	G	G	A	K	P	T	C	I	S	C	H	K

	100								**105**						**110**						**115**					
1)	L	K	K	K	D	-	-	-	-	K	K	P	T	G	P	T	A	C	-	-	G	K	C	H	T	T	N	
2)	-	-	-	-	-	-	-	-	S	M	K	K	G	-	-	P	T	K	C	-	-	T	E	C	H	P	K	N
3)	-	-	-	-	-	-	A	A	L	K	K	A	T	G	P	T	K	C	-	-	G	D	C	H	P	K	K	K
4)	E	V	A	G	A	D	A	A	K	K	K	D	-	-	L	T	G	C	K	K	S	K	C	H	E			
5)	E	T	A	G	A	D	K	E	K	K	K	E	-	-	L	T	G	C	K	G	S	K	C	H	S			
6)	D	K	A	G	D	D	-	-	L	K	K	K	-	-	L	T	G	C	K	G	S	A	C	H	P	S		

FIGURE 1.7. : Alignment of cytochrome c_3 sequences from the organisms:

1)*Dsm.b*-*Desulfomicrobium baculatum*, **2)*D.d*(EA)-*Desulfovibrio desulfuricans*** El Agheila Z, **3)*D.s*-*Desulfovibrio salexigens***, **4)*D.v*(H)-*Desulfovibrio vulgaris*** Hildenborough, **5)*D.v*(M)-*Desulfovibrio vulgaris*** Miyazaki, **6)***D.g*-*Desulfovibrio gigas*.** (From Moore & Pettigrew, 1991)

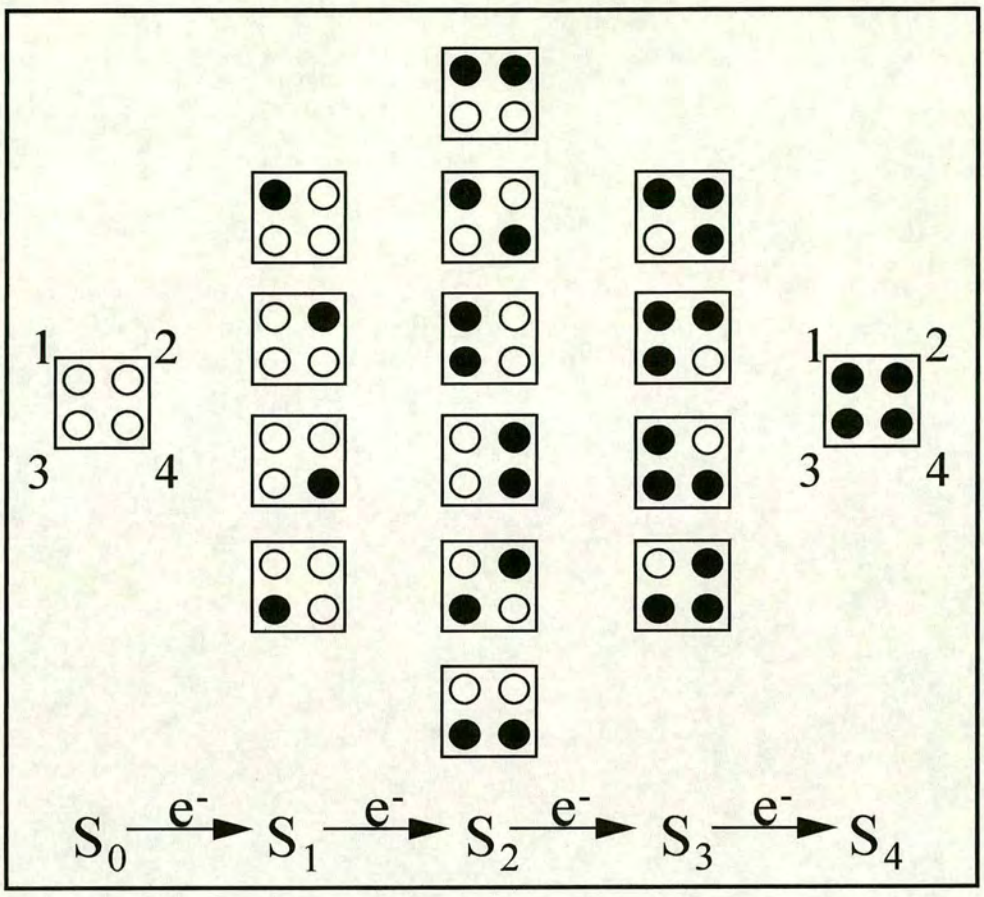

FIGURE 1.8. : A schematic representation of the redox states of cytochrome c_3. Each box denotes one of the 16 microstates with either ferri-haems (open circles) or ferro-haems (filled circles). The five macroscopic redox states (S_i) are indicated in columns. The addition of an electron between redox states corresponds to the macroscopic redox potentials of the protein. The numbers denote haem numbers. (After Fan *et al.*, 1990b).

Cytochromes c_3 are low potential proteins, thus strong reducing agents such as dithionite ($E^\circ \sim -500$ mV at pH 7.0) or the H_2 / H_{ase} (hydrogenase) system at pH > 7.0, are required to achieve full reduction. Estimates of the redox potentials for the proteins have been made using electrochemical methods (Bruschi *et al.*, 1984; Bianco & Haladjian, 1981; Niki *et al.*, 1984; Mus-Veteau *et al.*, 1992; Niviere *et al.*, 1988) and spectroelectrochemical data (Fan *et al.*, 1990a; Coletta *et al.*, 1991). The macroscopic potentials determined in these and other studies all lie between -30 mV and -400 mV, see table 1.

Redox titrations monitored by one-dimensional (1D) NMR have been carried out for the cytochromes c_3 from *D. gigas* (Picarra-Periera *et al.*, 1993; Santos *et al.*, 1984), *D. vulgaris* Miyazaki (Fan *et al.*, 1990a), *D. vulgaris* Hildenborough (Turner *et al.*, 1994) and show similar microscopic potentials for the four haems. The titrations also showed that the redox state of one or more haems influenced the micropotentials of the other haems (determined as the haem-haem interaction potentials). Furthermore, the pH dependence of individual haem micropotentials was demonstrated.

Redox linked pK_a values have been determined for the cytochromes from *D. gigas* (Coletta *et al.*, 1991; Santos *et al.*, 1984) and *D. vulgaris* Hildenborough (Turner *et al*, 1994). Abnormalities were noted in the visible spectrum of cytochrome c_3 reduction by hydrogenase and attributed to haem-haem interactions (Yagi *et al.*, 1984). Interactions have also been observed using EPR (More *et al.*, 1990), Mössbauer spectroscopy (Utuno *et al.*, 1980) and resonance Raman spectroscopy (Verma *et al.*, 1988). The interaction potentials determined by NMR take both positive and negative values and so cannot be explained simply on the basis of electrostatic effects.

Negative values are co-operative and positive values, anti-co-operative. The existence of negative values for interacting potentials have been explained in terms of a structural modification linked to the change in redox state of the molecule. Redox titrations of the cytochromes c_3 from *Dsm. baculatum* Norway 4 and *Dsm. baculatum* (DSM 1743) monitored by EPR (Gayda *et al.*, 1985; Gayda *et al.*, 1988; Moura *et al.*, 1988) and NMR have shown three micropotentials similar to those for *D. vulgaris*

and *D. gigas* (More *et al.*, 1990; Xavier *et al.*, 1979; Benosman *et al.*, 1989) and also a fourth which is considerably higher. No important haem-haem interactions were observed for the *Dsm. baculatum* proteins.

TABLE 1.1. : Macroscopic potentials determined for cytochromes c_3

Organism	Potential (mV)			
	E_1	E_2	E_3	E_4
Dsm. baculatum (Norway 4) [a]	-400	-365	-305	-165
Dsm. baculatum (Norway 4) [b]	-410	-370	-310	-210
D. vulgaris (Miyazaki) [c]	-360	-322	-300	-242
D. vulgaris (Hildenborough) wt [d]	-380	-350	-320	-280
D. vulgaris (Hildenborough) H70M [d]	-350	-320	-260	-80
D. gigas [e]	-330	-315	-295	-195
D. desulfuricans (Berre Sol) [f]	-375	-335	-305	-225
D. desulfuricans (El Agheila) [f]	-320	-290	-265	-235
D. desulfuricans (ATCC 27774) [g]	-380	-370	-260	-140
D. africanus - basic c_3 [h]	-290	-280	-260	-90
D. africanus - acidic c_3 [h]	-270	-260	-240	-210
D. elongatus [i]	-165	-165	-165	-30
T. commune [j]	-280	-280	-280	-140

References

a) Bianco & Haladjian (1981)
b) Dolla *et al.* (1987)
c) Sokol *et al.* (1980)
d) Mus-Veteau *et al.* (1992), wt is wild type c_3 and H70M is an axial ligand mutant
e) Nivière *et al.* (1988)
f) Bruschi *et al.* (1984)
g) Morais *et al.* (1995)
h) Pieulle *et al.* (1996)
i) Samain *et al.* (1986)
j) Hatchikian *et al.* (1984)

Some of the redox micropotentials determined by NMR and EPR are shown in Tables 2 and 3 respectively. The macroscopic redox potentials are predicted from the micropotentials and the inter-haem interaction potentials.

The intermolecular electron exchange rate for the cytochromes c_3 from *D. gigas* is slow on the NMR timescale. This means that a different set of signals is observed for the haem protons belonging to each different stage. For these proteins it is easy to follow the redox stages, as well as measuring the degree of oxidation of the haems and their different potentials (different microscopic potentials) at each stage. The slow inter-molecular exchange allowed assignment of redox potentials to specific haems in the structure. Two-dimensional (2D) NMR was used to follow the connectivities of haem methyl resonances, previously identified in the fully reduced state, throughout the five redox stages, up to the fully oxidised state (Picarra-Pereira *et al.*, 1993; Salgueiro *et al.*, 1992; Xavier *et al.*, 1993). The results agree only partly with those obtained from direct interpretation of 2D-NMR data acquired for the oxidised *D. vulgaris* proteins which were mainly based on tentative assignments of haem connectivities (Park *et al.*, 1991a; Park *et al.*, 1991b; Sola & Cowan, 1992). An attempt was made to assign the redox potential of haem HIV from *D. vulgaris* Hildenborough by making a mutation at one of the axial ligands. The potentiometric results obtained for the H70M enzyme are, however, thought to be ambiguous (Mus-Veteau *et al.*, 1992).

Despite the haem core similarity, some of the properties of the *Dsm. baculatum* c_3 differ considerably from those of the *Desulfovibrio* proteins. Firstly, the potential of one haem is more than 120 mV higher than those of the other three (Guerlesquin *et al.*, 1985; Moura *et al.*, 1988; Gayda *et al.*, 1985; Gayda *et al.*, 1988; Guigliarella *et al.*, 1990). Secondly, the cytochromes c_3 from *Dsm. baculatum* show fast intermolecular exchange on the NMR timescale (Coutinho *et al.*, 1993; Guerlesquin *et al.*, 1985) and so resolved haem methyl peaks corresponding to the different redox stages are not observed. Assignments of the higher potential haem (Coutinho *et al.*, 1993) and of the lowest one (Coutinho *et al.* 1995) were obtained by following the chemical shifts of selected resonances from the haems using 1D NMR data.

TABLE 1.2. : Microscopic redox potentials determined for cytochrome c_3 using nuclear magnetic resonance data. (After Coutinho & Xavier, 1994)

Organism	Redox potentials (mV)				pH
	e_1	e_2	e_3	e_4	
Dsm. baculatum [a]	-335	-296	-286	-120	7.8
D. vulgaris Miyazaki [b, O]	-340	-328	-302	-270	7.1
D. vulgaris Miyazaki [b, R]	-325	-291	-355	-321	
D. gigas [c, O]	-295	-260	-225	-180	5.5
D. gigas [c, R]	-255	-290	-255	-240	
D. gigas [c, O]	-360	-305	-280	-205	9.8
D. gigas [c, R]	-340	-285	-280	205	

References
a) Coutinho & Xavier (1994)
b) Fan *et al.* (1990b)
c) Coletta *et al.* (1991) & Santos *et al.* (1984)
O) Potentials when other haems are oxidised
R) Potentials when other haems are reduced

TABLE 1.3. : Microscopic redox potentials determined for cytochrome c_3 using electron paramagnetic resonance data. (from Coutinho & Xavier, 1994)

Organism	Redox potentials (mV)			
	e_1	e_2	e_3	e_4
Dsm. baculatum (DSM 1743) [a]	-355	-300	-280	-70
Dsm. baculatum (Norway 4) [b]	-355	-325	-270	-150
Dsm. baculatum (Norway 4) [c]	-345/ -352	-320/ -330	-275/ -300	-150
Dsm. baculatum (Norway 4) [d]	-355	-330	-300	-150
D. vulgaris (Miyazaki) [e]	-355/ -360	-335/ -330	-325/ -320	-250/ -220
D. vulgaris (Hildenborough) [f]	-365	-350	-320	-300
D. gigas [g]	-315	-306	-235	-235

References
a) Moura *et al.*, 1988.
b) Gayda *et al.*, 1985.
c) Gayda *et al.*, 1988.
d) Guigliarelli *et al.*, 1990.
e) Benosman *et al.*, 1989.
f) Coutinho & Xavier., 1994
g) Xavier *et al.*, 1979.

These assignments agree well with data obtained in a single-crystal EPR redox study (Guigliarelli *et al.*, 1990).

1.4.5. Genetics

The antigenic cross-reactivity of the cytochromes c_3 from different species of sulphate reducing bacteria shows considerable variability (Singleton *et al.*, 1982; Voordouw *et al.*, 1987). Even strains of a single species showed considerable variability when compared using PCR (Kwoh *et al.*, 1993). The gene for *D. vulgaris* Hildenborough cytochrome c_3 has been cloned and sequenced (Voordouw *et al.*, 1986). This gene was used to probe the genomes of 16 further strains of *Desulfovibrio*, using southern blotting to indicate the presence or absence of a similar gene (Voordouw *et al.*, 1987).

Attempts to functionally express the cytochrome c_3 gene of *D. vulgaris* Hildenborough in *E. coli* were unsuccessful, apparently because of the inability of *E. coli* to insert *c*-type haems (Pollock *et al.*, 1989). Functional expression of the *D. vulgaris* Hildenborough gene, and purification of holocytochrome c_3 was achieved in *D. desulfuricans* G200 (Voordouw *et al.*, 1990). The system using *D. desulfuricans* G200 has also been employed for site directed mutagenesis of the *D. vulgaris* Hildenborough cytochrome c_3 (Mus-Veteau *et al.*, 1992; Saraiva *et al.*, 1996). Successful production of *D. vulgaris* cytochrome c_3 was also achieved in the purple photosynthetic bacterium *Rhodobacter sphaeroides* (Cannac *et al.*, 1991), the authors were hopeful that this system may lead to protein over-production.

1.4.6. Kinetics

The presence of four haems in cytochrome c_3 allows the possibility of both intra-molecular, first-order electron transfer and inter-molecular, second-order electron transfer reactions.

The intra-molecular rate constants for cytochrome c_3 have not yet been determined but attempts have been made to estimate them. In NMR studies of cytochrome c_3 samples in slow inter-molecular exchange, the absence of individualised haem resonances indicates a fast exchange rate, $>10^5$ s^{-1}. Resonance

Raman results for *Desulfovibrio vulgaris* (Miyazaki) showed discrete bands, at positions characteristic of reduced and oxidised haems. This indicates that the lifetime of microstates is longer than the spectral timescale limit (Verma *et al.*, 1988). However, the transit time of electrons between haems could still be exceptionally fast. The postulated rates are still faster than most intra-molecular electron transfer (ET) processes in proteins containing multiple metal centres, with the obvious exception of the photosynthetic reaction centre. The short haem-haem distances and the extensive covalent and noncovalent linkages through the backbone probably help to facilitate intramolecular electron flow. More recent Resonance Raman results for *Desulfovibrio vulgaris* (Hildenborough) and *Desulfomicrobium baculatum* (Norway 4) cytochrome c_3 , did not indicate peak splitting (Kazanskaya *et al.*, 1996).

First-order ET rate constants have been calculated for a paired cytochrome c_3 ferredoxin complex using stopped flow data (Capeillere-Blandin *et al.*, 1986). The proteins were considered as a dimer and rate constants for the forward and back reactions were acquired. Cytochrome c_3 has also been studied in the presence of dithionite and methyl viologen radicals using pulse radiolysis (Van Leeuwen *et al.*, 1982, Favaudon *et al.*, 1978). The data provided the first indication that the four haems were kinetically nonequivalent during bimolecular reduction with inorganic redox partners. Stopped flow kinetic data for a reaction between *Dsm. baculatum* cytochrome c_3 and dithionite is biphasic. The fast phase, corresponds to reduction of 25 % of the total protein and the slow phase to, reduction of 75 % of the protein. Comparable biphasic data have also been observed for the cytochromes c_3 from *D. vulgaris* and *D. gigas* (Capeillere-Blandin *et al.*, 1986; Catarino *et al.*, 1991). The latter study used a network of thermodynamic parameters from another study (Coletta *et al.*, 1991) including haem micropotentials and interaction potentials, to establish intermolecular ET rates for each haem. Similar results were observed for *D. vulgaris* (Hildenborough and Miyazaki strains) reduced by small molecules followed by flash photolysis (Akutsu *et al.*, 1992). The ionic strength of the solution and the formal charge of the reductant were found to influence the rate constants.

1.4.7. Summary

In spite of the wealth of data which has been obtained for cytochrome c_3 from an increasing variety of sources, no physiological function has been conclusively assigned to any of the proteins. Even though the proteins are very small, and have well conserved haem orientations, they seem to show considerable differences in some of their properties *i.e.* haem midpoint potentials, isoelectric points, electron exchange rates.

Xavier and coworkers have related data from the *D. gigas* and *D. vulgaris* (Hildenborough) cytochromes c_3 to one of the postulated physiological functions, as an electron acceptor from hydrogenase (Xavier, 1985; Xavier, 1986; Coutinho & Xavier, 1994; Louro *et al.*, 1996; Louro *et al.*, 1997). When a multiredox centre protein is studied *in vitro*, all possible redox states are attained by the protein. For cytochrome c_3 this means that all 16 microstates (Figure 1.8.) are populated in accordance with the attendant 32 redox pairs (Xavier, 1986). Hence, the resulting data reflect the chemical equilibrium state of the protein. It is quite possible that *in vivo* a number of these states will not be accessible to the protein. This would result if electrons were given (or received) by a specific haem and then given (or received) so fast that chemical equilibrium conditions are not obtained.

The cooperativity (electron/electron) shown by the *D. gigas* cytochrome c_3 , gives it the properties necessary to function as a two electron donor/acceptor and a scheme has been proposed (Xavier, 1985: Xavier, 1986). In the scheme, transfer of two electrons only occurs after reduction/oxidation of a third haem. Thus, two haems are considered as regulatory (dispatcher centres) and the two positively cooperative haems, can then deliver two electrons rapidly. The regulatory haems overcome the need for selective electron transfer.

The functional significance of the cooperativity (proton/electron) in *D. vulgaris* (Hildenborough) cytochrome c_3 has also been considered. The thermodynamic relationship between electrons and protons participating in redox reactions, is commonly referred to as the redox-Bohr effect (Papa *et al.*, 1979). It is commonly used to explain proton-pumping across membranes, where it is referred to as the membrane-Bohr effect. The properties observed for cytochrome c_3 suggest that

it can support a concerted proton-assisted $2e^-$ step (Louro *et al.*, 1996; Louro *et al.*, 1997). The coupled uptake of protons and electrons would make the cytochrome c_3 an excellent partner for hydrogenase which catalyses the reaction:

$$H_2 \rightarrow 2H^+ + 2e^-$$

During physiological function, cytochrome c_3 could act as a "proton thruster" (Louro *et al*, 1997). This involves taking up protons and energised electrons, then releasing electrons and energised protons. This would allow energy transduction without the need for membrane confinement, in accordance with Williams (1978).

It is quite possible that the low molecular weight cytochromes c_3 found in different bacteria may fulfil different physiological functions. This hypothesis is supported by the discovery of two very different tetrahaem cytochromes c_3 in a single organism, *Desulfovibrio africanus* (Pieulle *et al.*, 1996). The cytochromes were referred to as the acidic c_3 and basic c_3 by the authors, reflecting differences in isoelectric point and other properties. The majority of cytochromes c_3 which have been identified so far are readily reduced by the periplasmic hydrogenase from the corresponding organism (*e g.* Pieulle *et al.*, 1996; Verma *et al.*, 1988; Bianco *et al.*, 1992). This is the case for basic *D. africanus* cytochrome c_3. The *D. africanus* acidic cytochrome c_3 on the other hand, is not reduced by hydrogenase in the absence of basic cytochrome c_3. In general, the basic cytochromes c_3 have conserved surface lysine residues. Complex formation can be facilitated by interaction between the lysine residues and complementary, negative residues on the surface of an acidic redox protein *e.g.* ferredoxin, flavodoxin and rubredoxin (Cambillau *et al.*, 1988; Stewart *et al.*, 1988; Guerlesquin *et al.*, 1984). Additionally, the cytochromes c_3 exhibit an asymmetrical charge distribution. This could produce a dipole moment and aid protein recognition (Cambillau *et al.*, 1988). The same type of interaction probably occurs between cytochrome c_3 and the periplasmic hydrogenases. The differing specificities of the *D. africanus* cytochromes c_3 could thus be rationalised on the basis of their differing electrostatic charges. Most importantly, the role of low potential cytochromes c_3 cannot be assumed to be as a coupling factor between hydrogenase and a respiratory electron transport chain.

1.5. Aims

During an attempt to purify the haem domain of *S. putrefaciens* NCIMB 400 flavocytochrome c_3, expressed in a flavocytochrome c_3 deficient strain of the bacterium (Gordon, 1996), another cytochrome c_3 was identified.

The main aims of the work described in part one of this thesis were to:

1. To purify the protein and obtain a biochemical and biophysical characterisation of it.

2. To sequence the cytochrome c_3 gene and flanking regions in the hope of obtaining information about the physiological function of the protein.

Part 1-Cytochrome c_3

Chapter 2 : *MATERIALS AND METHODS*

2.1. MEDIA AND GROWTH CONDITIONS

2.1.1. General

All plastic disposables were sterilised by autoclaving at 121°C for 20 min. as was all growth medium. Temperature sensitive solutions such as antibiotics were sterilised by filtration through 0.2 μm filters (Sartorius). Ultrapure deionised water (resistivity ~18 MΩ) was used for all solutions and high purity chemical were used throughout.

E. coli were grown at 37°C throughout and *S. putrefaciens* were grown at 23-25°C. Starter cultures (5 mL) were inoculated from agar plates using a sterile loop and used to inoculate large cultures (0.5 L). Large scale cultures were grown anaerobically in flasks typically containing 1/2 volume of culture media. Aerobic cultures were grown in flasks containing no more than 1/5 volume of medium. Bacteria were harvested by at 16000g for 10 minutes in a Sorvall RC-5B centrifuge and then stored at -20°C until required.

2.1.2. Bacterial strains used

S. putrefaciens NCIMB 400 - wild type

S. putrefaciens EG301 - Flavocytochrome c_3 deficient mutant

E. coli AR120

2.1.3. Luria-Bertani growth medium

per litre:

Bacto-tryptone	10 g
Bacto-yeast extract	5 g
NaCl	5 g (10 g for *S. putrefaciens*)

1.5 % agar was added to the above for plates

2.1.4. Long term bacterial storage

To maintain stocks of bacterial strains 70 μL DMSO (7 % v / v) was added to 1 mL of exponentially growing culture in a sterile microcentrifuge tube. The tube was

chilled on ice for 10 min. and then frozen at -80°C. The culture was recovered by scraping a small sample with a sterile pipette tip and transferring to an agar plate. The plate was then streaked for single colonies.

2.1.5. Antibiotics

Filter sterilised antibiotics were added to previously autoclaved broth and plates (once the temperature was below 50°C) in the following concentrations: Ampicillin 100 μg / mL, Kanamycin 50 μg / mL, Streptomycin 25 μg / mL, Rifampcin 10 μg / mL.

2.2. PROTEIN PURIFICATION

2.2.1. General

Unless otherwise stated, all steps were carried out at 4°C. Buffers were made up according to standard practise (Dawson R. M. C. et al., 1984). UV / visible spectroscopy between 250 nm and 800 nm was used to monitor the protein during purification.

2.2.2. Cell lysis

Anaerobically grown S. putrefaciens cells (100 g), frozen at -20°C were thawed. Using a homogeniser the cells were suspended in 200 mL of 100 mM sodium phosphate buffer (pH 7.0). The cells were sonicated, on ice, at full power for 1 min. total using a sonicator (HEAT SYSTEMS-ultrasonic processor). To separate cell debris from the soluble fraction, the lysed cells were spun at 39000g for 30 min.. The red supernatant was carefully decanted and the pellet of debris discarded.

2.2.3. Ammonium sulphate precipitation

The addition of ammonium sulphate causes salting-out of less soluble proteins. It is an excellent method for removing a large bulk of the unwanted protein from solution. The volume of supernatant containing soluble proteins was determined. Ammonium sulphate was added slowly to the supernatant at 4°C in order to make a

50 % saturated solution. The resultant solution was spun at 39000g in an SS-34 rotor for 20 min. The supernatant, which contains cytochrome c_3 was carefully pipetted away from the protein pellet and was ready for chromatography.

2.2.4. Chromatography

Hydrophobic interaction chromatography(HIC)

Hydrophobic columns consist of alkyl or aryl ligands, usually immobilised on a base matrix of hydrophilic carbohydrate. No single theory has been proposed to explain HIC. Most are based on the unfavourable entropy associated with water solvating the immobilised hydrophobic ligands and the solvent accessible hydrophobic groups of the protein. In high-salt solutions the hydrophobic protein groups will interact with the immobilised ligands and exclude water. As the salt concentration is decreased, more water is "free" to solvate the protein and ligands, and protein is eluted from the column.

The use of a hydrophobic column provides a useful method for desalting and purifying protein immediately subsequent to ammonium sulphate precipitation (Ziomek *et al.*, 1984). A column of Phenyl Sepharose CL-4B (Pharmacia) 2.5 cm by 10 cm was equilibrated with 100 mM phosphate pH 7.0 containing 50% saturated ammonium sulphate. The protein solution was loaded onto the column and washed with two volumes of the equilibration buffer. The protein was eluted with a gradient from 50%- 0% ammonium sulphate in 100 mM phosphate buffer pH 7.0. The fractions containing cytochrome c_3 were dialysed against two changes of phosphate buffer to remove residual salt prior to the next chromatography step.

Anion exchange column

Ion exchange chromatography uses the difference in net charges between proteins to effect separation. An example is DE-52 which contains diethyl-aminoethyl groups bound to a supporting cellulose matrix. The side groups bear a positive charge and interact specifically with proteins passing down the column. Negatively charged

proteins bind to the amino groups resulting in longer retention times. Neutral and positively charged proteins bind less favourably resulting in short retention times.

DE-52 (Whatman) was equilibrated according to the manufacturer's instructions in 100 mM phosphate buffer pH 7.0. Column dimensions were typically 2.5 cm diameter and 10 cm length. The soluble cell lysate was loaded straight onto the column resulting in a tight red band. Two column volumes of 100 mM phosphate buffer were used to elute impurities before a gradient was set up. Elution of cytochrome c_3 was achieved using a stepwise gradient of 0-250 mM NaCl in 100 mM Phosphate buffer pH 7.0, fractions were collected.

Gel filtration chromatography

Gel filtration chromatography utilises the huge distribution of molecular weights found in proteins. Beads of cross-linked dextran make up the gel and result in a three dimensional network of molecular pores. Buffer carrying protein flows around beads and through the pores. Small proteins can enter the pores but larger ones are excluded. The net result is fast elution of large proteins and retention of smaller ones.

Sephadex G-50 was degassed and packed under gravity in a large column (2 cm diameter, 150 cm length), with 20 mM phosphate buffer pH 7.0. Samples from the previous chromatographic step were too dilute to be directly applied to the column. The fractions with absorbance at around 407 nm were pooled and spun in centricon concentrators (Vivascience) with a molecular weight cut-off of 5000 Da. When the sample volume reached 2 mL, it was loaded onto the column and run with 20 mM phosphate. Once the cytochrome bands reached the end of the column, fractions were collected. The fractions were checked for an oxidised Soret peak at 407 nm and the purest were pooled. Cytochrome c_3 typically eluted after 8 hours.

Hydroxyapatite chromatography

Hydroxyapatite is insoluble calcium phosphate. The mode of action is most likely due to electrostatic effects from the ions present. Instead of single isolated charges (c.f. anion and cation exchangers), the crystalline lattice consists of adjacent positive and negative charges. A simplistic view is that dipole on the protein surface

can interact with dipoles on the lattice surface. Separation is achieved as a result of the different interaction strengths of different proteins.

Hydroxyapatite Bio-Gel (Bio-Rad) was prepared in a slurry following the manufacturers instructions (particular care being taken to remove fine particles). A column of size 2 cm diameter by 10 cm length was poured with 20 mM phosphate pH 7.0 as the starting buffer. The purest fractions from the previous step were diluted with an equal volume of deionised water and loaded onto the column. The column was washed with two volumes of 20 mM phosphate buffer followed by a linear gradient (20 mM-100 mM phosphate). Fractions were collected and assessed by spectrometrically.

2.2.5. Polyacrylamide gel electrophoresis (PAGE)

Tris-Glycine buffer system

A discontinuous buffer system is employed for separation of proteins. The optimal molecular weight range is varied by changing the acrylamide content (%) in the separating gel (see below). Gels were cast in mini-PROTEAN (Bio-Rad) apparatus and all chemicals were electrophoresis grade. Gels were run at 200 V for 45 minutes.

Stock Solutions

- Acrylamide / Bisacrylamide Mix

  Protogel (30 % T, 2.67 % C) Acrylamide, 37.5:1 acrylamide / bis ratio
- 1.5 M Tris-HCl, pH 8.8 (stored @ 4°C)

  Tris base 18.15 g / 100 mL, adjust pH with 1 N HCl
- 0.5 m Tris-HCl, pH 6.8 (stored @ 4°C)

  Tris Base 6 g / 100 mL, adjust pH with 1 N HCl
- 10 % SDS

  Sodium dodecylsulphate 10 g / 100 mL
- 5X Running Buffer (stored @ 4°C)

  Tris base 1.5 g / 100 mL

Glycine 7.2 g / 100 mL

SDS 0.5 g / 100 mL

- 4X Sample Buffer

  Distilled water 4.0 mL

  0.5 M Tris-HCl, pH 6.8

  Glycerol 0.8 mL

  10 % SDS

  2-β-mercaptoethanol

  0.05 % (w / v) bromophenol blue

- TEMED (N, N, N', N'-tetramethylethylenediamine)
- 10 % w/v Ammonium persulphate (made up fresh in dH_20)

4 % Stacking Gel Composition

Solution	**Volume (μL)**
d H_2O	3050
30 % Acrylamide stock	650
0.5 M Tris-HCl	1250
10 % SDS	50
10 % Ammonium persulphate	25
TEMED	5

Variable Separating Gel Composition

	Solution volume (μL) for required % acrylamide gel		
Solution	**10 %**	**12%**	**15 %**
d H_2O	1900	1600	1100
30 % Acrylamide stock	1700	2000	2500
1.5 M Tris-HCl	1300	1300	1300
10 % SDS	50	50	50
10 % Ammonium persulphate	50	50	50
TEMED	2	2	2

Coomassie Staining

Gels were soaked in stain solution for approximately 30 min. and then in destain for 1-3 hours. Prior to drying the gels were soaked in distilled water.

- Gel Stain

  1 g / L Coomassie blue R-250 in 40 % methanol, 10 % ethanoic acid

- Destain

  40 % Methanol, 10 % ethanoic acid

Haem Staining

Haem staining determines the location of cytochrome bands in the gel. The gel was equilibrated in solution 1 for 5 min., then transferred to the TMBZ solution where it was incubated in the dark for 15 min.. The stain was developed by adding 1 mL of 30 % hydrogen peroxide solution. Once sufficient colour had developed, the gel was fixed in solution 1 and soaked in distilled water before drying.

- Solution 1

  0.25 M sodium acetate, pH 5.2 in 30 % aqueous methanol solution

- TMBZ solution

  400 mg / mL TMBZ in solution 1

Tris-Tricine buffer system

The discontinuous tris-tricine system (Schägger & von Jagow, 1987; Schägger, 1994) allows resolution of small proteins of molecular weight 1-100 kDa at a much lower percentage acrylamide in the gel than glycine-SDS-PAGE systems. Resolution of small proteins and peptides is achieved without the inclusion of urea in the gel. The tris-glycine system operates well over a broad range of molecular weight, however proteins below 20 kDa are not separated from the bulk SDS in the stacking gel. The use of tricine overcomes these stacking problems.

A mini-gel system (BIO-RAD mini-PROTEAN II) was used for all experiments. All gels consisted of a stacking gel, a spacer gel and a separating gel. The solutions were made up as detailed below and the APS and TEMED solutions were added to promote polymerisation immediately prior to pouring. The separating gel was poured first to a length of ~4.5 cm and then the spacer gel was carefully layered on top using a syringe, to a length of 1 cm. Distilled water was carefully layered on top of the gel solution to exclude air during polymerisation. After 30 min. the water was removed and the stacking gel was poured and left to polymerise. Samples and markers were prepared by addition of 1/4 volume of sample buffer and heating to 95°C for 5 min. The gel was run in a refrigerator at 4°C with a potential of 150 V across the gel for approximately 3 hours or until the dye front from the loading buffer was at the end of the gel. The gel was stained for approximately 1 hour and then destained for 2 hours.

Stock Solutions

- Acrylamide / Bisacrylamide Mix (store @ 4°C)

  BIO-RAD (40 % T, 3.3 % C) Acrylamide, 29:1 acrylamide / bis ratio
- Anode Buffer, pH 8.9

  0.2 M Tris-HCl
- Cathode Buffer, pH 8.25

  0.1 M Tris-HCl

  0.1 M Tricine

  0.1 % SDS
- Gel Buffer, pH 8.45

  3 M Tris-HCl

  0.3 % SDS
- Sample Buffer (4X)

  30 mL Na-SDS (20 % w/v)

  15 g Glycerol

  0.91 g Tris

  Adjust pH to 6.8-7.0 with HCl

Make up to 47 mL with dH_2O

Dissolve 40 mg Coomassie® blue G

Add 3 mL mercaptoethanol, store at room temperature

- 10 % APS (Ammonium Persulphate) made fresh
- TEMED (N, N, N', N'-tetramethylethylenediamine)
- Gel Stain

  0.025 % Coomassie® Blue G

  10 % Acetic Acid solution
- Gel Destain

  10 % Acetic Acid Solution

Gel Composition

Solution	**Separating Gel (16 %)**	**Spacer Gel (10 %)**	**Stacking Gel (4 %)**
40 % Acrylamide	6 mL	1.5 mL	1.25 mL
Gel Buffer	5 mL	2 mL	3.1 mL
dH_2O	1.5 mL	2.5 mL	8.15 mL
80 % Glycerol	2 mL	———	———
10 % APS	75 µL	30 µL	100 µL
TEMED	7.5 µL	3 µL	10 µL
Total Volume (mL)	15 mL	6 mL	12.5 mL

2.3. REDOX POTENTIOMETRY

Haem group redox potentials were measured using the method of Dutton (1978). A nitrogen atmosphere glove box with oxygen level < 5 ppm was used and temperature was maintained at 25°C . Spectra were recorded with a Shimadzu 1201 spectrometer. Potential were measured with a WPA meter and Russell platinum electrode, containing a silver / silver chloride reference system (potential +196 mV relative to SHE). The electrode was calibrated using the Fe (III) / Fe (II) couple. Mediators were used to aid electron transfer between the protein and the electrode.

Mediators are chosen to give a wide potential span and varied between experiments to ensure that chemical interaction is not occurring. The following were used:

Methyl viologen	MV	-446 mV
Benzyl viologen	BV	-359 mV
Flavin mononucleotide	FMN	-205 mV
Hydroxynapthaquinone	HNQ	-145 mV
Phenazine methosulphate	PMS	+60 mV

A selection of mediators were added to a solution of approximately 2 μM oxidised cytochrome (5-8 mL) in 100 mM phosphate buffer. Mediator concentration was around 20 μM in the working solution. Small volumes of a freshly made sodium dithionite solution (10 mM) were introduced with a microliter syringe, so as to shift the potential downwards a few mV. The spectrum of the haem α and β peaks were recorded after each addition as was the potential. Once the protein had been fully reduced, oxidation was carried out with stepwise additions of potassium ferricyanide (10 mM), to ensure that the process is reversible.

2.4. NMR SPECTROSCOPY (recorded by Dr. Emma Beattie and Lez Holden)

Approximately 0.5 mL of 0.2 mM cytochrome c_3 solution was used, dissolved in 20 mM phosphate buffer, pH 7.0. Pre-saturation of the H_2O peak was required before a 1D pulse sequence was applied. Chemical shifts were assigned relative to the H_2O peak at δ 4.8 ppm.

2.5. EPR SPECTROSCOPY

All measurements were made at 10 K using a Bruker ER 200D spectrometer fitted with a cryostat and helium transfer system (Oxford instruments). Samples contained ~0.2 mM protein in 100 mM phosphate buffer pH 7.0.

2.6. MOLECULAR BIOLOGY

Buffers were made according to standard recipes (Sambrook et al., 1989) and sterilised by autoclaving before use.

2.6.1. Oligonucleotide primers (5' to 3')

PCR

$C_3$1 - CAC GAA TTC GAR TTY CAY GTN GAR ATG

$C_3$2 - GCG AAG CTT YTT NAR NGG YTC NCC

Sequencing

$C_3$3 - GTT TTC ACA GCC ACC

$C_3$4 - CTT CTG CAT CAT TTG C

$C_3$5 - ATA CCT CTT TAT AGG

$C_3$6 - CAT GTA ACT CGA TGG

$C_3$7 - CAA TGC ACT TAG TAG

$C_3$9 - CAA TGT ACT GCG TTA CC

$C_3$10 - GCT GTT ATG TAG CGC TC

$C_3$11 - CCT GGA TGT TAC GAC G

$C_3$12 - ATC ATA TTG ACC TTG CC

$C_3$13 - CTA AGT TGT TAT ATG TG

$C_3$14 - CAG ACT TAC ATT TAG CC

2.6.2. Isolation of the cytochrome c_3 Gene (carried out by Dr. Euan Gordon)

Two PCR primers were designed from protein sequence and codon usage data from known *Shewanella* sequences. Two rounds of PCR were used to amplify the coding sequence from *S. putrefaciens* genomic DNA. The single product obtained was purified and ligated into vector pTZ19r, resulting recombinant clones were sequenced, confirming the fragment identification. Plasmid DNA was used to generate a radioactive probe for a Southern blot. Positive hybridisation was seen with 4kb *NsiI* digested fragments. Bands of this size were purified from a similar gel and ligated into

PstI cut pTZ18r, forming a library. Two positive clones were obtained, these were used to determine the DNA sequence of the insert.

2.6.3. DNA sequencing (carried out in conjunction with Dr. Euan Gordon)

Single stranded DNA preparation

The 4 kb fragment containing the cytochrome c3 gene was inserted into the phagemid vector pTZ18r which has an *f1* origin of replication. Two clones, pEG700 and pEG700r were used for production of all single stranded DNA. The only difference between the two clones is the orientation of the insert. This allowed production of both DNA strands for sequencing.

Bacteria containing the relevant vector were grown to mid-log phase and then infected with helper phage M13 KO7 (m.o.i.~1) and shaken for 1 hour at 37°C. 400μL of infected culture was added to a 250 mL flask with selective medium (10 mL) containing 70 μg / mL kanamycin for selection of phage uptake. The culture was shaken vigorously overnight at 37°C.

A microcentrifuge tube filled with 1.5 mL of culture was spun at 13000 x g for 5 minutes to remove cells. To precipitate the phage, 1.2 mL supernatant was added to 0.3 mL of 2.5 M NaCl / 20 % PEG 8000. The solution was mixed and incubated at room temperature for 15 min. before centrifugation, 5 min. at 13000 x g. All supernatant was removed and the pellet was resuspended in 100 μL of TE buffer. The solution was extracted with 50 μL phenol:chloroform:isoamyl alcohol (25:24:1) mixture and then with 50 mL chloroform:isoamyl alcohol (25:1) mixture. To precipitate the DNA, 0.1 volume sodium acetate (pH 5.2) and 3 volumes of ethanol were added, followed by incubation at -20°C for 1 hour. A DNA pellet was obtained after centrifugation, 13000 x g for 10 min. at 4°C. The pellet was washed with 80 % ethanol from the freezer, dried and suspended in 50 μL TE buffer ready for use.

Manual Sequencing Reactions

Sequencing of single stranded DNA was achieved using the Sequenase™ Version 2.0 kit (Amersham). The primers used for sequencing are listed in Section 2.6.1. The procedure consists of three steps. Firstly, primers are annealed to the single stranded template. Secondly, the primers are extended and radio-label is incorporated into the DNA. Finally, the inclusion of dideoxy nucleotide of a single type causes the extension reaction to stop at the location of that base.

To anneal primer and template, 1 μg of ~3 ng μL^{-1} solution was added to 7 μL of template (approximately 1 μg DNA) and 2 mL of 5 x reaction buffer (200 mM Tris-HCl, pH 7.5; 100 mM $MgCl_2$; 250 mM NaCl) and heated to 65°C for 2 min. in a water bath. The mixture was allowed to cool slowly and iced, once it had reached 35°C.

For DNA labelling, the following were added to the 10 μL annealing mixture: 1 x labelling mix (1.3 μM each dGTP, dTTP, dCTP), 5 μCi [α-^{35}S]dATP, 1 μL 0.1 M DTT, 0.5 units Sequenase enzyme in enzyme dilution buffer (10 mM Tris-HCl pH 7.5, 5 mM DTT, 0.5 mg / mL BSA). The mixture was incubated at room temperature or below for 5 min..

The four termination reaction mixtures contained ddATP, ddCTP, ddGTP and ddTTP (2. 5 μL) in pre-warmed tubes at 37-45°C, to which 3.5 μL of labelled DNA was added. After 5 min., 4 μL of STOP solution (98 % formamide, 10 mM EDTA pH 8, 0.025 % xylene cyanol, 0.025 % bromophenol blue) was added. The reactions were used immediately or stored at -20°C. For sequences with high G-C ratio, termination mixes containing dITP instead of dGTP were used.

- dGTP Termination Mixtures

ddTTP- 80 μM dTTP, dCTP, dGTP, dATP, 8 μM ddTTP, 50 mM NaCl

ddCTP- 80 μM dTTP, dCTP, dGTP, dATP, 8 μM ddCTP, 50 mM NaCl

ddGTP- 80 μM dTTP, dCTP, dGTP, dATP, 8 μM ddGTP, 50 mM NaCl

ddATP- 80 μM dTTP, dCTP, dGTP, dATP, 8 μM ddATP, 50 mM NaCl

- dITP Termination Mixtures

ddTTP- 80 μM dTTP, dCTP, dITP, dATP, 8 μM ddTTP, 50 mM NaCl

ddCTP- 80 μM dTTP, dCTP, dITP, dATP, 8 μM ddCTP, 50 mM NaCl

ddITP- 160 μM dITP, 80 mM dTTP, dCTP, dATP, 1.6 μM ddITP, 50 mM NaCl

ddATP- 80 μM dTTP, dCTP, dITP, dATP, 8 μM ddATP, 50 mM NaCl

2.6.4. Denaturing polyacrylamide gel electrophoresis

Gel solutions (60 mL) consisted 6 % acrylamide, 8 M urea dissolved in TE buffer (10 mM Tris-HCl, 1 mM EDTA pH 8.0). Glass plates were carefully cleaned, one plate was silanised and they were clamped with 0.4 mm spacers. The gel was polymerised with 10 % ammonium persulphate (150 μL) and TEMED (150 μL) and left to set for 1 hour. The gel was clamped vertically in a BRL sequencing tank, immersed in TE buffer and run at 60 W for 1 hour to pre-warm. The samples were denatured by heating to 75°C for 2 min., loaded onto the gel and run at 60W.

Once electrophoresis was complete, the gel was transferred to a sheet of filter paper and soaked in 15 % methanol / 5 % acetic acid for 5 min. to remove urea. The gel was dried at 80°C and autoradiography was performed in direct contact with the film at room temperature.

Sequencing compressions were resolved by adding 40 % formamide to the standard gel mixture.

2.6.5. Sequence Analysis

All sequencing data was analysed using the GCG version 9.0 program (University of Wisconsin).

Part 1-Cytochrome c_3

Chapter 3 : *RESULTS AND DISCUSSION*

3.1. PROTEIN PURIFICATION AND CHARACTERISATION

3.1.1. Introduction

Shewanella putrefaciens can utilise an unparalleled variety of terminal electron acceptors when respiring anaerobically. As was stated in Chapter 1, *Shewanella* synthesizes a large number of *c*-type cytochromes during anaerobic respiration. A previous study attempted to identify the cytochromes produced in response to different terminal acceptors by *Shewanella* NCIMB400 (Morris, 1987). One of the *c*-type cytochromes made in response to anaerobiosis is flavocytochrome c_3. Flavocytochrome c_3 functions as a respiratory fumarate reductase and consists of a haem and flavin domain. The smaller domain contains four bis-histidine ligated haems with low redox potentials (Pealing *et al.*, 1995). The haem domain has similar biophysical properties to the *Desulfovibrio* cytochromes c_3, but shows little sequence similarity with them.

Morris also observed a cytochrome which bound very tightly to anion exchange columns. However, little further analysis of this protein was carried out. It appears that this protein is a low molecular weight cytochrome c_3 which is related to the cytochrome domain of flavocytochrome c_3. We have identified the gene which encodes this cytochrome c_3 from *Shewanella* NCIMB400 and cloned it. We have purified the protein to homogeneity and carried out a biochemical and biophysical studies of it. The cytochromes c_3 were until recently, thought to be prevalent only in the strictly anaerobic, sulphate-reducing bacteria. However, they have now been identified in more diverse bacteria such as the purple phototrophic bacterium H1R (Ambler, 1991). A cytochrome c_3 has also been identified in the *Shewanella putrefaciens* MR-1 strain (Tsapin *et al.*, 1996). A typical purification table for cytochrome c3 is shown in figure 3.1.

Figure 3.1.: Purification table for cytochrome c_3 based on 100g wet weight of *Shewanella* NCIMB400. Cytochrome c_3 concentration based on absorbance measurements taken at 407 nm.

Step	Total c_3 (mg)	Ratio (A_{407} : A_{280})	Yield (%)	Purification factor
Cell lysate	15.4	0.149	100	1
Phenyl sepharose	13.2	1.0	86	6.7
DE-52	10.3	4	67	26.9
Gel filtration	6.2	10.8	40	72.5
Hydroxyapatite	2.3	16	16	107.4

3.1.2. Molecular weight determination

3.1.2.1. Polyacrylamide gel electrophoresis

Denaturing polyacrylamide gel electrophoresis is a useful technique for determining the molecular weight of proteins. The protein sample is treated with SDS, heat and a reducing agent in order to fully denature it. SDS molecules induce protein is unfolding and bind to it. Approximately one SDS molecule binds for every two amino acids, giving the protein a large net negative charge. When the SDS-protein complex is run through a cross-linked acrylamide gel matrix (using an applied electric field), separation of different sized proteins is effected. The mobility of a protein is generally proportional to the log of its molecular weight. Proteins used as molecular weight markers are chosen because they follow this behaviour. However, ideal behavior is not always observed for a variety of reasons. *Shewanella* NCIMB400 cytochrome c_3 does not migrate as a single tight band on gels run with either tris-tricine or tris-glycine buffer. Instead we see a broad band at around 16000 Da. This behaviour is probably a result of incomplete unfolding of the protein due to the 16 linkages (8 thioether and 8 iron ligands) between the backbone and the four haems. This structural stability would not allow typical denaturation with the SDS, perhaps resulting in a lower net charge and unexpectedly low mobility. There could also be a strong tendency for this small protein to refold.

3.1.2.2. Electrospray mass spectrometry

Electrospray ionization is a particularly effective method for analysing small proteins and polymers. The technique is very sensitive and detection limits in the sub-femtomole range have been obtained. Electrospray spectra can yield molecular masses for proteins because the ionisation method is capable of attaching many charges to large molecules. The net result is that a polypeptide of molecular mass 60000 Da with, 30-60 net positive charge, has a mass-to-charge ratio (m/z) of 1000-2000 which is well within the mass range of most modern spectrometers. From Figure 3.2. and Figure 3.3., the molecular mass of the major peak is 11778 Da. This is in excellent agreement with the calculated mass from the protein sequence, plus four haems (see

later). The results from the mass spectra support the hypothesis that the molecular weight determined by gel electrophoresis is anomalous.

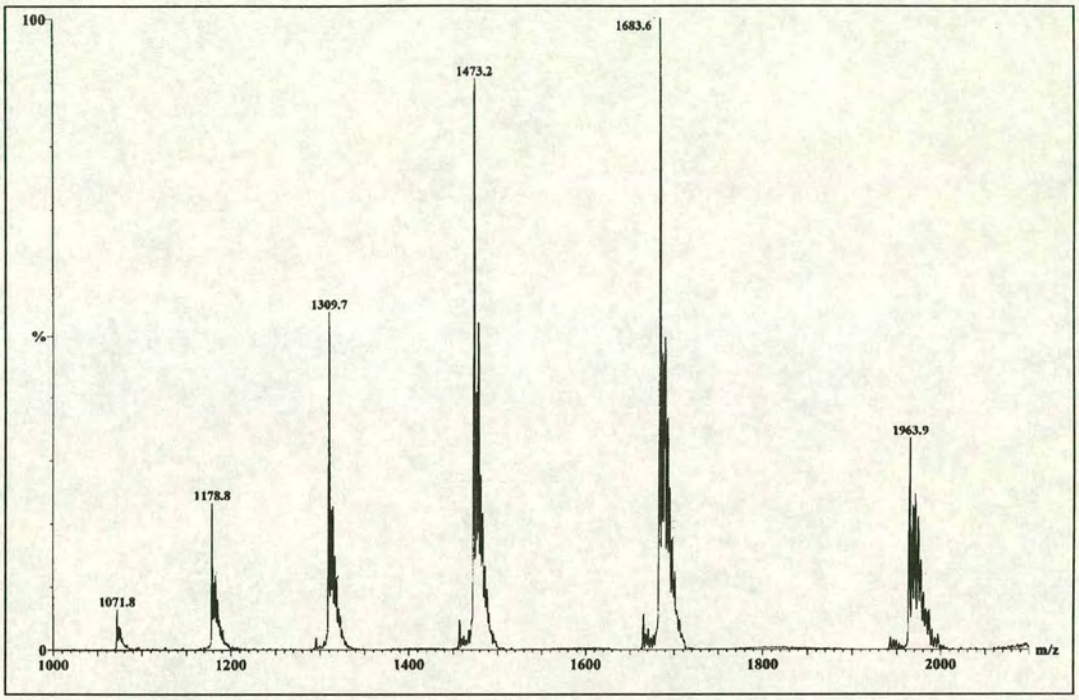

Figure 3.2. : Mass spectrum of the cytochrome c_3 sample showing mass to charge ratios. The peaks correspond to protein molecules with net charge ranging from 11(far left) to 6 (far right).

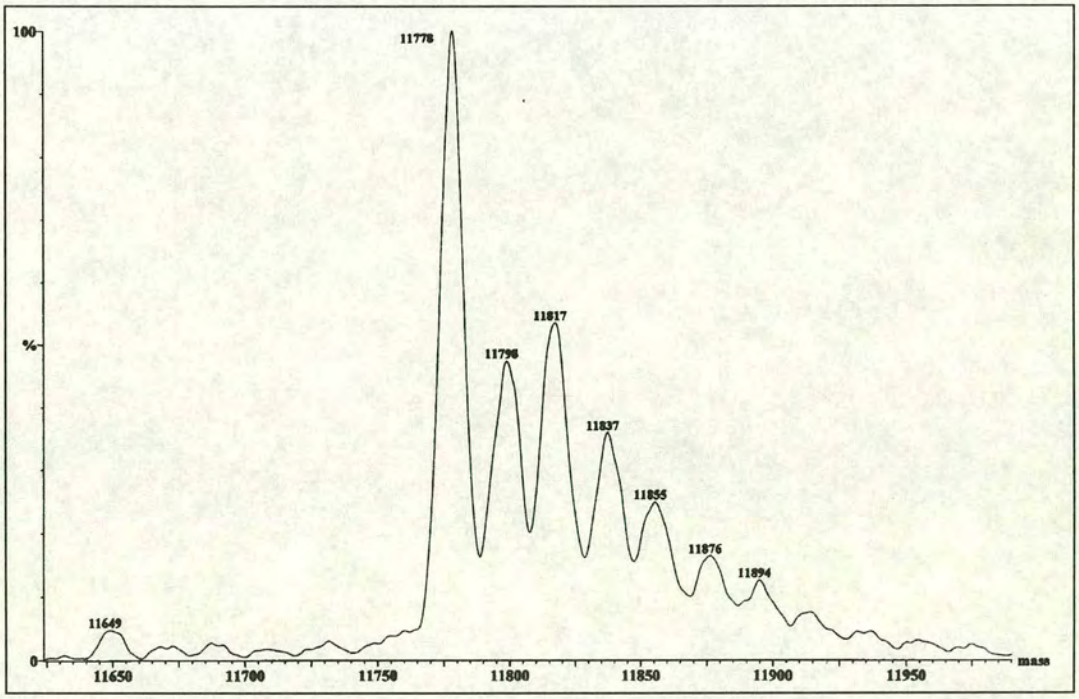

Figure 3.3. : Mass spectrum showing molecular weight values yielded by analysis of Figure 3.1.

3.1.3. Redox potentiometry

The macroscopic redox potentials of cytochromes c_3 from a number of sources have been measured using EPR, NMR, cyclic voltammetry and spectroscopic titrations (see Section 1.4.4.). The potentials of the different cytochromes c_3 show a very considerable variation. This is in spite of the highly conserved haem-core architecture in the structures solved so far. For example, cytochrome c_3 from *Desulfomicrobium baculatum* has potentials spanning over 200 mV, ranging from -165 to -400 mV (Bianco & Haladjian, 1981). *Desulfovibrio gigas* cytochrome c_3, on the other hand, has potentials which span less than 100 mV from -235 to -315 mV (Cusanovich *et al.*, 1994).

The spectra in Figure 3.4. were obtained for the α/β region of the *S. putrefaciens* cytochrome c_3 spectrum during a redox titration and are corrected to allow for concentration changes (due to evaporation) during the experiment. The absorbance data were summed and averaged over the region between the two isosbestic points at 510 and 560 nm, rather than using a single wavelength value. It was assumed the protein was fully oxidised (or reduced) when no further spectral change was seen on addition of oxidant (or reductant). The data are shown in Figure 3.5. Using the non linear least squares method, the data was fitted to an equation containing two Nernst functions with Microcal Origin. This yields macroscopic midpoint potentials, with values of -58 ± 10 and -200 ± 10 mV (relative to SHE). We attempted to fit the data to a function containing four Nernst equations but found it fitted badly and yielded two pairs of potentials. The pairs of potentials were almost identical to those obtained from the two Nernst equation function.

Similar redox behaviour was observed for the four haems of flavocytochrome c_3, which titrate in a pairwise fashion, at approximately -220 and -320 mV (Morris *et al.*, 1994). The haem potential values determined for cytochrome c_3 are higher than those for flavocytochrome c_3. A recent re-examination of flavocytochrome c_3 gave potentials closer to, but still lower than those of cytochrome c_3 (M. Doherty - personal communication). The differences in potential are not entirely suprising. Flavocytochrome c_3 has a large flavin domain bound to the cytochrome domain and shows differences in its amino acid sequence.

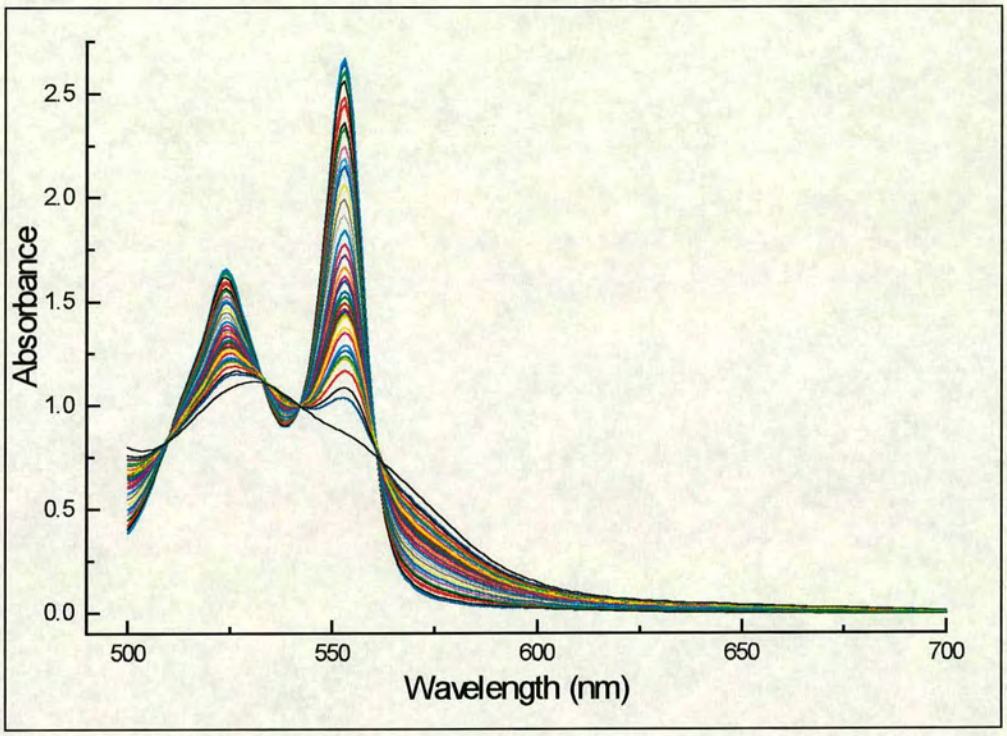

Figure 3.4. : Spectra obtained during a redox titration of cytochrome c_3, performed as described in materials and methods section.

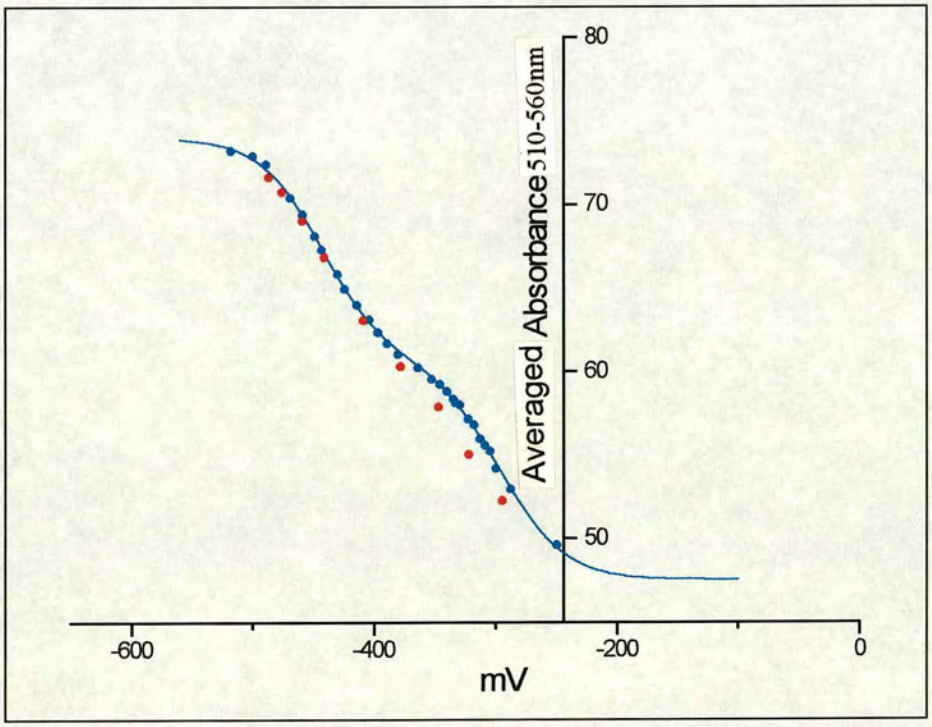

Figure 3.5. : Data from a redox titration of cytochrome c_3; points in blue correspond to reduction with sodium dithionite, points in red correspond to oxidation with potassium ferricyanide. The blue trace is fitting of the data to two Nernst equations. All potential values are relative to the calomel electrode (*i.e.* SHE -244 mV)

The cytochrome c_3 from *Desulfobulbus elongatus,* the haems appear to titrate in two stages (Samain *et al.*, 1986). The first stage corresponds to one haem and the second, to the remaining three haems (based on the magnitude of the spectral change).

It is apparent from NMR and EPR titrations that many of the cytochromes c_3 have closely spaced redox potentials. In cyclic voltammetry and pulse polarography experiments, different numbers of haem potentials are resolved for some cytochromes c_3 (Bruschi *et al.*, 1984; Niviere *et al.*, 1988). Four distinct potentials have never been resolved using theses techniques Although our data fit well to the equation describing two pairs of potentials, it is possible that cytochrome c_3 for *S. putrefaciens* has four discrete redox potentials.

3.2. SPECTROSCOPIC TECHNIQUES

3.2.1. Optical spectroscopy

This technique monitors transitions between different electronic states. Most electronic transitions observed in the visible region are between haem π bonding and π anti-bonding orbitals or between ligand and iron (charge transfer or CT transitions). In the UV region of the spectrum, most transitions are due to movement of electrons between ligand π bonding and π anti-bonding orbitals. Other contributions to the spectrum come from aromatic amino acids (tyrosine, tryptophan and phenylalanine). The absorption of the haem dominates the spectra. The characteristic haem absorptions (in order of increasing energy) are named α, β & γ (or Soret) bands. The very intense Soret band usually lies between 390 nm and 430 nm and the α & β bands lie between 500 and 600 nm. Each class of cytochrome has a characteristic spectrum. The exact position of absorption peaks due the haem aromatic system are affected by the ligation, and hence spin state, of the iron and by the substituents on the haem. The spectrum in Figure 3.6. shows peaks at positions, consistent with other cytochromes c_3.

The oxidised and reduced spectra of *S. putrefaciens* cytochrome c_3 are shown in Figure 3.6. The oxidised Soret peak lies at 407 nm and the oxidised α/β band lies at 532 nm. The reduced Soret band lies at 417.5 nm and the α & β bands lie at 551.5 nm and 521.5 nm respectively.

Two methods were used to estimate an extinction coefficent for the haem Soret peak. The first is based on a theoretical value extinction coefficient calculated from the contribution of the aromatic amino acids and per haem at 280 nm. The program, protparam at http://expasy.hcuge.ch/chi-bin/protparam, gives a protein only extinction coefficient of 1280 M^{-1} cm^{-1}. The haem contribution was calculated using the extinction per haem of 13850 M^{-1} cm^{-1} (Moore & Pettigrew, 1990). This yields an overall coefficient of ε_{280}=56680 M^{-1} cm^{-1}. Using this value an extinction coefficient of $\varepsilon_{417.5}$=793500 M^{-1} cm^{-1} was calculated for the reduced Soret peak. The second method used the bicinchoninic acid assay method to quantitate the protein concentration. BSA (bovine serum albumin) was used as a standard. The extinction coefficient for the reduced Soret band was calculated as 507700 M^{-1} cm^{-1} based on the protein concentration.

The value obtained using BSA as a standard is prone to quite a large error. The standard does not even contain the same chromophores and the experiment may give different results if cytochrome *c* were used as a standard. However the two results lie within the same order of magnitude. The value based on theoretical contributions from each chromophore lies close to that determined for *Shewanella* NCIMB400 flavocytochrome c_3 (Morris *et al.*,1994)

The sequence for *Shewanella* NCIMB400 cytochrome c_3 contains three methionine residues which could act as axial ligands to iron. However, the absence of the characteristic band at 695 nm eliminates this possibility. Also, the methionines could only provide a maximum 3 of the total 8 ligation to haems. Since only one type of haem is seen by UV-visible, EPR and resonance Raman spectroscopy, heterogeneity of ligands is unlikely. The most likely ligands to the haem irons are the eight histidine residues present in the protein.

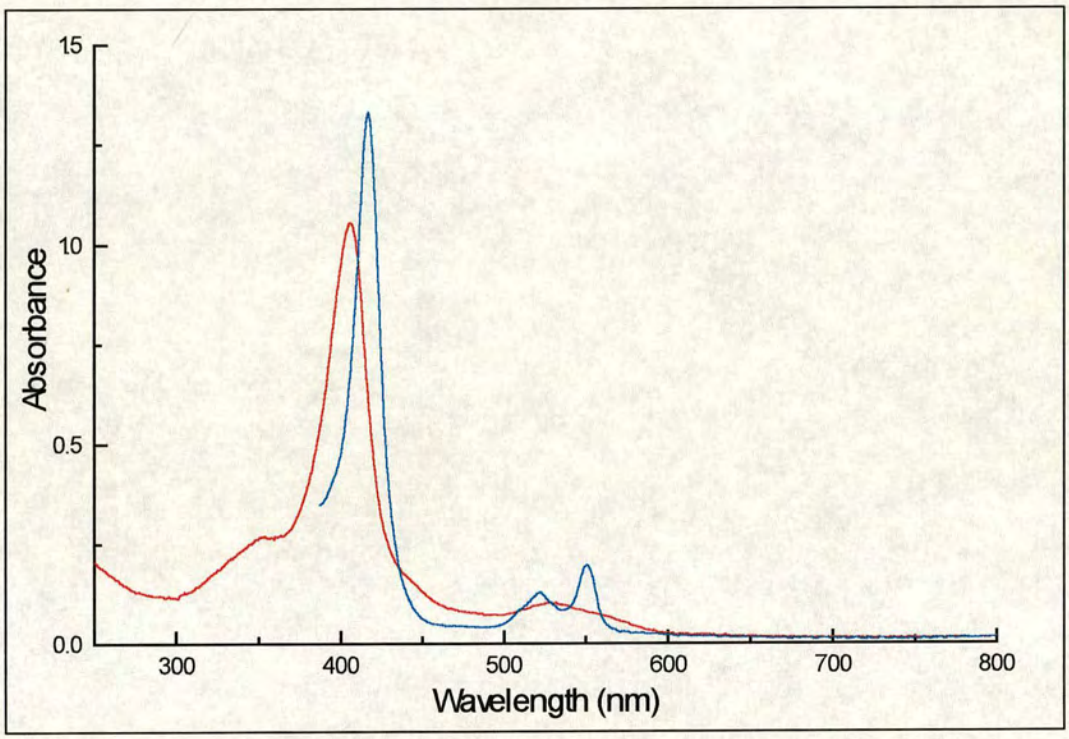

Figure 3.6. : UV-visible absorbtion spectrum of the oxidised (red trace) and reduced (blue trace) states of cytochrome c_3. Reduction was performed with sodium dithionite which has a large spectral contribution below 350 nm.


EX BIBL UNIV. GRONINGEN

3.2.2. NMR spectroscopy (Spectra run by Dr. Emma Beattie and Lez Holden.)

NMR studies of proteins are usually restricted to small soluble proteins because of problems such as signal strength and line broadening in large molecules. Large protein molecules in solution have slow tumbling rates, which enhance relaxation processes and result in large linewidths. The problems of enhanced relaxation are also encountered in proteins containing paramagnetic centres, *i.e.* unpaired electrons (Moore & Pettigrew, 1990). Paramagnetic centres cause through-bond and through-space (or dipolar) relaxation effects. As a result, the haem and axial ligand resonances are most strongly affected. The broadening generally increases with the number of unpaired electrons present and is particularly pronounced in high spin cytochromes such as cytochrome *c'*. A further effect induced by paramagnetic centres is an increase of the spectral width. Most resonances found in proteins usually occur in the -2 to 10 ppm region (hence the cluttered nature of one dimensional protein NMR spectra). However, paramagnetic centres induce large shifts of up to 100 ppm or more.

Cytochromes c_3 are, in fact, ideal proteins for NMR studies. This fact is reflected in the proliferation of literature (*e.g.* Moura *et al.*, 1977; McDonald *et al.*, 1974; Park & Kang, 1996a; Salgueiro *et al.*, 1997a & b - and references therein) on the subject. The proteins are very soluble allowing them to be used at high concentrations. The low molecular weight (12-14 kDa) of the proteins means that the tumbling rate in solution is fast. Hence, relaxation rates are relatively slow, leading to narrow linewidths. The bis-his ligation of the haem iron make it low-spin. This means that, a fully oxidised cytochrome c_3 containing four d^5 configuration iron atoms, has four unpaired electrons. The effects on chemical shift, like the relaxation effects are most pronounced in the haem and axial ligand resonances. The one dimensional ^{1}H-NMR spectra of oxidised cytochromes c_3, typically have haem methyl resonances shifted as far as 35-40 ppm.. *Shewanella* NCIMB400 cytochrome c_3 is no exception as can be seen in Figure 3.7.

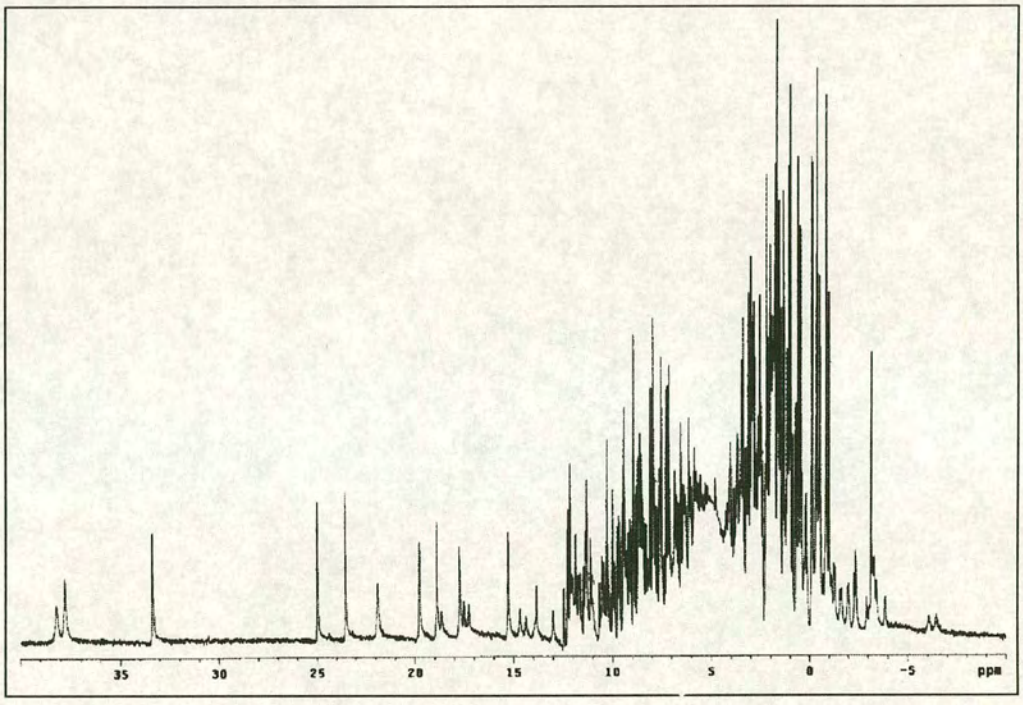

Figure 3.7. : One-dimensional ^{1}H nuclear magnetic resonance spectrum of *Shewanella* NCIMB400 cytochrome c_3

3.2.3. EPR spectroscopy (Run by Dr. W. J. Ingledew - St. Andrews University)

Electron paramagnetic resonance spectroscopy detects unpaired electrons. The magnetic moments of electrons are much larger than for nuclei. As a result much lower magnetic field strengths are required for EPR than for NMR. The technique is sensitive to the distribution of electrons around the paramagnetic centre and hence structural data can be inferred. The different haems in a molecule of cytochrome c_3 are characterised by g tensors which have only slight differences. This results in an important overlap between the spectra relative to each haem (Gayda *et al.*, 1988). For EPR redox titrations spectral simulations are used to resolve the individual peaks.

As has already been noted, fully oxidised or ferricytochrome c_3 contains four paramagnetic haems per protein molecule. The spectrum of the protein in the oxidised state is shown in Figure 3.8. A single set of g-values at $g_x = 1.53$, $g_y = 2.22$ and $g_z = 2.83$ is observed for *S. putrefaciens* cytochrome c_3. These values lie well within the range commonly observed for low spin, six coordinate, bis-histidine ligated haemoproteins (Walker *et al.*, 1984). The spectrum obtained for *Dsm. baculatum* cytochrome c_3 in the fully oxidised state has peaks at $g_x = 1.52$, $g_y = 2.28$ and $g_z = 2.95$ and similar peak shapes to *Shewanella* NCIMB400 cytochrome c_3 (Gayda *et al.*, 1988).

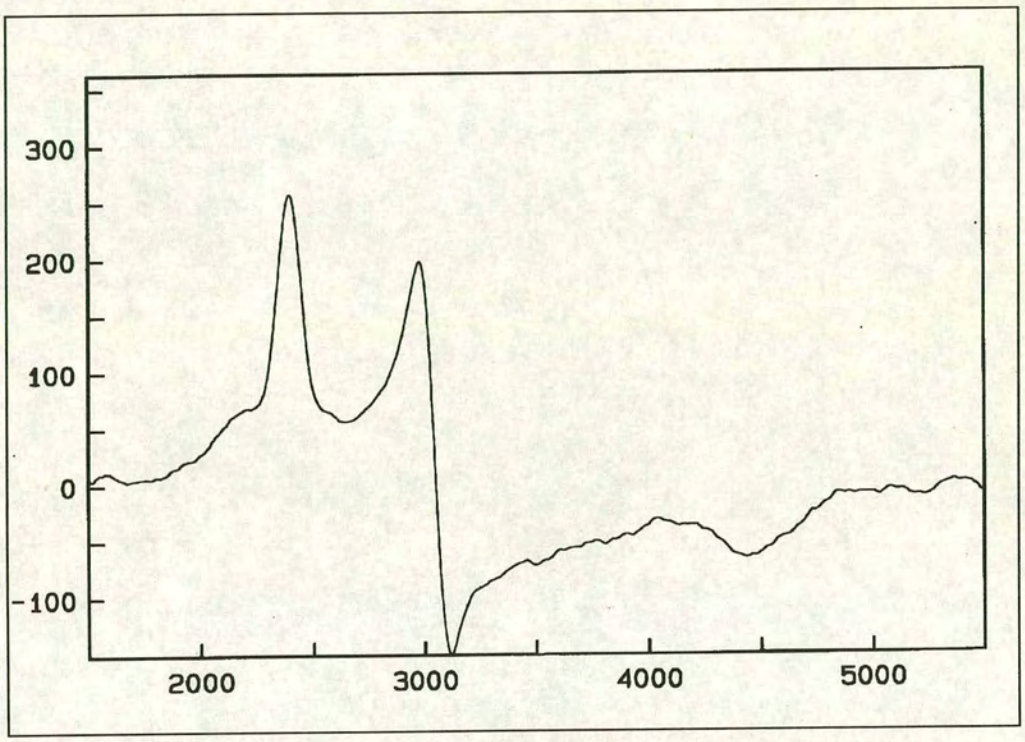

Figure 3.8. : Electron paramagnetic resonance of *Shewanella* NCIMB400 cytochrome c_3 obtained at 10 K. A single set of signals are observed, comprising; g_z=2.83, g_y=2.22 & g_x=1.53.

3.2.4. Resonance Raman spectroscopy (Spectra run by Dr. Luca Quaroni - Dept. of Pure and Applied Chemistry, Strathclyde University)

Resonance Raman spectroscopy is a vibrational technique which has been used extensively in the study of haemoproteins. The technique involves irradiating the molecule under study with monochromatic light at a frequency corresponding to an electronic transition using a laser. The electronic transitions used are usually the α, β and Soret bands of the haem. In practice, the excitation values used are limited by the available laser lines. The laser frequency of 514.5 nm is commonly used, even though it does not correspond exactly to an absorption maximum of the haem. When a protein is excited at or near the absorption maximum of haem, the resulting haem signals will be much more intense than other backbone contributions. The resulting spectrum thus gives information about the haem; the oxidation state, the axial ligation and the spin state.

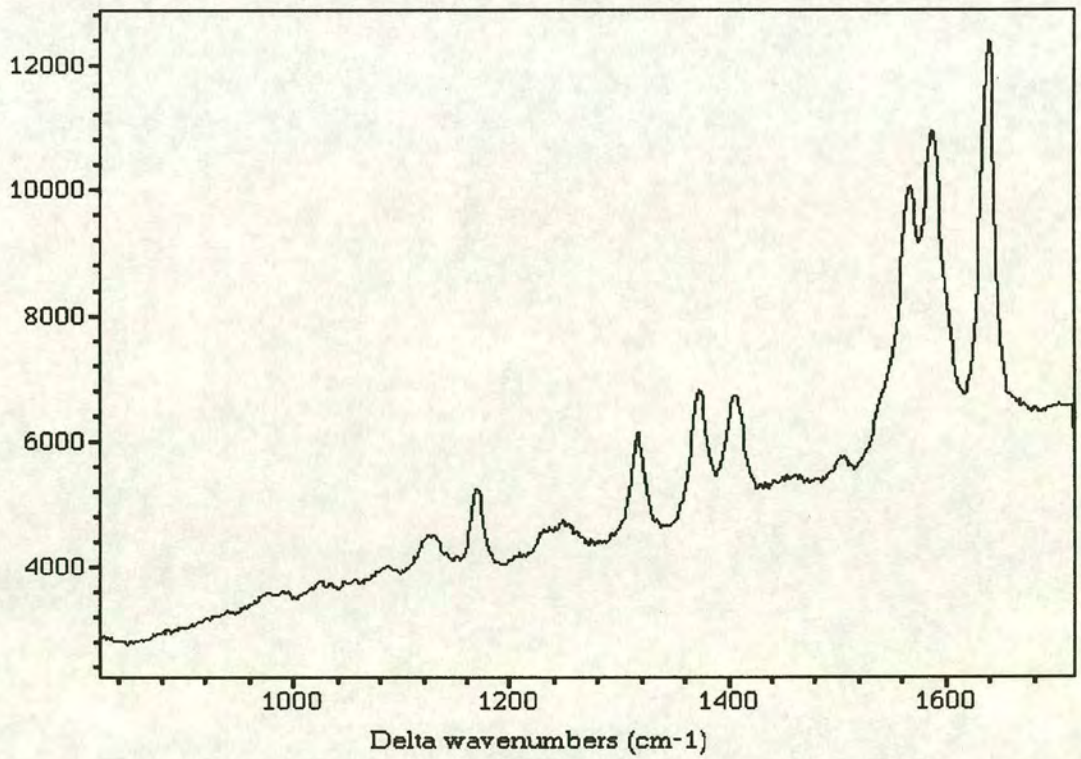

Figure 3.9. : Resonance Raman spectrum of *Shewanella* NCIMB400 cytochrome c_3 obtained by irradating with laser light at 514.5 nm.

A number of bands which are characteristic markers of the haem spin and oxidation state, are found in the 1300-1700 cm^{-1} region of the spectrum for cytochromes c_3 (Kazanskaya *et al.*, 1996). The stretching frequencies are seen at distinct and different positions in the fully oxidised states. Splitting of the main bands at intermediate oxidation states has been reported for *Desulfovibrio vulgaris* (Miyazaki), (Verma *et al.*, 1988) but not for *Desulfovibrio vulgaris* (Hildenborough) and *Desulfomicrobium baculatum* (Norway 4), (Kazanskaya *et al.*, 1996).

The spectrum of oxidised *Shewanella* NCIMB400 cytochrome c_3 is shown in Figure 3.9. The observed stretching frequencies are compared with those obtained for oxidised *D. vulgaris* (Miyazaki) in table 1. The NCIMB400 bands lie very close to those from the other two proteins. The presence of the oxidation state marker at 1373 nm indicates that the haem is in the Fe^{3+} state. The position of the spin-state sensitive bands (ν_2) and (ν_3) at 1588 nm and 1506 nm respectively, indicate that all 4 haems are low spin. The spin-state / coordination-state marker 1639 nm confirms that the protein is six coordinate and low-spin.

Table 1: Stretching frequencies determined for *Shewanella* NCIMB400 cytochrome c_3 using Resonance Raman spectroscopy compared with two other cytochrome c_3 (using the nomenclature of Abe *et al.*, 1978).

Stretching Mode	*Shewanella* cyt c_3	*D. v* (M) cyt c_3	*D.v* (H) cyt c3
ν_{10}	1639	1636	1637
ν_2	1588	1585	1587
ν_{11}	1566	1566	1565
ν_3	1506	1506	not given
ν_{29}	1406	1409	1407
ν_4	1373	1374	1374
ν_{21}	1317	1319	not given

Values for *D.v* (M), *D. vulgaris* (Miyazaki) cytochrome c_3 taken from Verma *et al.*, 1988; values for *D.v* (H), *D. vulgaris* (Hildenborough) taken from Kazanskaya *et al.*, 1996.

3.3. CLONING AND SEQUENCING THE CYTOCHROME c_3 GENE

The gene encoding cytochrome c_3 was cloned by Dr. Euan Gordon (ICMB, University of Edinburgh) using PCR primers designed on the basis of amino acid analysis data to create a library probe, as described in the methods section. Sequence was obtained using the dideoxy chain-termination method. The plasmid (pEG700) construct containing a 4 kb insert from the *Shewanella* NCIMB400 genome was used to generate single stranded template DNA.

3.3.1. Sequence analysis

In Figure 3.10 we can see the amino acid sequence translated from the the gene sequence for *Shewanella* NCIMB400 cytochrome c_3, *cctA*. A putative periplasm directing leader sequence is also indicated in Figure 3.10. A leader sequence is common to all of the known cytochromes c_3 which are known to be exported into the periplasm (LeGall & Peck, 1987). The coding region is 333 bp long and the signal sequence indicated is 25 amino acids in length. There are three consecutive ATG codons within the putative signal sequence. However, initiation from any of these sites does not give an N-terminal secretory sequence characteristic of periplasmic proteins. It appears most likely that translation initiates at a GTG codon; this is a low usage start codon. Although GTG encodes valine when it is within a coding sequence, it is translated as an N-formyl methionine when it is the initiator codon. The resulting signal sequence which is shown in magenta in Figure 3.10 has a long hydrophobic region and a basic N-terminus (Nielson *et al.*, 1997). A putative ribosome binding site, shown in Figure 3.10, lies just 9 bp from the GTG codon which is consistent with it being the site of translation initiation. Immediately downstream from the stop codon is an invert repeat region (shown by arrows in Figure 3.10.)which is common in bacterial Rho-independent transcriptional terminators, implying that *cctA* is not cotranscribed with any other coding sequence.

Downstream from the *cctA* gene is a second coding sequence in the same orentation. The sequence encodes a putative protein product similar to the molybdenum containing nitrate and formate reductases. The reading frame is

particularly closely related to the assimilatory nitrate reductases (41% identical with a cyanobacterial sequence, Figure 3.11 A). Assimilatory nitrate reductases are cytoplasmically located enzymes involved in the utilisation of nitrate as a nitrogen source. The initiation codon for the nitrate reductase lies 285 bp downstream of the *cctA* termination codon. Upstream of *cctA* is another reading frame, again in the same orientation. This coding sequence shows extensive similarity with the 3-hydroxyisobutyrate dehydrogenases (31% identical with *E. coli* sequence, Figure 3.11. B). In bacteria, these cytoplasmic NAD-dependent enzymes are required for valine catabolism. The coding sequence lies 395 bp away from the *cctA* gene.

As no function has yet been ascribed to this cytochrome c_3, any sequence information is potentially useful. In bacteria, genes with related function are often (but not always) located together as an operon. The operon has a single promoter site and results in a single, polycistronic mRNA transcript molecule. This means all of the genes can be expressed simultaneously. Related genes are not always nested together in an operon. This appears to be the case with *Shewanella putrefaciens* cytochrome c_3. The two coding sequences flanking *cctA* are clearly unrelated to anaerobic respiration and neither of them have periplasm directing signal sequences. It is likely that *cctA* is transcribed as a monocistronic RNA and so no information about its physiological function can be inferred from neighbouring sequences.

Figure 3.10. : The sequence determined for the cloned fragment of the *Shewanella putrefaciens* genome, containing the cytochrome c_3 gene, *cctA*. The cytochrome c_3 protein sequence is shown in red with the putative periplasm directing leader sequence indicated in magenta. The underlined region of protein sequence has also been obtained from amino acid sequencing. The putative ribosome binding site is shown in uppercase as are the sequences similar to the Rho-independent terminator. Two other coding sequences with the same orientation as the cctA gene are indicated in light blue (see section 3.3.1.).

```
    aaccgcttcagcagatgttgcacgtgaaattgccgcgtacattgagccacttaacatcgc
  1 ---------+---------+---------+---------+---------+---------+ 60
    ttggcgaagtcgtctacaacgtgcactttaacggcgcatgtaactcggtgaattgtagcg
     T  A  S  A  D  V  A  R  E  I  A  A  Y  I  E  P  L  N  I  A

    attcttagacgcgccagtttcaggtggtcaagccggtgccgaaaatggtgcgttaacggt
 61 ---------+---------+---------+---------+---------+---------+ 120
    taagaatctgcgcggtcaaagtccaccagttcggccacggcttttaccacgcaattgcca
     F  L  D  A  P  V  S  G  G  Q  A  G  A  E  N  G  A  L  T  V

    gatgatgggtggtgaccaagctcattttgatactgttaaacccgtcatatcggcatacag
121 ---------+---------+---------+---------+---------+---------+ 180
    ctactacccaccactggttcgagtaaaactatgacaatttgggcagtatagccgtatgtc
     M  M  G  G  D  Q  A  H  F  D  T  V  K  P  V  I  S  A  Y  S

    ctgcgctgaattgttagggccagttggggcggggcagttgactaaaatggttaaccaaat
181 ---------+---------+---------+---------+---------+---------+ 240
    gacgcgacttaacaatcccggtcaaccccgccccgtcaactgattttaccaattggttta
     C  A  E  L  L  G  P  V  G  A  G  Q  L  T  K  M  V  N  Q  I

    ttgtattgctggtgtagtgcaaggcctcgcagagggacttcattttgctaaaagtgctgg
241 ---------+---------+---------+---------+---------+---------+ 300
    aacataacgaccacatcacgttccggagcgtctccctgaagtaaaacgattttcacgacc
     C  I  A  G  V  V  Q  G  L  A  E  G  L  H  F  A  K  S  A  G

    tttagatggcttaaaagtgattgaagtgatcagcaaagggcgggcacaaagctggcagat
301 ---------+---------+---------+---------+---------+---------+ 360
    aaatctaccgaattttcactaacttcactagtcgtttcccgcccgtgtttcgaccgtcta
     L  D  G  L  K  V  I  E  V  I  S  K  G  R  A  Q  S  W  Q  M

    ggaaaatcgctataaaacgatgtggcaaggtcaatatgattttggttttgctatcgattg
361 ---------+---------+---------+---------+---------+---------+ 420
    ccttttagcgatattttgctacaccgttccagttatactaaaaccaaaacgatagctaac
     E  N  R  Y  K  T  M  W  Q  G  Q  Y  D  F  G  F  A  I  D  W

    gatgcgtaaagatttgggtattgcattagatgaagcccgtcgtaatggtagccatttacc
421 ---------+---------+---------+---------+---------+---------+ 480
    ctacgcatttctaaacccataacgtaatctacttcgggcagcattaccatcggtaaatgg
     M  R  K  D  L  G  I  A  L  D  E  A  R  R  N  G  S  H  L  P

    ggtagccgcattagttgatcaattttattctgaagttcaagcaatgaaaggtaatcgctg
481 ---------+---------+---------+---------+---------+---------+ 540
    ccatcggcgtaatcaactagttaaaataagacttcaagttcgttactttccattagcgac
     V  A  A  L  V  D  Q  F  Y  S  E  V  Q  A  M  K  G  N  R  W

    ggatacttctagtttacttgctcgcttagaaaagtctcgcagttaatataaacactaagt
541 ---------+---------+---------+---------+---------+---------+ 600
    cctatgaagatcaaatgaacgagcgaatcttttcagagcgtcaattatatttgtgattca
     D  T  S  S  L  L  A  R  L  E  K  S  R  S  *  Y  K  H  *  V

    tgttatatgtgtaaatgtagccccaatatcgattggggctttttattggctataagcca
601 ---------+---------+---------+---------+---------+---------+ 660
    acaatatacacatttacatcggggttatagctaaccccgaaaaaataaccgatattcggt
     V  I  C  V  N  V  A  P  I  S  I  G  A  F  L  L  A  I  S  Q

    atacattagcctttgctgtattagcttgtttctgctcttaagatgatttattgactaaaa
661 ---------+---------+---------+---------+---------+---------+ 720
    tatgtaatcggaaacgacataatcgaacaaagacgagaattctactaaataactgatttt
     Y  I  S  L  C  C  I  S  L  F  L  L  L  R  *  F  I  D  *  K
```

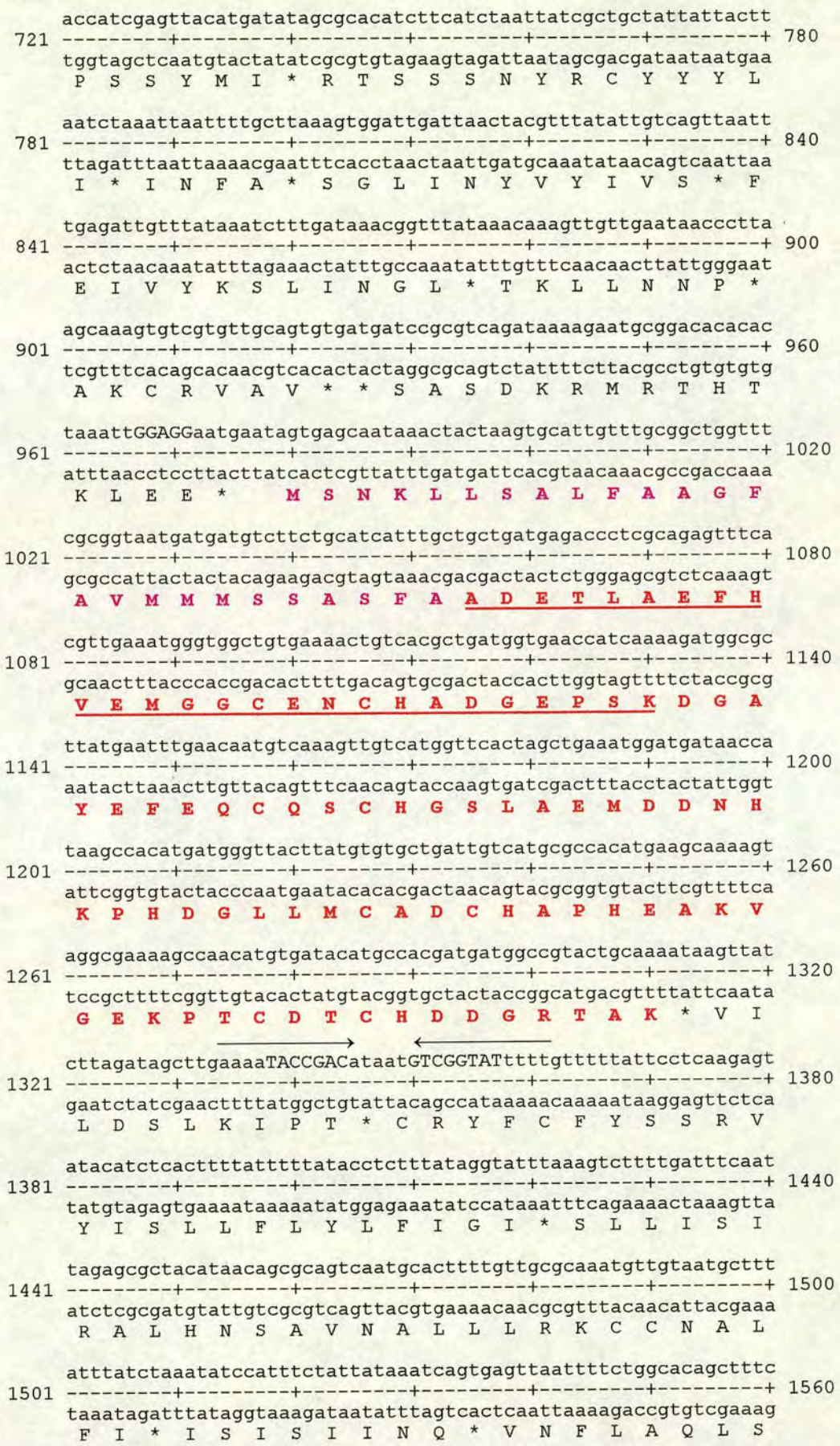
accatcgagttacatgatatagcgcacatcttcatctaattatcgctgctattattactt
721 780
tggtagctcaatgtactatatcgcgtgtagaagtagattaatagcgacgataataatgaa
P S S Y M I * R T S S S N Y R C Y Y Y L
aatctaaattaattttgcttaaagtggattgattaactacgtttatattgtcagttaatt
781 840
ttagatttaattaaaacgaatttcacctaactaattgatgcaaatataacagtcaattaa
I * I N F A * S G L I N Y V Y I V S * F
tgagattgtttataaatctttgataaacggtttataaacaaagttgttgaataacccttа
841 900
actctaacaaatatttagaaactatttgccaaatatttgtttcaacaacttattgggaat
E I V Y K S L I N G L * T K L L N N P *
agcaaagtgtcgtgttgcagtgtgatgatccgcgtcagataaaagaatgcggacacacac
901 960
tcgtttcacagcacaacgtcacactactaggcgcagtctatttcttacgcctgtgtgtg
A K C R V A V * * S A S D K R M R T H T
taaattGGAGGaatgaatagtgagcaataaactactaagtgcattgtttgcggctggttt
961 1020
atttaacctccttacttatcactcgttatttgatgattcacgtaacaaacgccgaccaaa
K L E E * M S N K L L S A L F A A G F
cgcggtaatgatgatgtcttctgcatcatttgctgctgatgagaccctcgcagagtttca
1021 1080
gcgccattactactacagaagacgtagtaaacgacgactactctgggagcgtctcaaagt
A V M M M S S A S F A A D E T L A E F H
cgttgaaatgggtggctgtgaaaactgtcacgctgatggtgaaccatcaaaagatggcgc
1081 1140
gcaactttacccaccgacacttttgacagtgcgactaccacttggtagttttctaccgcg
V E M G G C E N C H A D G E P S K D G A
ttatgaatttgaacaatgtcaaagttgtcatggttcactagctgaaatggatgataacca
1141 1200
aatacttaaacttgttacagtttcaacagtaccaagtgatcgactttacctactattggt
Y E F E Q C Q S C H G S L A E M D D N H
taagccacatgatgggttacttatgtgtgctgattgtcatgcgccacatgaagcaaaagt
1201 1260
attcggtgtactacccaatgaatacacacgactaacagtacgcggtgtacttcgttttca
K P H D G L L M C A D C H A P H E A K V
aggcgaaaagccaacatgtgatacatgccacgatgatggccgtactgcaaaataagttat
1261 1320
tccgcttttcggttgtacactatgtacggtgctactaccggcatgacgttttattcaata
G E K P T C D T C H D D G R T A K * V I
cttagatagcttgaaaaTACCGACataatGTCGGTATttttgtttttattcctcaagagt
1321 1380
gaatctatcgaacttttatggctgtattacagccataaaaacaaaaataaggagttctca
L D S L K I P T * C R Y F C F Y S S R V
atacatctcacttttatttttatacctctttataggtatttaaagtcttttgatttcaat
1381 1440
tatgtagagtgaaaataaaaatatggagaaatatccataaatttcagaaaactaaagtta
Y I S L L F L Y L F I G I * S L L I S I
tagagcgctacataacagcgcagtcaatgcacttttgttgcgcaaatgttgtaatgcttt
1441 1500
atctcgcgatgtattgtcgcgtcagttacgtgaaaacaacgcgtttacaacattacgaaa
R A L H N S A V N A L L L R K C C N A L
atttatctaaatatccatttctattataaatcagtgagttaattttctggcacagctttc
1501 1560
taaatagatttataggtaaagataatatttagtcactcaattaaaagaccgtgtcgaaag
F I * I S I S I I N Q * V N F L A Q L S

```
     gcagtaccttaccatgagatagtcaaagtgaaagggtagatgtatgtcagtggtccaatc
1561 ---------+---------+---------+---------+---------+---------+ 1620
     cgtcatggaatggtactctatcagtttcactttcccatctacatacagtcaccaggttag
      Q  Y  L  T  M  R  *  S  K  *  K  G  R  C  M  S  V  V  Q  S

     aagttgtgcttattgtggtgtcggatgcggtgttagcgtgtcttcaaataaaccgaattg
1621 ---------+---------+---------+---------+---------+---------+ 1680
     ttcaacacgaataacaccacagcctacgccacaatcgcacagaagtttatttggcttaac
      S  C  A  Y  C  G  V  G  C  G  V  S  V  S  S  N  K  P  N  W

     gaccgatgtcgatgctgcagatttaatactagtcggtgacaacaagcatccagctaatta
1681 ---------+---------+---------+---------+---------+---------+ 1740
     ctggctacagctacgacgtctaaattatgatcagccactgttgttcgtaggtcgattaat
      T  D  V  D  A  A  D  L  I  L  V  G  D  N  K  H  P  A  N  Y

     cggtcatttatgtgccaaaggtgaacgcttactcgacagtttagcccaacccaatgtact
1741 ---------+---------+---------+---------+---------+---------+ 1800
     gccagtaaatacacggtttccacttgcgaatgagctgtcaaatcgggttgggttacatga
      G  H  L  C  A  K  G  E  R  L  L  D  S  L  A  Q  P  N  V  L

     gcgttaccctaaacttcgttctggtatgccacttgattgggacaaggcgagcaccttaat
1801 ---------+---------+---------+---------+---------+---------+ 1860
     cgcaatgggatttgaagcaagaccatacggtgaactaaccctgttccgctcgtggaatta
      R  Y  P  K  L  R  S  G  M  P  L  D  W  D  K  A  S  T  L  I

     tgctgatacctttgcgaaaaccattgcagaacatggtccagattcagtcgcactgtatct
1861 ---------+---------+---------+---------+---------+---------+ 1920
     acgactatggaaacgcttttggtaacgtcttgtaccaggtctaagtcagcgtgacataga
      A  D  T  F  A  K  T  I  A  E  H  G  P  D  S  V  A  L  Y  L

     ttctggccaattactcactgaagattattatgttgccaacaagtttgctaaaggcttttt
1921 ---------+---------+---------+---------+---------+---------+ 1980
     aagaccggttaatgagtgacttctaataatacaacggttgttcaaacgatttccgaaaaa
      S  G  Q  L  L  T  E  D  Y  Y  V  A  N  K  F  A  K  G  F  L

     aaaaacggctaacgtcgatactaactcacgcttatgtatgtcgtcagcggtgagcgcaat
1981 ---------+---------+---------+---------+---------+---------+ 2040
     tttttgccgattgcagctatgattgagtgcgaatacatacagcagtcgccactcgcgtta
      K  T  A  N  V  D  T  N  S  R  L  C  M  S  S  A  V  S  A  M

     gcagcgtgcctttggtgaagatgtagttcctggatgttacgacgatctagagcaagctga
2041 ---------+---------+---------+---------+---------+---------+ 2100
     cgtcgcacggaaaccacttctacatcaaggacctacaatgctgctagatctcgttcgact
      Q  R  A  F  G  E  D  V  V  P  G  C  Y  D  D  L  E  Q  A  D

     tgtgatagtgcttgtaggggccaataccgcttggactcatcccgttctttttcaaagaat
2101 ---------+---------+---------+---------+---------+---------+ 2160
     acactatcacgaacatccccggttatggcgaacctgagtagggcaagaaaaagtttctta
      V  I  V  L  V  G  A  N  T  A  W  T  H  P  V  L  F  Q  R  I

     tttagccgcaataaaagccaataatgctcagttagtggtaatcgacccgttatcaacagc
2161 ---------+---------+---------+---------+---------+---------+ 2220
     aaatcggcgttattttcggttattacgagtcaatcaccattagctgggcaatagttgtcg
      L  A  A  I  K  A  N  N  A  Q  L  V  V  I  D  P  L  S  T  A

     cacagcaaaacaagcagacttacatttagccattaaaccgggcgctgatttaacattatt
2221 ---------+---------+---------+---------+---------+---------+ 2280
     gtgtcgttttgttcgtctgaatgtaaatcggtaatttggcccgcgactaaattgtaataa
      T  A  K  Q  A  D  L  H  L  A  I  K  P  G  A  D  L  T  L  F
     tcatggcttactcggttacctagcagatcaaaatcgtgtcgaccacgcgtatattgccgc
2281 ---------+---------+---------+---------+---------+---------+ 2340
     agtaccgaatgagccaatggatcgtctagttttagcacagctggtgcgcatataacggcg
      H  G  L  L  G  Y  L  A  D  Q  N  R  V  D  H  A  Y  I  A  A

     acatacagaaggctttgatactgtggttttgcaggcgcaacaattaagtgccaatttagc
2341 ---------+---------+---------+---------+---------+---------+ 2400
     tgtatgtcttccgaaactatgacaccaaaacgtccgcgttgttaattcacggttaaatcg
      H  T  E  G  F  D  T  V  V  L  Q  A  Q  Q  L  S  A  N  L  A
```

```
    cgatcttgccacgcaagtcggtgtttcagtcactcagctgacgcaattctatcaacttgt
2401 ---------+---------+---------+---------+---------+---------+ 2460
    gctagaacggtgcgttcagccacaaagtcagtgagtcgactgcgttaagatagttgaaca
     D  L  A  T  Q  V  G  V  S  V  T  Q  L  T  Q  F  Y  Q  L  V

    agccaacaataaaaaagtacttacggcatcttgtcaggggttaatcagtcaaccattgg
2461 ---------+---------+---------+---------+---------+---------+ 2520
    tcggttgttatttttcatgaatgccgtagaacagtcccccaattagtcagttggtaacc
     A  N  N  K  K  V  L  T  A  S  C  Q  G  V  N  Q  S  T  I  G

    caccgatgcaaccaatgcgatgattaactgccacctcgcgttagggcacattggtcaagc
2521 ---------+---------+---------+---------+---------+---------+ 2580
    gtggctacgttggttacgctactaattgacggtggagcgcaatcccgtgtaaccagttcg
     T  D  A  T  N  A  M  I  N  C  H  L  A  L  G  H  I  G  Q  A

    tggttgtggtttttttcgttaacagggcagcctaatgccatgggcggtcgtgaggttgg
2581 ---------+---------+---------+---------+---------+---------+ 2640
    accaacaccaaaaaaaagcaattgtcccgtcggattacggtacccgccagcactccaacc
     G  C  G  F  F  S  L  T  G  Q  P  N  A  M  G  G  R  E  V  G

    tgggttggccactcagttagcatgccatatgggtttttcacaaccggagcagcagttatt
2641 ---------+---------+---------+---------+---------+---------+ 2700
    acccaaccggtgagtcaatcgtacggtatacccaaaaagtgttggcctcgtcgtcaataa
     G  L  A  T  Q  L  A  C  H  M  G  F  S  Q  P  E  Q  Q  L  L

    agctgatttttggaaagttgatagtattgcggatcaaaaaggattggttgcagttgagat
2701 ---------+---------+---------+---------+---------+---------+ 2760
    tcgactaaaaacctttcaactatcataacgcctagtttttcctaaccaacgtcaactcta
     A  D  F  W  K  V  D  S  I  A  D  Q  K  G  L  V  A  V  E  M

    gtttgatgcccttgccgaaggtaaaatcaaagcga
2761 ---------+---------+---------+----- 2795
    caaactacgggaacggcttccattttagtttcgct
      F  D  A  L  A  E  G  K  I  K  A
```

3.3.2. Protein sequence data

After export into the periplasm, the N-terminal signal sequence of *c*-type cytochromes is cleaved. From the amino acid sequencing data, this appears to be the case for *S. putrefaciens* cytochrome c_3. The mature cytochrome c_3 protein, inferred from the gene sequence is only 86 amino acids in length, smaller than the *Desulfovibrio* & *Desulfomicrobium* proteins which typically contain 107-118 residues. The only reported cytochrome c_3 which is smaller is the protein from H1R at 84 amino acids in length (Ambler, 1991). The predicted molecular mass for *S. putrefaciens* protein would be 9316 Da (excluding the haem groups). The haem binding motifs found in *S. putrefaciens* cytochrome c_3 are all of the type CXXCH (where X is any amino acid). This is unlike the *Desulfovibrio* proteins which all contain at least one CXXXXCH motif (Coutinho & Xavier, 1994, Moore & Pettigrew, 1990). Attachment of four haems at the CXXCH motifs would yield a molecular weight of 11780 Da, which is in excellent agreement with the mass spectrometry data (section 3.1.1.2.). The protein has a very high content of acidic residues (10 aspartate, 10 glutamate) and few positive residues (5 lysine, 1 arginine). This gives a net charge of -14 to the polypeptide.

The amino acid sequence has been aligned with those available in protein databases. The highest similarity was observed with the cytochrome domain of flavocytochrome c_3 (Pealing *et al.*, 1992) and the cytochrome c_3 from the organism H1R (Ambler, 1991) which can be seen in Figure 3.12. The similarity with *Desulfovibrio* cytochromes c_3 is more distant and the haem attachment motifs are about all that is conserved. If haem attachment and ligation is consistent with other cytochromes c_3, all of the 8 cysteine and 8 histidine residues in the sequence will be involved.

Figure 3.11. : Sequence alignments of the polypeptide sequences predicted by the reading frames flanking the *cctA* with close relatives.

A: The reading frame downstream from *cctA* (blue sequence) aligned with the nitrate reductase from *Synechococcus sp.* (black sequence, Swissprot entry NARB_SYNP7; Omata *et al.*, 1993).

B: (OVERLEAF) The reading frame upstream from *cctA* (black sequence) aligned with the sequence of 3-hydroxyisobutyrate dehydrogenase from *E. coli* (blue sequence, Swissprot entry YHAE_ECOLI; Komine & Inokuchi, 1991). The alignments were produced using the program GAP (Wisconsin Package Version 9.0, Genetics Computing Group (GCG).)

A

```
  1 MFDLSKFLPVITPLMIDTAKTLCPYCGVGCGLEAVPPAQPGRATVRDREG
                    .   .. | |||||||. .|   .|    |   :
  1 ...............MSVVQSSCAYCGVGCGV.SVSSNKPNWTDVDAADL
                  .         .         .         .        .
 51 TPIWQIRGDRQHPSSQGMVCVKGATVAESVSKSR.LKYPMFRASLDDPFT
      :    || .||.. | .| ||  . :|...   |:||  |. :
 35 ILV....GDNKHPANYGHLCAKGERLLDSLAQPNVLRYPKLRSGM.....
                  .         .         .         .        .
100 EISWDEALDRLCDRIQQTQADYGKDGICFYGSGQFQTEDYYIAQKLVKGC
     : ||.|   : |   .| |::| | :  | |||  |||||:| |  ||
 76 PLDWDKASTLIADTFAKTIAEHGPDSVALYLSGQLLTEDYYVANKFAKGF
                  .         .         .         .        .
150 LGTNNFDTNSRLCMSSAVSAYSLCLGSDGPPACYEDLDLADCLLIVGSNT
    | | | |||||||||||||||     | |  | ||:||: || :.:||.||
126 LKTANVDTNSRLCMSSAVSAMQRAFGEDVVPGCYDDLEQADVIVLVGANT
                  .         .         .         .        .
200 AECHPILFNRYRKRHKQGGTNLIVVDPRCTPTAEVADLHLALKPGSDVAL
    |  ||:|| |     |     |:|:||  | ||. ||||||:|||.|. |
176 AWTHPVLFQRILAAIKANNAQLVVIDPLSTATAKQADLHLAIKPGADLTL
                  .         .         .         .        .
250 LNGLGWLLYQMGYVKKDFIANQTEGFEDWLAIIEDYPPQRT..AELTGLA
     .||   |     |   :||  ||||:  .   :          |   |..
226 FHGLLGYLADQNRVDHAYIAAHTEGFDTVVLQAQQLSANLADLATQVGVS
                  .         .         .         .        .
298 VAELVRAADLIASAQRWLSLWSMGVNQSIQGTAKATSLINLHLLTRQIGL
    | :| .   |:|. .: |.    |||||  ||    .:|| ||     ||
276 VTQLTQFYQLVANNKKVLTASCQGVNQSTIGTDATNAMINCHLALGHIGQ
                  .         .         .         .        .
348 PGCGPFSLTGQPNAMGGRETGGLAHLLPGYRKVIDPQHRADVETIWGLPM
     ||| ||||||||||||||| ||||  |  :      |: .  .   |   .
326 AGCGFFSLTGQPNAMGGREVGGLATQLACHMGFSQPEQQL.LADFW..KV
                  .         .         .         .        .
398 GSISPQPGRTAWQMIEGLEQGAVGFLWVAATNPAVSLPDVKRAQAALKRS
     ||. | |  | :| : | :| :
373 DSIADQKGLVAVEMFDALAEGKIKA.........................
```

Figure 3.11. B

```
101 IAPLASREISEALKAKGIDMLDAPVSGGEPKAIDGTLSVMVGGDKAIFDK 150
    .   .|||.  :.   |  ||||||||:  | .| |.||.|||.| ||
  2 ASADVAREIAAYIEPLNIAFLDAPVSGGQAGAENGALTVMMGGDQAHFDT 51
              .          .          .          .
151 YYDLMKAMAGSVVHTGEIGAGNVTKLANQVIVALNIAAMSEALTLATKAG 200
      .. | . . .  | :||| .||: ||: :|  :  :.| |  |  ||
 52 VKPVISAYSCAEL.LGPVGAGQLTKMVNQICIAGVVQGLAEGLHFAKSAG 100
              .          .          .          .
201 VNPDLVYQAIRGGLAGSTVLDAKAPMVMDRNFKPGFRIDLHIKDLANALD 250
    ..   | : |  | | |  :: :   .    :  || ||   |||  |||
101 LDGLKVIEVISKGRAQSWQMENRYKTMWQGQYDFGFAIDWMRKDLGIALD 150
              .          .          .
251 TSHGVGAQLPLTAAVMEMMQALRADGLGTADHSALACYYEKLAKVEVTR 299
    .   |. ||. | | :    ..|      | |.|    ||

151 EARRNGSHLPVAALVDQFYSEVQAMKGNRWDTSSLLARLEKSRS..... 194
```

```
          1          11         21         31         41       50
Sh  c3    ADETLAEFHV EMGGCENCH. ADGEPSKDG. AYEFEQCQSC HGSLAEMDDN
H1R c3    AD.VLADMHA EMSGCETCH. ADGAPSEDG. AHEAAACADC HGGLADMEAP
Fcc c3    AD.NLAEFHV QNQECDSCHT PDGELSNDSL TYENTQCVSC HGTLAEVAET
MR1 c3    ADQKLSDFHA ESGGCESCH

          51         61         71         81         91
Shp c3    HKPHD..... ....GLLMCA DCHAPHEAKV GEKPTCDTCH DDGRTAK
H1R c3    HPAHD..... ....GMLECT DCHMMHEDEV GSRPACDACH DDGRTA
Fcc c3    TKHEHYNAHA SHFPGEVACT SCHSAHEKSM ...VYCDSCH SFDFNMPYAK
```

Figure 3.12. : Alignment of the amino acid sequences of cytochrome c_3 from *Shewanella* NCIMB400 (Sh c_3) with; the cytochrome c_3 from the purple phototrophic bacterium H1R (H1R c_3), a partial sequence of flavocytochrome c_3 from *Shewanella* NCIMB 400 (Fcc c_3) corresponding to the N-terminal haem domain and the N-terminal sequence of the cytochrome c_3 from *S. putrefaciens* MR-1 (MR1 c_3). The amino acid residues highlighted in red indicate the well conserved haem binding motif.

3.4. CONCLUSIONS

The variety of biochemical and genetic data collected for the *Shewanella* NCIMB400 protein allow its designation as a cytochrome c_3. The electrospray mass spectrometry data, along with inferred protein sequence from the *cct*A gene provide complementary information about the size of the protein. It appears to be one of the smallest cytochromes c_3 yet identified.

The electrochemical data for the cytochrome indicates macroscopic potentials within the range observed for cytochromes c_3. It would be interesting to determine the microscopic potentials for the protein as its amino acid sequence is significantly different form the well studied *Desulfovibrio* proteins.

The preliminary data indicate that the protein is an excellent candidate for study by NMR. Given the size of the protein, it could be possible to determine the complete three dimensional structure. However, this requires good protein over-production system to allow isotopic labelling of the protein. The host bacteria needs to be capable of inserting *c*-type haems efficiently, something which is apparently ruled out in *E. coli*. The paramagnetic nature of the oxidised haems should allow assignment of haem methyl peaks and examination of haem cooperativities and microscopic potentials.

The EPR spectrum from *Shewanella* NCIMB400 cytochrome c_3 indicates a single set of g-values, but as mentioned in discussion the peaks are probably compound in nature. The signals from the four haems are unresolved, indicating similar environments for the unpaired electrons.

The *cctA* gene sequence has failed to provide clues to the function of the protein. The cytochrome c_3 from *Shewanella* NCIMB400 is produced from a small, monocistronic RNA. Its low redox potential and production during anaerobiosis suggest it could be involved in an anaerobic electron transport chain.

Future work

One priority is the identification of the physiological role of the protein. The majority of the experimental evidence obtained for the *Desulfovibrio* species points to cytochrome c_3 being involved in accepting electrons from periplasmic hydrogenase. *Shewanella* NCIMB400 is able to respire using hydrogen so this is a possible function. A strain of *Shewanella* NCIMB400 has now been constructed with the cytochrome c_3 gene deleted from the bacterial genome. Studies of the phenotype of this mutant should give an indication of the protein's function (Anne Hill-work in progress).

The three-dimensional structure of Shewanella NCIMB400 cytochrome c_3 is also of great interest. It is evident that the protein has a high sequence homology with the cytochrome domain of flavocytochrome c_3, the three dimensional structure of which has proved elusive. Current work (Pauline Cuthbertson) is concentrating on crystallisation of cytochrome c_3.

Part 1-Cytochrome c_3

REFERENCES

REFERENCES

Abe M., Kitagawa T., Kyogoku Y., (1978) Resonance Raman spectra of octaethylporphyrinato-Ni (II) and *meso*-deuterated and ^{15}N substituted derivatives. II. A normal coordinate analysis, *J. Chem. Phys.*, **69**, 4526-4534.

Ambler R. P., (1980) The structure and classification of cytochromes *c*. In: Robinson A. B., Kaplan N. O., eds., From cyclotrons to cytochromes, Academic press, London, 263-279.

Ambler R. P., (1991) Sequence variability in bacterial cytochrome *c*, *Biochim. Biophys. Acta*, **1058**, 42-47.

Akutsu H., Hazzard J. H., Bartsch R. G., Cusanovich M. A., (1992) Reduction kinetics of the four hemes of cytochrome c_3 from *Desulfovibrio vulgaris* by flash photolysis, *Biochim. Biophys. Acta*, **1140**, 144-156.

Anraku Y., (1988) Bacterial electron transport chains, *Ann. Rev. Biochem.*, **57**, 101-132.

Arnold R., DiChristina T., Hoffman M., (1990) Regulation of dissimilative Fe (III) reduction in *Shewanella putrefaciens*, *Appl. Environ. Microbiol.*, **56**, 2811-2817.

Benosman H., Asso M., Bertrand P., Yagi T., Gayda J., (1989) EPR study of the redox interactions in cytochrome c_3 from *Desulfovibrio vulgaris* Miyazaki, *Eur. J. Biochem.*, **182**, 51-55.

Bianco P., Haladjian J., (1981) Current-potential responses for a tetrahemic protein- a method for determining the individual half-wave potentials of cytochrome c_3 from *Desulfovibrio desulfuricans* strain Norway, *Electrochim. Acta*, **26**, 1001-1004.

Bianco P., Haladjian J., Bruschi M., Guerlesquin F., (1992) Reactivity of [Fe] and [Ni-Fe-Se] hydrogenases with their oxido-reduction partner : the tetrahaem cytochrome c_3, *Biochem. Biophys. Res. Comm.*, **189**, 633-639.

Bowman J. P., McCammon S. A., Nichols D.S., Skerratt J. H., Rea S. M., Nichols S. D., McMeekin T. A., (1997) *Shewanella gelidimarina sp. nov.* and *Shewanella frigidimarina sp. nov.*, novel Antarctic species with the ability to produce eicosapentaenoic acid (20:5 omega 3) and grow aerobically by dissimilatory Fe(III) reduction, *Int. J. Syst. Bact.* , **47**, 1040-1047.

Bruschi M., (1981) The primary structure of the tetrahaem cytochrome c_3 from *Desulfovibrio desulfuricans* (strain Norway 4), *Biochim. Biophys. Acta*, **671**, 219-226.

Bruschi M., Loutfi P., Bianco P., Haladjain J., (1984) Correlation studies between structural and redox properties of cytochromes c_3, *Biochem. Biophys. Res. Com.*, **120**, 384-389.

Cambillau C., Frey M., Mosse J., Guerlesquin F., Bruschi M., (1988) Model of a complex between the tetrahemic cytochrome c_3 and the ferredoxin I from *Desulfovibrio desulfuricans* (Norway strain), *Proteins: Struct. Func. Gen.*, **4**, 63-70.

Cannac V., Caffrey M. S., Voordouw G., Cusanovich M. A., (1991) Expression of the gene encoding cytochrome c_3 from the sulfate reducing bacterium *Desulfovibrio vulgaris* Hildenborough in the purple photosynthetic bacterium *Rhodobacter sphaeroides*, *Arch. Biochem. Biophys.*, **286**, 629-632.

Capeillere-Blandin C., Guerlesqin F., Bruschi M., (1986) Rapid kinetic studies of the electron-exchange reaction between cytochrome c_3 and ferredoxin from *Desulfovibrio desulfuricans* Norway strain and their individual reactions with dithionite, *Biochem. Biophys. Acta*, **848**, 279-293.

Catarino T., Coletta M., LeGall J., Xavier A. V., (1991) Kinetic study of the reduction mechanism for *Desulfovibrio gigas* cytochrome c_3, *Eur. J. Biochem.*, **202**, 1107-1113.

Coletta M., Catarino T., LeGall J. Xavier A. V., (1991) A thermodynamic model for the cooperative functional properties of the tetrahaem cytochrome c_3 from *Desulfovibrio gigas*, *Eur. J. Biochem.*, **202**, 1101-1106.

Coutinho I. B., Turner D. L., LeGall J., Xavier A. V., (1993) Characterization of the structure and redox behaviour of cytochrome c_3 from *Desulfovibrio baculatus* by ^1H nuclear magnetic resonance spectroscopy, *Biochem. J.*, **294**, 899-908.

Coutinho I. B., Xavier A. V., (1994) Tetraheme Cytochromes, *Meth. Enz.*, **243**, 119-140.

Coutinho I. B., Turner D. L., LeGall J., Xavier A. V., (1995) NMR studies and redox titration of the tetraheme cytochrome c_3 from *Desulfomicrobium baculatum.*, *Eur. J. Biochem.*, **230**, 1007-1013.

Cusanovich M. A., Hazzard J. H., Wilson G. S., (1994) Cytochrome c_3: properties and recent insights, *Advances in Chemistry Series-Biomembrane Electrochemistry*, **235**, 471-489.

Czjzek M., Payan F., Guerlesquin F., Bruschi M., Haser R., (1994) Crystal structure of cytochrome c_3 from *Desulfovibrio desulfuricans* Norway at 1.7Å resolution, *J. Mol. Biol.*, **243**, 653-667.

Dawson R. M. C., Elliot D. C., Elliot W. H., Jones K. M., (1984) Data for Biochemical Research-3rd edition, Clarendon Press, Oxford.

Derby H. A., Hammer B. W., (1931) Observations on butter showing surface taint. *Iowa Agri. Exp. Stat. Res. Bull.*, **145**, 289-416.

Devereax R., He S., Doyle C. L., Oackland S., Stahl P. A., LeGall J., Whitman W. B., (1990) Diversity and origin of Desulfovibrio species-phylogenetic definition of a family, *J. Bacteriol.*, **172**, 3609-3619.

DiChristina T., (1992) Effects of nitrate and nitrite on dissimilatory iron reduction by *Shewanella putrefaciens* 200, *J. Bacteriol.*, **174**, 1891-1896.

Dolla A., Cambillau C., Bianco P., Haladjian J., Bruschi M., (1987) Structural assignment of the heme potentials of cytochrome c_3, using a specifically modified arginine, *Biochem. Biophys. Res. Comm.*, **147**, 818-823.

Dolla A., Leroy G., Guerlesquin F., Bruschi M., (1991) Identification of the site of interaction between cytochrome c_3 and ferredoxin using peptide mapping of the cross linked complex, *Biochim. Biophys. Acta*, **1058**, 171-177.

Dutton P. L., (1978) Redox Potentiometry: determination of midpoint potentials of oxidation-reduction components of biological electron-transfer systems, *Meth. Enz.*, **54**, 411-435.

Fan K., Akutsu H., Niki K., Higuchi N., Kyoguku Y., (1990a) Determination of the macroscopic formal potentials of cytochrome c_3 of *Desulfovibrio vulgaris*, Miyazaki F, through the combined use of ^{1}H NMR and an optically transparent thin-layer electrode cell, *J. Electroanal. Chem.*, **278**, 295-306.

Fan K., Akutsu H., Kyoguku Y., Niki K., (1990b) Estimation of the microscopic redox potentials of *Desulfovibrio vulgaris* , Miyazaki F, and partial assignments of heme groups, *Biochemistry*, **29**, 2257-2263.

Favaudon V., Ferradini C., Pucheault J., Gilles L., LeGall J., (1978), *Biochem. Biophys. Res. Commun.*, **84**, 435.

Gauthier G., Gauthier M., Christen R., (1995) Phylogenetic analysis of the genera *Alteromonas*, *Shewanella* and *Moritella* using genes encoding the small-subunit rRNA sequences and division of the genus into two genera, *Alteromonas* (emended) and *Pseudoalteromonas* (gen. nov.) and proposal of twelve new species combinations. *Intl. J. Syst. Bacteriol.*, **45**, 755-761.

Gayda J. P., Bertrand P., More C., Guerlesquin F., Bruschi M., (1985) EPR potentiometric titrations of c_3-type cytochromes, *Biochim. Biophys. Acta*, **829**, 262-267.

Gayda J. P., Benosman H., Bertrand P., More C., Asso M., (1988) EPR determination of interaction redox potentials in a multiheme cytochrome: cytochrome c_3 from *Desulfovibrio desulfuricans* Norway, *Eur. J. Biochem.*, **177**, 199-206.

Gordon E. H. J., (1996) The physiological role of a novel flavocytochrome *c* from *Shewanella putrefaciens*. PhD Thesis, The University of Edinburgh.

Gordon E. H. J., Pealing S. L., Chapman S. K., Ward F. B., Reid G. A., (1998) Physiological function and regulation of flavocytochrome c_3, the soluble fumarate reductase from *Shewanella putrefaciens* NCIMB400, *Microbiology* (In Press).

Guerlesquin F., Bruschi M., Bovier-Lapierre G., (1984) Electron transfer mechanism and interaction studies between cytochrome c_3 and ferredoxin, *Biochimie*, **66**, 93-99.

Guerlesquin F., Bruschi M., Wuthrich K., (1985) NMR studies of cytochrome c_3 from *Desulfovibrio desulfuricans* Norway strain, *Biochim. Biophys. Acta*, **530**, 296-303.

Guerlesquin F., Dolla A., Bruschi M, (1994) Involvement of electrostatic interactions in cytochrome *c* complex formations, *Biochimie*, **76**, 515-523.

Guigliarelli T., Bertrand P., More C., Haser R., Gayda J. P., (1990) Single-crystal electron paramagnetic resonance study of cytochrome c_3 from *Desulfovibrio desulfuricans* Norway strain. Assignment of the heme midpoint potentials, *J. Mol. Biol.*, **216**, 161-166.

Haser R., Pierrot M., Payan F., Astier J. P., Bruschi M., LeGall J., (1979) Structure and sequence of the multihaem cytochrome c_3, *Nature*, **282**, 806-810.

Hatchikian E. C., Papavassiliou P., Bianco P., Haladjian J., (1984) Characterization of cytochrome c_3 from the thermophilic sulfate reducer *Thermodesulfobacterium commune*, *J. Bacteriol.*, **159**, 1040-1046.

Higuchi Y., Bando S., Kusonoki M., Matsuura Y., Yasuoka N., Kakudo M., Yamanaka T., Yagi T., Inokuchi H., (1981) The structure of cytochrome c_3 from *Desulfovibrio vulgaris* Miyazaki at 2.5 Å resolution, *J. Biochem.*, **89**, 1659-1662.

Higuchi Y., Kusonoki M., Matsuura Y., Yasuoka N., Kakudo M., (1984) Refined structure of cytochrome c_3 at 1.8 Å resolution, *J. Mol. Biol.*, **172**, 109-139.

Kazanskaya I., Lexa D., Bruschi M., Chottard G., (1996) Electron transfer in tetrahemic cytochrome c_3: Spectroelectrochemical evidence for a conformational change triggered by heme IV reduction, *Biochemistry*, **35**, 13411-13418.

Komine Y., Inokuchi H., (1991) precise mapping of the *rnpB* gene encoding the RNA component of RNase-P in *Escherichia coli* K12, *J. Bacteriol.*, **173**, 670-676.

Kwoh, D. Y., Vedvick T. S., McCue A. F., Gevertz D., (1993) Rapid comparison of the cytochrome c_3 gene from nine strains of *Desulfovibrio vulgaris* using polymerase chain reaction amplification, *Can. J. Microbiol.*, **39**, 402-411.

Lazzazera B. A., Beinert H., Khoroshilova N., Kennedy M. C., Kiley P. J., (1996) DNA binding and dimerization of the Fe S-containing protein from *Escherichia coli* are regulated by oxygen, *J. Biol. Chem.*, **271**, 2762-2768.

Ledyard K. M., Butler A., (1997) Structure of putrebactin, a new dihydroxamate siderophore produced by *Shewanella Putrefaciens*, *JBIC*, **2**, 93-97.

Lee J. V., Gibson D. M., Shewan J. M., (1977) A numerical taxonomy of some *Pseudomonas* -like bacteria, *J. Gen. Microbiol.*, **98**, 439-451.

LeGall J., Postgate J. R., (1973) The physiology of sulphate reducing bacteria, *Adv. Microb. Physiol.*, **10**, 81-133.

LeGall J., Peck H. D. Jr., (1987) Amino-terminal amino-acid sequences of electron transfer proteins from gram-negative bacteria as indicators of their cellular-localisation-the sulfate reducing bacteria, *FEMS Microbiol. Rev.*, **46**, 35-40.

LeGall J., Fauque G., (1988) Dissimilatory reduction of sulphur compounds: In Biology of anaerobic microorganisms, Zehnder A. J. ed., John Wiley and sons, New York, 587-639.

Long H. F., Hammer B. W., (1941) Classification of organisms important in dairy products. III. *Pseudomonas putrefaciens. Iowa. Agric. Exp. Stn. Bull.*, **2850**, 176-195.

Louro R. O., Catarino T., Salgueiro C. A., LeGall J., Xavier A. V., (1996) Redox-Bohr effect in the tetrahaem cytochrome c_3 from *Desulfovibrio vulgaris*: a model for energy transduction mechanisms, *JBIC*, **1**, 34-38.

Louro R. O., Catarino T., LeGall J., Xavier A. V., (1997) Redox-Bohr effect in electron/proton energy transduction: cytochrome c_3 coupled to hydrogenase works as a 'proton thruster' in *Desulfovibrio vulgaris*, *JBIC*, **2**, 488-491.

Lovely D. R., Phillips E. J. P., Lonergan D. J., (1989) Hydrogen and formate oxidation coupled to dissimilatory reduction of iron or manganese by *Alteromonas putrefaciens*, *Appl. Env. Microbiol.*, **55**, 700-706.

MacDonall M. T., Colwell R. R., (1985) Phylogeny of the *Vibrionaceae* and recommendation for two new genera, *Listonella* and *Shewanella*. *Syst. Appl. Microbiol.*, **6**, 171-182.

Matias P. M., Frazäo C., Morais J., Coll M., Carrondo M. A., (1993) Structure analysis of cytochrome c_3 from *Desulfovibrio vulgaris* Hidenborough at 1.9 Å resolution , *J. Mol. Biol.*, **234**, 680-699.

Matias P. M., Morais J., Coelho R., Carrondo M. A., Wilson K., Dauter Z., Sieker L., (1996) Cytochrome c_3 from *Desulfovibrio gigas* - crystal structure at 1.8 angstrom resolution and evidence for a specific calcium binding site, *Prot. Sci.*, **5**, 1342-1354.

McDonald C. C., Phillips W. D., LeGall J., (1974) Proton magnetic resonance studies of *Desulfovibrio* cytochromes c_3, *Biochemistry*,**13**, 1952-1959.

Mitchell P., (1961) Coupling of phosphorylation to electron transport and hydrogen transfer by a chemiosmotic mechanism, *Nature*, **191**, 141-148.

Moore G. R., Pettigrew G. W, (1990) Cytochromes *c*: Evolutionary, Structural and Physicochemical Aspects, Springer -Verlag, Heidelberg, Germany.

Morais J., Nuno Palma P., Frazão C., LeGall J., Moura I., Moura J. J. G., Carrondo M. A., (1995) Structure of the tetraheme cytochrome from *Desulfovibrio desulfuricans* ATCC 27774: X-ray diffraction and electron paramagnetic resonance studies, *Biochemistry*, **34**, 12830-12841.

More C., Gayda J. P., Bertrand P., (1990) Simulations of the g-strain broadening of the low-spin hemoprotein EPR-spectra based on the T2G hole model, *J. Magn. Res.*, **90**, 486-499.

Morris C. J., (1987) The cytochromes of *S. putrefaciens*, PhD. Thesis, The University of Edinburgh.

Morris C. J., Gibson D. M., Ward F. B., (1990) Influence of respiratory substrate on the cytochrome content of *Shewanella putrefaciens*, *FEMS Microbiol. Lett.*, **69**, 259-262.

Morris C. J., Black A. C., Pealing S. L., Manson F. D. C., Chapman S. K., Reid G. A., Gibson D. M., Ward F. B., (1994) Purification and properties of a novel cytochrome: flavocytochrome *c* from *Shewanella putrefaciens*, *Biochem. J.*, **302**, 587-593.

Moura J. J. G., Xavier A. V., Cookson D. J., Moore G. R., Williams R. J. P., (1977) Redox states of cytochrome c_3 in the absence and presence of ferredoxin, *FEBS Lett.*, **81**, 275-280.

Moura I., Teixeira M., Huynh B. H., LeGall J., Moura J. J. G., (1988) Assignment of individual heme EPR signals of *Desulfovibrio baculatus* (strain 9974) tetraheme cytochrome c_3 - a redox equilibria study, *Eur. J. Biochem.*, **176**, 365-369.

Moura J. J. G., Santos H., Moura I., Legall J., Moore G. R., Williams R. J. P., Xavier A. V., (1982) NMR redox studies of *Desulfovibrio vulgaris* cytochrome c_3 - electron transfer mechanisms, *Eur. J. Biochem.*, **127**, 151-155.

Mus-Veteau I., Dolla A., Guerlesquin F., Payan F., Czjek M., Haser R., Bianco P., Haladjian J., Rapp-Giles B. J., Wall J. D., Voordouw G., Bruschi M., (1992) Site-directed mutagenesis of tetraheme cytochrome c_3 - modification of oxidoreduction potentials after heme axial ligand replacement, *J. Biol. Chem.*, **267**, 16851-16858.

Myers C. R., Nealson K. H., (1988a) Microbial reduction of manganese oxides: Interactions with iron and sulphur. *Geochim. et Cosmochim. Acta.*, **52**, 2727-2732.

Myers C. R., Nealson K. H., (1988b) Bacterial manganese reduction and growth with manganese oxide as the sole electron acceptor, *Science*, **240**, 1319-1321.

Myers C. R., Myers J. M., (1992) Localization of cytochromes to the outer membrane of anaerobically grown *Shewanella putrefaciens* MR-1, *J. Bacteriol.*, **174**, 3429-3438.

Myers C. R., Myers J. M., (1993a) Ferric reductase is associated with the membranes of anaerobically grown *Shewanella putrefaciens* MR-1, *FEMS Microbiol. Letts.*, **114**, 215-222.

Myers C. R., Myers J. M., (1993b) Role of menaquinone in the reduction of fumarate, nitrate, iron (III) and manganese (IV) by *Shewanella putrefaciens* MR-1, *FEMS Microbiol. Lett.*, **114**, 215-222.

Myers C. R., Myers J. M., (1997a) Cloning and sequencing of *cymA*, a gene encoding a tetraheme cytochrome c required for reduction of iron (III), fumarate and nitrite by *Shewanella putrefaciens* MR-1, *J. Bacteriol.*, **179**, 1143-1152.

Myers C. R., Myers J. M., (1997b) Outer membrane cytochromes of *Shewanella putrefaciens* MR1: spectral analysis and purification of the 83 kDa c-type cytochrome, *Biochim. Biophys. Acta*, **1326**, 307-318.

Myers C. R., Myers J. M., (1997c) Isolation and characterisation of a transposon mutant of *Shewanella putrefaciens* MR-1 deficient in fumarate reductase. *Letts. Applied Microbiol.*, **25**, 162-168.

Nealson K. H., Myers C. R., (1990) Iron reduction by bacteria: a potential role in the genesis of banded iron foundations, *Am. J. Sci.*, **290**, 35-45.

Nealson K. H., Saffarini D., (1994) Iron and manganese in anaerobic respiration: environmental significance, physiology and regulation, *Ann. Rev. Microbiol.*, **48**, 311-343.

Nicholls D. G., Ferguson S. J., (1992), Bioenergetics-2nd edition, Academic Press.

Nielson H., Engelbrecht J., Brunak S., vonHeijne G., (1997) Identification of prokaryotic and eukaryotic signal peptides and prediction of their cleavage sites, *Prot. Eng.*, **10**, 1-6.

Niki K., Kawasaki K., Nishimura N., Higushi Y., Yasuoka N., Kakudo M., (1984) Electrochemical and structural studies of tetra-heme proteins from *Desulfovibrio* - standard potentials of the redox sites and heme-heme interactions, *J. Electroanal. Chem.*, **168**, 275-286.

Nivière V., Hatchikian E. C., Bianco P., Haladjian J., (1988) Kinetic studies of electron transfer between hydrogenase and cytochrome c_3 from *Desulfovibrio gigas*. Electrochemical properties of cytochrome c_3 , *Biochem. Biophys. Acta*, **935**, 34-40.

Nozue H., Hayashi T., Hashimoto Y., Ezaki T., Hamasaki K., Ohwada K., Terawaki Y., (1992) Isolation and characterisation of *Shewanella Alga* from human clinical specimens and emendation of the description of *S. alga* Simidu *et al.*, 1990, 335. *Int. J. Syst. Bact.*, **42**, 628-634.

Obuekwe C. O., Westlake D. W. S., Cook F. D., Costerton J. W., (1981) Surface changes in mild steel coupons from the action of corrosion-causing bacteria, *Appl. Env. Microbiol.*, **41**, 766-774.

Odom J. M., Peck H. D., (1981) Hydrogen cycling as a general mechanism for energy coupling in the sulfate reducing bacteria *Desulfovibrio-sp.*, *FEMS Microbiol. Lett.*, **12**, 47-50.

Omata T., Andriesse X., Hirano A., (1993) Identification and characterisation of a gene cluster involved in nitrate transport in the cyanobacterium *Synechococcus* sp. PCC7942, *Mol. Gen. Genet.*, **236**, 193-202.

Papa S., Guerrieri F., Izzo G., (1979), Redox Bohr effects in the cytochrome system of mitochondria, *FEBS Lett.*, **105**, 213-216.

Park J., Kano K., Morimoto Y., Higushi Y., Yasuoka N., Ogata M., Niki K., Akutsu H., (1991a) 1H NMR studies on ferricytochrome c_3 from *Desulfovibrio vulgaris* Miyazaki F and its interaction with ferredoxin I, *J. Biomol. NMR*, **1**, 271-282.

Park J., Kano K., Niki K., Akutsu H., (1991b) Full assignment of heme redox potentials of cytochrome c_3 of *D. vulgaris* (Miyazaki) by ^{1}H NMR, *FEBS Lett.*, **285**, 149-151.

Park J., Kang S. W., Shin J., (1995) Assignment of the redox potentials of cytochrome c_3 of *Desulfovibrio vulgaris* Hildenborough by ^{1}H NMR, *Bull. Korean Chem. Soc.*, **16**, 968-971.

Park J., Ohmura T., Kano K., Sagara T., Niki K., Kyogoku Y., Akutsu H., (1996a) Regulation of the redox order of four hemes by pH in cytochrome c_3 from *D. vulgaris* Miyazaki F, *Biochim. Biophys. Acta*, **1293**, 45-54.

Park J., Kang S. W., (1996b) Effects of ionizable groups on the redox potentials of cytochrome c_3 from *D. vulgaris* Miyazaki F, *Bull. Korean Chem. Soc.*, **17**, 820-826.

Pealing S. L., Black A. C., Manson F. D. C., Ward F. B., Chapman S. K., Reid G. A., (1992) Sequence of the gene encoding flavocytochrome *c* from *Shewanella putrefaciens* that is a soluble fumarate reductase related to the membrane-bound enzyme from other bacteria, *Biochemistry*, **31**, 12132-12140.

Pealing S. L., (1994) Flavocytochrome *c* from *Shewanella putrefaciens*: a soluble fumarate reductase, PhD. Thesis, University of Edinburgh.

Pealing S. L., Cheesman M. R., Reid G. A., Thomson A. J., Ward F. B., Chapman S. K., (1995) Spectroscopic and kinetic studies of the tetrahaem flavocytochrome *c* from *Shewanella putrefaciens* NCIMB400, *Biochemistry*, **34**, 6153-6158.

Perry K. A., Kostka J. E., Luther G. W., Nealson K. H., (1993) Mediation of sulphur speciation by a Black Sea facultative anaerobe, *Science*, **259**, 801-803.

Pettigrew G. W., Moore G. R., (1987) Cytochromes *c*: biological aspects, Springer - Verlag, Heidelberg, Germany.

Picarra-Pereira A., Turner D. L., LeGall J., Xavier A. V., (1993) Structural studies on *Desulfovibrio gigas* cytochrome c_3 by 2-dimensional ^{1}H nuclear magnetic resonance spectroscopy, *Biochem. J.*, **294**, 909-915.

Pierrot M., Haser R., Frey M., Payan F., Astier J., (1982) Crystal structure and electron transfer properties of cytochrome c_3, *J. Biol. Chem.*, **257**, 14341-14348.

Pieulle L., Haladjian J., Bonicel J., Hatchikian E. C., (1996) Biochemical studies of the *c*-type cytochromes of the sulfate reducer *Desulfovibrio africanus*. Characterisation of two tetraheme cytochromes c_3 with different specificity. *Biochim. Biophys. Acta*, **1273**, 51-61.

Pollock W. B. R., Chemerika P. J., Forrest M. E., Beatty J. T., Voordouw G., (1989) Expression of the gene encoding cytochrome c_3 from *Desulfovibrio vulgaris*

(Hildenborough) in *Escherichia coli*: export and processing of the apoprotein, *J. Gen. Microbiol.*, **135**, 2319-2328.

Postgate J. R., (1954) Presence of cytochrome in an obligate anaerobe, *Biochem. J.*, **54,** proceedings xi.

Postgate J. R., (1984) *The sulphate reducing bacteria* (2nd edn), Cambridge University Press, Cambridge.

Reid G. A., Gordon E. H. J., (1998) Phylogeny of marine and freshwater *Shewanella*: reclassification of *S. putrefaciens* NCIMB400 as *S. frigidimarina*, *Int. J. Syst Bacteriol.*, (In Press).

Saffarini D. A., Nealson K. H., (1993) Sequence and genetic characterization of *etrA*, an *fnr* analog that regulates anaerobic respiration in *Shewanella putrefaciens* MR-1, *J. Bacteriol.*, **175**, 7938-7944.

Saffarini D. A., DiChristina T. J., Bermudes D., Nealson K. H., (1994) Anaerobic respiration of *Shewanella putrefaciens* requires both chromosomal and plasmid-borne genes, *FEMS Microbiol. Lett.*, **119**, 271-278.

Samain E., Albagnac G., Legall J., (1986) Redox studies of the teraheme cytochrome c_3 isolated from the propionate-oxidising, sulfate reducing bacterium *Desulfobulbus elongatus*, *FEBS Letts.*, **204**, 247-250.

Salgueiro C.A., Turner D. L., Santos H., LeGall J., Xavier A. V., (1992) Assignment of the redox potentials to the four haems in *Desulfovibrio vulgaris* cytochrome c_3 by 2D-NMR, *FEBS Lett.*, **314**. 155-158.

Salgueiro C. A., Turner D. L., LeGall J., Xavier A. V., (1997a) Reevaluation of the redox and redox-Bohr cooperativity in tetrahaem *Desulfovibrio vulgaris* (Miyazaki F) cytochrome c_3, *JBIC*, **2**, 343-349.

Salgueiro C. A., Turner D. L., Xavier A. V., (1997b) Use of paramagnetic NMR probes for structural analysis in cytochrome c_3 from *Desulfovibrio vulgaris*, *Eur. J., Biochem.*, **244**, 721-734.

Sambrook J., Fritsch E. F., Maniatis T., (1989) Molecular cloning: a laboratory manual, 2nd edition, Cold Spring Harbour Laboratory Press, Cold Spring Harbour, NY.

Santos H., Moura J. J. G., Moura I., LeGall J., Xavier A. V., (1984) NMR studies of electron transfer mechanisms in a protein with interacting redox centres: *Desulfovibrio gigas* cytochrome c_3, Eur. J. Biochem., **141**, 283-296.

Saraiva L. M., Salgueiro C. A., LeGall J., van Dongen W. M. A. M., Xavier A. V., (1996) Site directed mutagenesis of a phenylalanine residue strictly conserved in cytochromes c_3, *JBIC*, **1**, 542-550.

Schägger H., von Jagow G., (1987) Tricine-sodium dodecyl sulfate-polyacrylamide gel electrophoresis for the separation of proteins in the range from 1 to 100 kDa. *Anal. Biochem.*, **166**, 368-379.

Schägger H., (1994) Electrophoretic Isolation of membrane proteins from acrylamide gels, *Appl. Biochem. Biotech.*, **48**, 185-203.

Semple K. M., Westlake D. W. S., (1987) Characterisation of iron-reducing *Alteromonas putrefaciens* strains from oil field fluids. *Can. J. Microbiol.*, **33**, 366-371.

Shinkai W., Hase T., Yagi T., Matsubara, H., (1980), *J. Biochem.*, **87**, 1747-1756.

Singleton R., Denis J., Campbell L. L., (1982) Cytochrome c_3 from the sulfate reducing anaerobe *Desulfovibrio africanus* Benghazi: Antigenic properties, *J. Bac.*, **152**, 527-529.

Sokol W. F., Evans P. H., Niki K., Yagi T., (1980), *J. Electroanal. Chem.*, **108**, 107-115.

Sola M., Cowan J. A., (1992) Assignment of heme resonances in the 1H NMR spectrum of oxidised *Desulfovibrio vulgaris* (Hildenborough) cytochrome c_3 , *Inorg. Chem. Acta*, **202**, 241-251.

Stewart D. E., Legall J., Moura I., Moura J. J. G., Peck H. D., Xavier A. V., Weiner P. K., Wampler J. E., (1988) A hypothetical model of the flavodoxin-tetraheme cytochrome c_3 complex of sulfate reducing bacteria, *Biochemistry*, **27**, 2444-2450.

Stewart D. E., Wampler J. E., (1991) Molecular-dynamics simulations of the cytochrome c_3-rubredoxin complex from *Desulfovibrio vulgaris*, *Proteins: Struct. Func. Gen.*, **11**, 142-152.

Tsapin A. I., Nealson K. H., Meyers T., Cusanovich M.A., Van Beeumen J., Crosby L. D., Feinberg B. A., Zhang C., (1996) Purification and properties of a low -redox-potential tetraheme cytochrome c_3 from *Shewanella* putrefaciens, *J. Bact.*, **178**, 6386-6388.

Turner D. L., Salgueiro C. A., Catarino T., LeGall J., Xavier A. V., (1994) Homotropic and heterotropic cooperativity in the tetrahaem cytochrome c_3 from *Desulfovibrio vulgaris*, *Biochim. Biophys. Acta*, **1187**, 232-235.

Turner D. L., Salgueiro C. A., Catarino T., LeGall J., Xavier A. V., (1996) NMR studies of the cooperativity in the tetrahaem cytochrome c3 from *Desulfovibrio vulgaris*, *Eur. J. Biochem.*, **241**, 723-731.

Utuno M., Ono K., Kimura K., Inokuchi H., Yagi T., (1980) , *J. Phys.* (Paris), **41**, 957.

Van Leeuwen J. W., Van Dijk C., Grande H. J., Veeger C., (1982) A pulse radiolysis study of cytochrome c_3, *Eur. J. Biochem.*, **127**, 631-637.

Verma A. L., Kimura K., Nakamura A., Yagi T., Inokuchi H., Kitagawa T., (1988) Resonance Raman studies of hydrogenase -catalysed reduction of cytochrome c_3 by hydrogen. Evidence for heme-heme interactions, *J. Am. Chem. Soc.*, **110**, 6617-6623.

Voordouw G., Brenner S., (1986) Cloning and sequencing of the gene encoding cytochrome c_3 from *Desulfovibrio vulgaris* (Hildenborough), *Eur. J. Biochem.*, **159**, 347-351.

Voordouw G., Kent H. M., Postgate J. R., (1987) Identification of the genes for hydrogenase and cytochrome c_3 in *Desulfovibrio*, *Can. J. Microbiol.*, **33**, 1006-1010.

Voordouw G., Pollock W. B. R., Bruschi M., Guerlesquin F., Rapp-Giles B. J., Wall J. D., (1990) Functional expression of *Desulfovibrio vulgaris* Hildenborough cytochrome c_3 in *Desulfovibrio desulfuricans* G200 after conjugational gene transfer from *Escherichia coli*, *J. Bac.*, **172**, 6122-6126.

Walker F. A., Reis D., Balke V. L., (1984) Models of the cytochromes-b_5. Electron paramagnetic resonance studies of low spin iron(III) tetraphenylporhyrins, *JACS*, **106**, 6888-6898.

Williams, R. J. P., (1978) The history and the hypothesis concerning ATP-formation by energised protons, *FEBS Letters*, **85**, 9-19.

Xavier A. V., Moura J. J. G., LeGall J., DerVartanian D. V., (1979) , *Biochimie*, **61**, 689.

Xavier A. V., (1985) Electron/proton transfer mechanisms in the tetraheme cytochrome c_3, Frontiers in Bioinorganic Chemistry, Ed. A. V. Xavier, VCH, Germany.

Xavier A. V., (1986) Energy transduction coupling mechanisms in multiredox center proteins, *J. Inorg. Biochem.*, **28**, 239-243.

Xavier A. V., Turner D. L., Santos H., (1993) Two-dimensional nuclear magnetic resonance of paramagnetic metalloproteins, *Methods Enzymol.*, **127**, 151-155.

Yagi T., Honya M., Tamiya N., (1968) Purification and properties of hydrogenases of different origins, *Biochim. Biophys. Acta.*, **153**, 699-705.

Yagi T., (1984) Spectral and kinetic abnormality during the reduction of cytochrome c_3 catalysed by hydrogenase with hydrogen, *Biochim. Biophys. Acta*, **767**, 288-294.

Ziomek E., Williams R. E., Martin W. G., (1984) Application of hydrophobic chromatography to the large scale purification of *Desulfovibrio desulfuricans* cytochrome c_3, *Prep. Biochem.*, **14**, 75-85.

Part 2-Flavocytochrome b_2

Chapter 4 : *INTRODUCTION*

4.1. PROTEIN-MEDIATED ELECTRON TRANSFER

4.1.1. Introduction

Probably the simplest of all chemical reactions, is the transfer of a single electron between two redox centres. Generally, no making or breaking of bonds is involved. The simplicity is paramount when a single donor and acceptor species are present. An example of this, is the self exchange reaction between oxidised and reduced species of a metal ion in solution (*e.g.* Fe^{3+} (aq) accepting an electron from Fe^{2+} (aq)). Even for such a simple system a number of parameters need to be considered when describing electron transfer. These include; ligand reorganisation energies, solvent sphere dipoles and solvent reorganisation energies.

In biological systems the situation is more complex, a typical cell contains many different donor and acceptor redox-proteins. Greater complication is added by the size of these proteins. Even small proteins contain tens of amino acids, with hundreds of atoms contributing to their redox characteristics. However, simple protein models and formalisms do allow predictions of biological function and electron transfer rates.

In the chemiosmotic theory, (outlined in Chapter 1) the central feature of bacterial energy transduction is creation of a transmembrane proton gradient. The gradient is built up in a number of steps which require electron transfers between specific pairs of proteins. In eukaryotes, most cellular ATP is generated by the transfer of electrons from NADH to oxygen, again building up a proton gradient. Nature has evolved a number of mechanisms to ensure that guided electron-transfer reactions occur. One important consideration is selection of the correct physiological partner proteins.

Fundamental processes such as photosynthesis, respiration and nitrogen fixation rely on many electron transfers. Many specialised proteins have evolved to perform these divese processes. Prosthetic groups such as haem, flavins, quinones, copper and iron sulphur clusters, are commonly found in redox proteins. Redox proteins can contain a single redox centre (*e.g.* rubredoxin, flavodoxin, azurin) or

multiple centres (*e.g.* flavocytochrome *c*, cytochromes c_3, photosynthetic reaction centre). They can be relatively simple, soluble entities or part of complex, highly organised membrane bound systems. The redox cofactors have well defined midpoint potentials in aqueous solutions. Inside the protein environment, these are modulated and 'fine tuned' to meet the specifications of the system. This allows a variety of functions to be performed with relatively few components.

4.1.2. Factors affecting protein-mediated electron transfer

Two stoichiometric mechanisms have been found to describe redox reactions where a metal centre is involved (Taube, 1984). The first, is the inner-sphere mechanism where the coordination spheres of the reacting centres share a bridging ligand. This bridging ligand provides a pathway during electron transfer. The second, is the outer sphere mechanism where the two complexes come into contact, but do not share a ligand during electron transfer. The outer sphere process occurs via through-space overlap of orbitals, but does not require the making or breaking of any bonds. On the basis of activation-energy requirements and steric and electronic considerations it has been argued that haem, iron-sulphur and copper containing redox proteins would favour an outer sphere mechanism (Wherland & Gray, 1977). Many theoretical descriptions of outer-sphere electron transfer processes have been made. One of the most developed is that of Marcus which has been adapted and applied to biological systems (Marcus, 1968; Marcus, 1996). Well established theory exists describing the factors which influence protein mediated electron transfer (*e.g.* Moser & Dutton, 1996; Chapman & Mount, 1995; Tollin *et al.*, 1986)

First, the factors which determine the kinetics and mechanisms of biological electron transfer will be outlined. We can consider a simplified reaction where a donor, **D** transfers an electron to an acceptor, **A** such that:

$$\underset{\text{reactants}}{\mathbf{D} + \mathbf{A}} \rightarrow \underset{\text{products}}{\mathbf{D}^{+} + \mathbf{A}^{-}}$$

The electron transfer typically occurs if the two species are in close proximity such that they form an encounter complex. If the electron transfer process is radiationless and no energy is lost or gained during the reaction, then the combined energy of the system must stay constant until after the electron has transferred. This is a fundamental characteristic of electron transfer reactions.

The Franck-Condon principle applies; *i.e.* the electron redistribution event is significantly rapid to prevent change in the nuclear coordinates of the reactants whilst it occurs. This approximation generally applies to biological systems. As a consequence **D** and **A** need to approach an optimum configuration, with equal internuclear distances and energies for both states, for electron transfer to occur. The optimised configuration will have higher energy than either reactants or products. As a result, this energy barrier is an important factor in determining the overall rate. The higher the energy the lower the overall electron transfer rate.

Marcus theory represents the reactants and their immediate environment as a simple harmonic oscillator potential along a reaction coordinate (Figure 4.1.). The bottom of the potential well corresponds to the equilibrium geometry of the donor. The products are represented by a similar harmonic potential, except it lies displaced further along the reaction coordinate and lowered in potential by ΔG (the free energy of the electron transfer reaction). It is common to refer to ΔG as the driving force of the reaction, it is proportional to the difference in acceptor and donor redox potentials. The reorganisation energy (λ) represents the change in geometry which must occur upon transfer of the electron. It is defined as, the energy required to distort the equilibrium geometry of the reactants to the equilibrium geometry of the products, without actually transferring the electron. In a simple, non-adiabatic electron transfer reaction, the height of intersection of the two parabolas above the bottom of the reactant parabola is analogous to the activation energy of the transition state in a traditional (adiabatic) chemical reaction. It is thus denoted as ΔG^*, and a simple relationship is given in Equation 1.

$$\Delta G^* = (\Delta G + \lambda)^2 / 4\lambda \qquad (1)$$

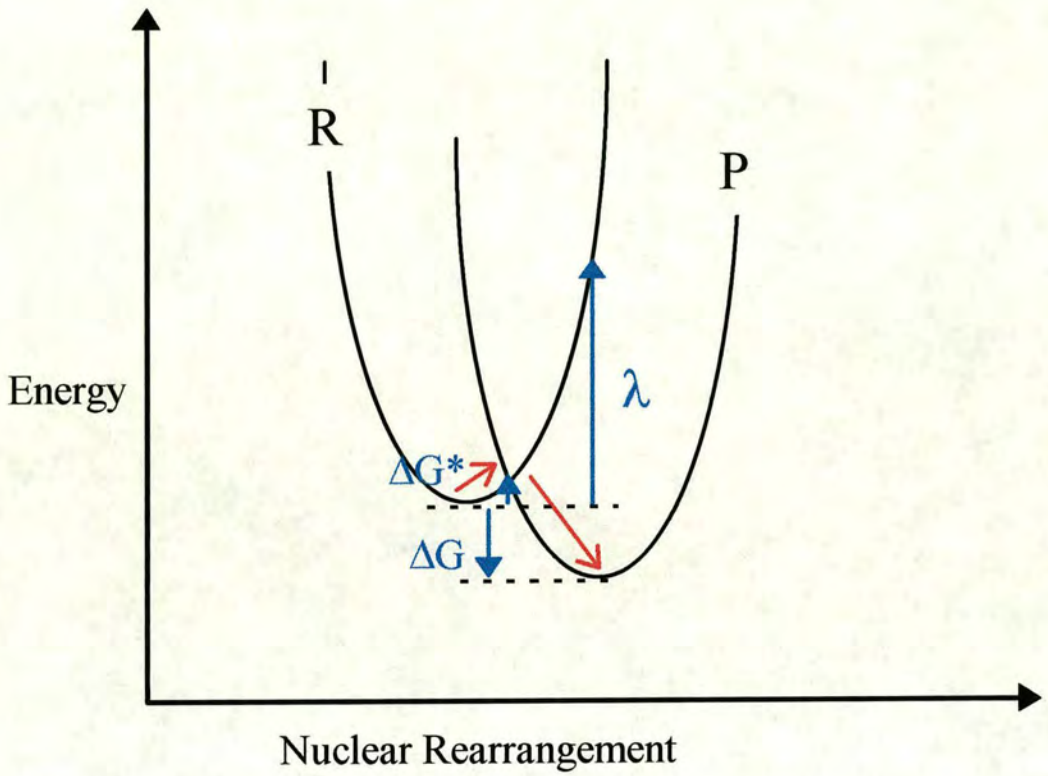

Figure 4.1. : Plot of nuclear rearrangement against free energy for the reactants (**R**) and products (**P**) during a non-adiabatic electron transfer reaction. Reaction proceeds via the route indicated by red arrows. In the Marcus theory description, the nuclear motion of reactants and products follow the simple harmonic oscillator potential. The bottom of the potential well corresponds to equilibrium geometry. The blue arrows indicate vectors for; free energy change of the reaction (**ΔG**), activation energy barrier (**ΔG***) and the reorganisation energy, required to move from the equilibrium reactant coordinates to the product equilibrium geometry without transfer of the electron (λ). (After Moser & Dutton, 1996)

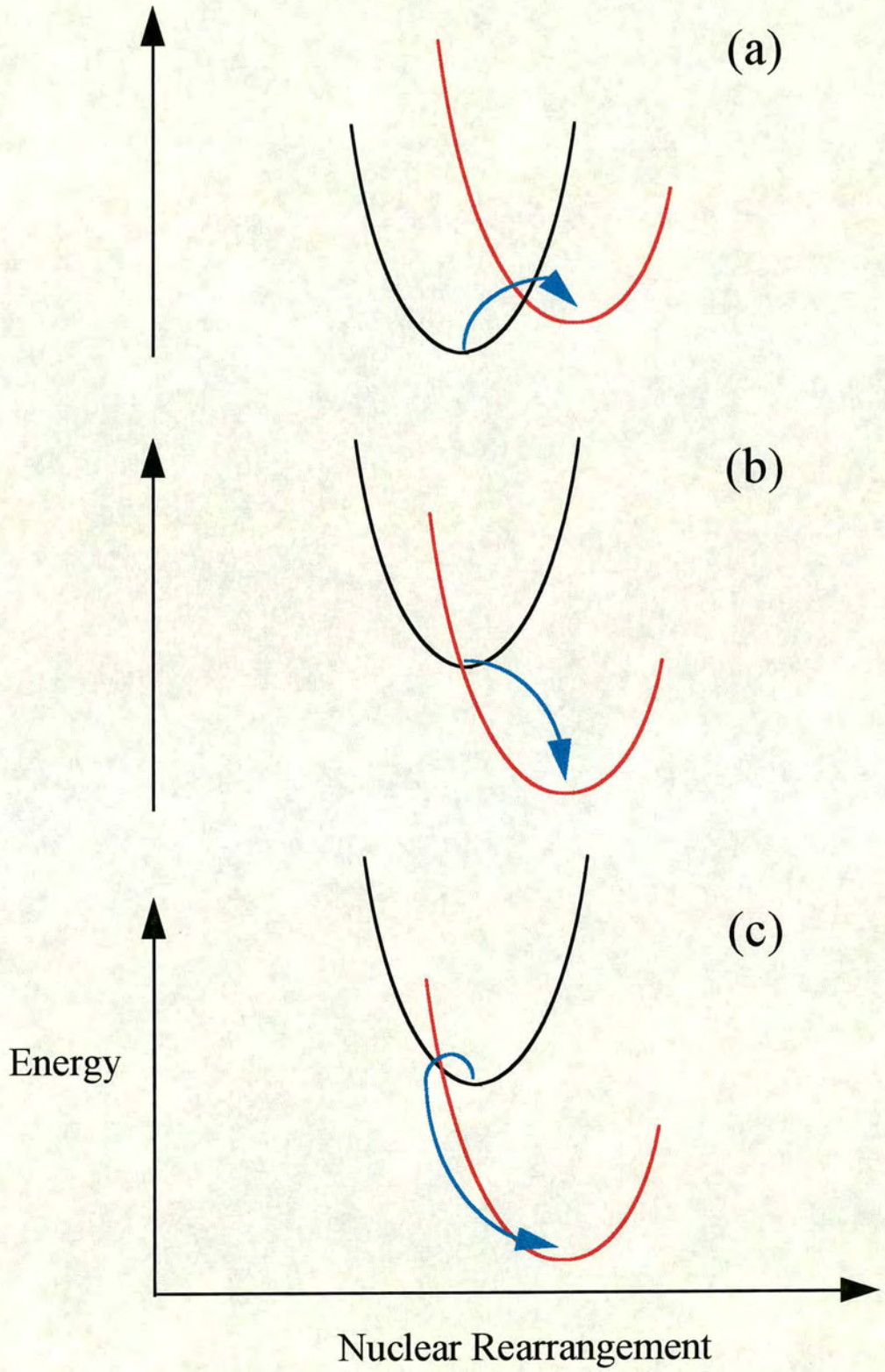

Figure 4. 2. : Typical energy profiles for the (a) *normal* ($\Delta G + \lambda > 0$), (b) *activationless* ($\Delta G + \lambda = 0$), and (c) *inverted* ($\Delta G + \lambda < 0$) regions predicted by Marcus theory. The black curve denotes reactants and the red curve denotes products, the blue arrows indicate the reaction pathway. (After Chapman & Mount, 1995).

These quantities are all shown in Figure 4.1. The activation energy predicts a simple Gaussian dependence of the electron transfer rate on free energy given by Equation 2:

$$k_{et} = k_{max}\ e^{-(\Delta G + \lambda)^2/4\lambda kT} \qquad (2)$$

Where: k_{et} is the observed electron transfer rate, k_{max} is the electron transfer rate when ΔG^* is zero, **k** is the Boltzmann constant and **T** is the absolute temperature.

Since λ is always positive, the term $(\Delta G + \lambda)$ determines the rate of reaction. Three cases can be distinguished for Equation 2: when $(\Delta G + \lambda)$ is greater than zero, equal to zero, and less than zero. These conditions are shown in Figure 4.2. (a, b & c) and are referred to as the *normal*, *activationless* and *inverted* regions respectively. Using Equations 1 & 2 we can calculate the variation in k_{et} with ΔG. This variation is shown in Figure 4.3. As the driving force of the reaction (ΔG) is increased the reaction rate rises to a maximum k_{max} when ΔG^* is at a minimum. The reaction is *activationless* at this point. Paradoxically, Marcus theory predicts a fall in electron transfer rate for any further increase in thermodynamic driving force. The existence of this *inverted* region is due to an increase in the energy barrier of the system. Several systems have demonstrated the existence of this region (*e.g.* Closs *et al.*, 1986; Miller *et al.*, 1984).

In the simplest model, the activationless electron transfer rate constant (k_{max}) is governed by two factors: the donor to acceptor distance and the intervening medium. The two factors influence the amount of overlap between donor and acceptor electronic orbitals. Orbital overlap decays exponentially with distance in accordance with Equation 3:

$$H_{AB} = H^0_{AB}\ e^{-\frac{1}{2}\beta(d-d_0)} \qquad (3)$$

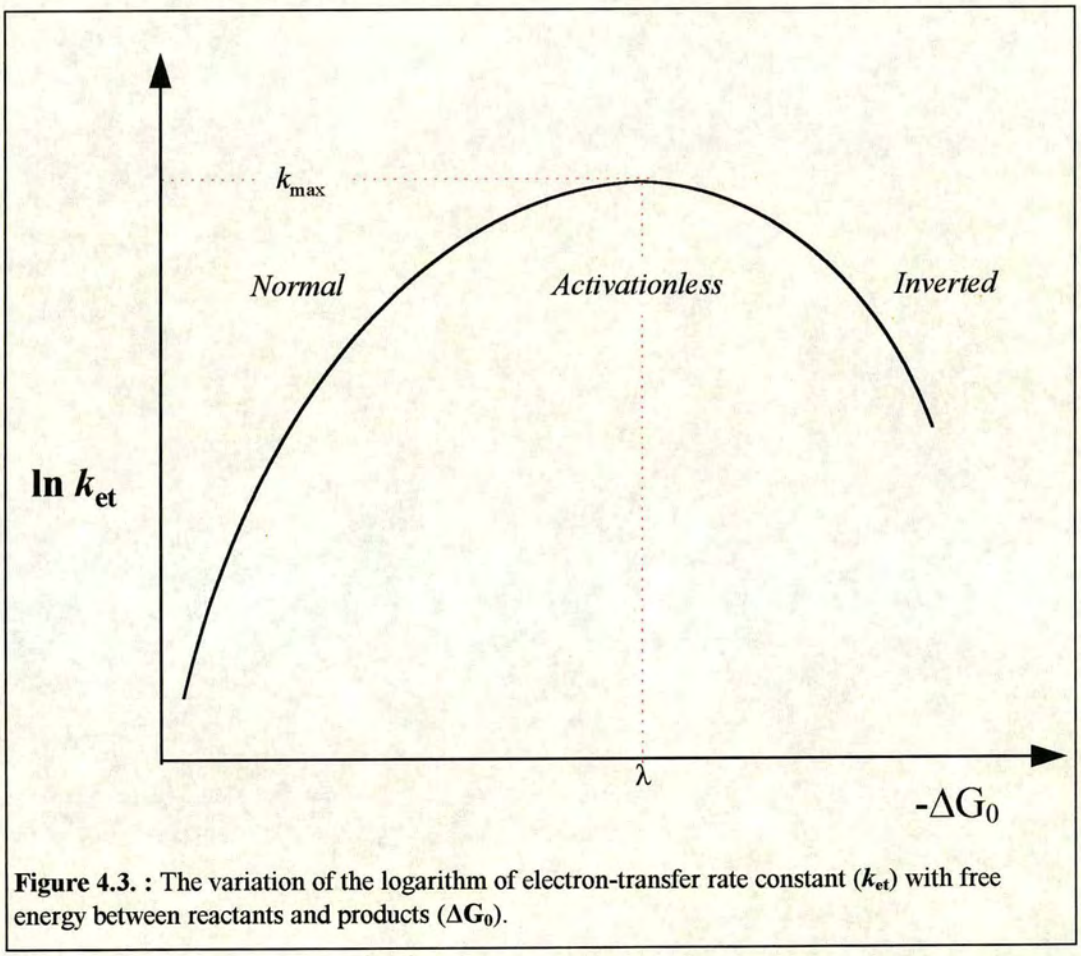

Figure 4.3. : The variation of the logarithm of electron-transfer rate constant (k_{et}) with free energy between reactants and products (ΔG_0).

The electron-transfer rate constant (k_{et}) is proportional to the tunnelling matrix element H_{AB}. The electronic coupling at close contact (d_0) is H^0_{AB} and the coefficient β is the rate of decay (in $Å^{-1}$) of coupling with distance d. A large β value, means electron transfer is only seen over short distances, e.g. β=2.8 $Å^{-1}$ *in vacuo*. A single β value of 1.4 $Å^{-1}$ provides a good estimate of k_{et} at any distance in the case of the photosynthetic reaction centre (Moser *et al.*, 1992; Moser & Dutton, 1992).The β values obtained for intraprotein electron transfer lie between the value for a vacuum and a rigid covalent linkage (β=0.7 $Å^{-1}$). Having a single β value means that protein can be thought of as an organic glass, *i.e.* the intervening medium is approximated as being homogeneous. This provides a reasonable description of the optimised photosynthetic reaction centre system but many proteins are best considered as consisting of a heterogeneous matrix (Winkler & Gray, 1992). An alternative approach, considering many different tunnelling pathways has been used to explain long distance electron transfer in proteins (Beratan *et al.*, 1987; Beratan *et al.*, 1991).

Quantum mechanical considerations such as electron tunnelling, modify the theory to account for the relative temperature insensitivity of observed electron transfer (Beratan & Onuchic, 1996; DeVault, 1984).

4.1.3 Intramolecular electron transfer in proteins

Marcus theory has been applied to experimental data from redox proteins using relatively simple equations with only three parameters. In order to apply the theory it is necessary to have a well defined structure and kinetic and thermodynamic models. These allow determination of d, ΔG_0 and k_{et} respectively. Replacement and alteration of cofactors, along with site directed mutagenesis allow variation of ΔG. The rate constants obtained allow a plot of log k_{et} v. ΔG^0 from which approximations of λ and k_{max} can be made, in accordance with Equation 2 (Moser *et al.*, 1995).

The bacterial photosynthetic reaction centre has provided a wealth of data since solution of the first structure from *Rhodopseudomonas viridis* (Deisenhofer *et al.*, 1985). The system consists of a number of membrane spanning polypeptides which bind 13 redox centres in close proximity. The system has been successfully used to study protein mediated electron transfer and determine rate constants (Moser *et al.*,

1992; 1995). The electron transfer rate constant data, which varies over 12 orders of magnitude (with distances from 3.6 Å to over 20 Å) yields a straight line plot for log k_{max} against distance and a β value of 1.4 $Å^{-1}$. In this case then, the protein medium appears to behave homogeneously, meaning that edge-to-edge distance from donor to acceptor is the main factor affecting rate.

Other approaches which have been used to study intraprotein electron transfer have involved; labelling the protein with inorganic redox reagents (Winkler & Gray, 1994; Winkler *et al.*, 1982) and replacing the haem groups in some proteins with porphyrin or zinc-containing porphyrin, both of which have useful photochemical properties (Ho *et al.*, 1985; Winkler & Gray, 1992). Commonly ruthenium has been attached to surface histidine residues of proteins, which were naturally occurring or introduced by mutagenesis (Winkler & Gray, 1992; Bjerrum *et al.*, 1995). The ruthenium atom introduces a photochemically active redox centre into the protein molecule. By engineering several binding sites for the ruthenium atom, it is possible to obtain rates for a variety of cofactor separations. In conjunction with ruthenation, swapping haems for zinc substituted porphyrins allows variation of the driving force (Axup *et al.*, 1988; Winkler and Gray, 1992).

4.2. *Saccharomyces cerevisiae* FLAVOCYTOCHROME b_2

4.2.1. Introduction

Flavocytochrome b_2 was first identified in 1928 (Bernheim, 1928). Since then it has been extensively studied and the ensuing literature has been reviewed (Lederer, 1991; Chapman *et al.*, 1991). The gene encoding the protein has been cloned and sequenced (Guiard *et al.*, 1985). The gene is over-expressed in *E. coli* (Black *et al.*, 1989) allowing over production of protein and construction of site directed mutants (Reid *et al.*, 1988). The structure of the enzyme is known and it has been used as a model for studying both intra-protein and inter-protein electron transfer.

4.2.2. Physiological function

Flavocytochrome b_2 is a soluble enzyme found in the intermembrane space of yeast mitochondria (Figure 4.4.). The protein contains the cofactors flavin mononucleotide (FMN) and protohaem IX, non-covalently bound. The enzyme is a primary dehydrogenase in one of the aerobic respiratory chains of the mitochondrion. This allows the yeast to respire L-lactate (Pajot & Claisse, 1974) even if the main respiratory chain is blocked. Flavocytochrome b_2 catalyses the oxidation of L-lactate to pyruvate and subsequently passes electrons on to its physiological partner, cytochrome *c*.

4.2.3. Three dimensional structure

Flavocytochrome b_2 has been isolated from the yeast *Saccharomyces cerevisiae* and the 2.4 Å resolution, X-ray crystal structure of native wild-type enzyme has been solved (Xia & Matthews, 1990). The structure of the recombinant enzyme, purified from *E. coli* has been determined more recently (Tegoni and Cambillau, 1994). The wild-type contains a product molecule, pyruvate, bound at the active site. The recombinant enzyme was crystallised with a molecule of sulphite covalently bound at the active site. The presence of the highly charged sulphite causes perturbation of some residues at the active site, as will be discussed later. The

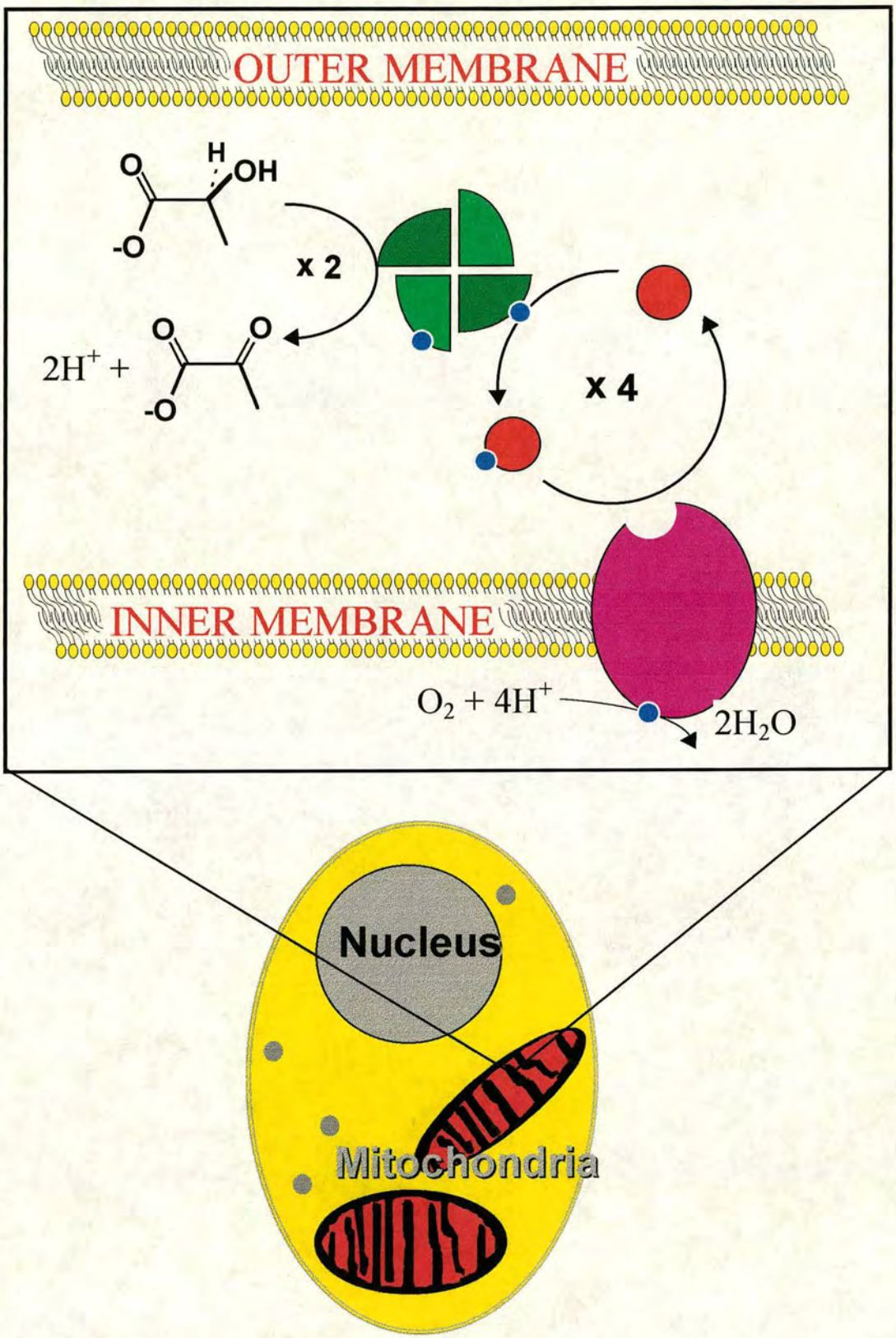

Figure 4.4.: Location and physiological function of flavocytochrome b_2. In the box, the green tetramer represents flavocytochrome b_2, the red circle represents cytochrome *c*, the membrane bound component is cytochrome *c* oxidase and the blue dots represent electrons.

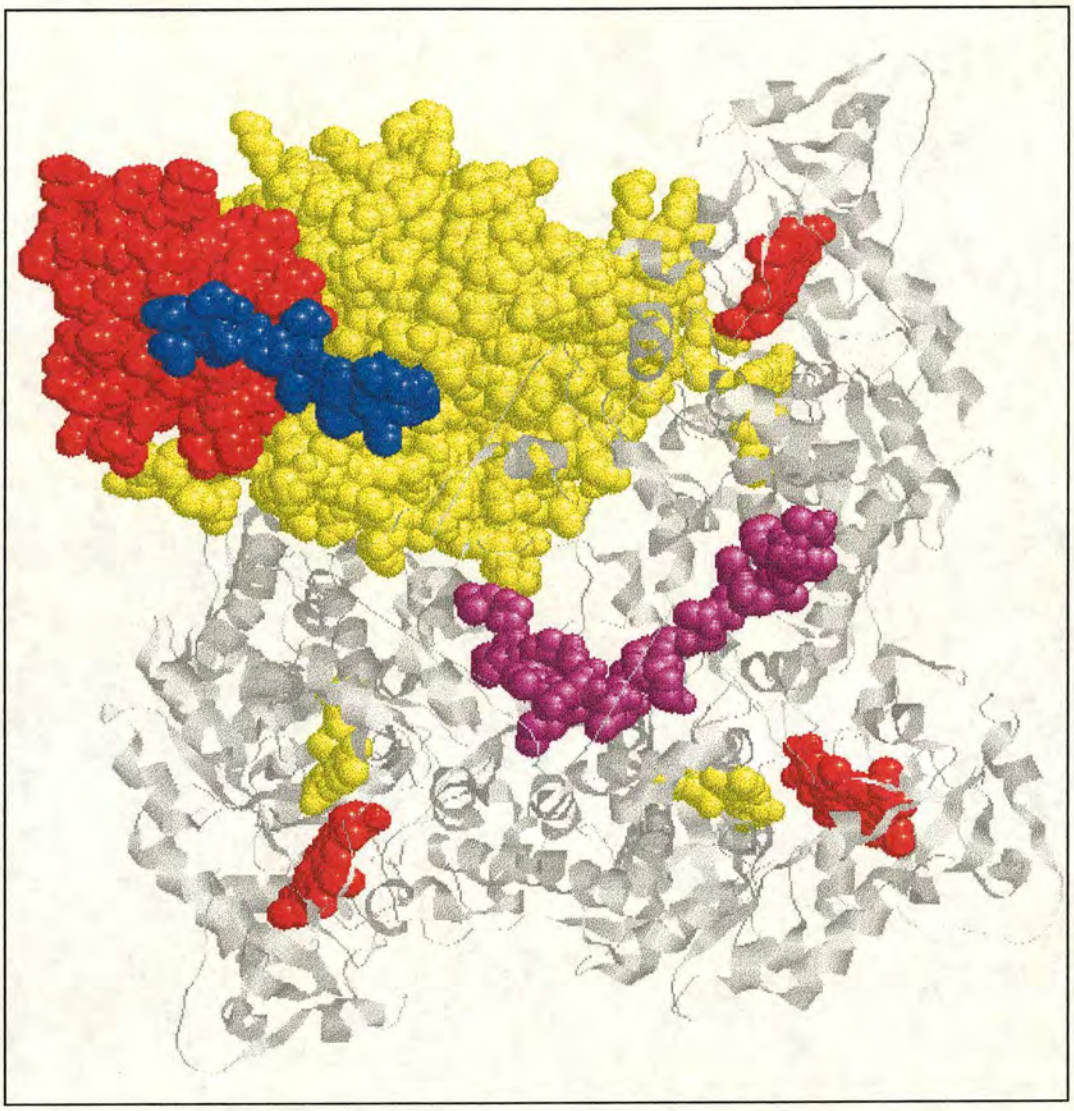

Figure 4.5. : The flavocytochrome b_2 tetramer. One subunit is shown in spacefill representation and the other three are shown in ribbon format, with the flavins in yellow and the haems in red. The different parts of the molecule are indicated on the spacefilled monomer. The red portion represents the haem domain, the blue portion is the hinge, the flavin domain is in yellow and the C-terminal tail is in purple.

recombinant enzyme also lacks the first 5 amino acids, which was an artefact of the cloning procedure (Black *et al.*, 1989). The recombinant enzyme retains full activity, even with this modification.

Flavocytochrome b_2 exists as a homotetramer (Figure 4.5.), with a molecular weight of 230 kDa (monomer weight 57.5 kDa). The monomers consist of two distinct domains. At the N-terminus of the protein (residues 1 to 100) is the haem binding domain, termed the haem core. The haem core structure closely resembles that of cytochrome b_5 family of proteins (Guiard & Lederer, 1979). The second domain (residues 101 to 487), called the flavin domain, has a classic $\alpha_8\beta_8$ TIM barrel structure. The flavin domain has a very similar structure to the related proteins, spinach glycolate oxidase and trimethylamine dehydrogenase (Scrutton, 1994; Lindquist *et al.*, 1991). It seems likely that the domain structure of the protein has arisen through a gene fusion at some stage. The flavin domain is responsible for binding FMN and also contains the protein active site. A short length of peptide, residues 89-103 (Sharp *et al.*, 1994), termed the hinge joins the flavin and haem domains together. The remainder of the protein, residues 488-511, is termed the tail. The tail forms important inter sub-unit contacts which help to maintain the quaternary structural integrity.

The crystal structure of the wild-type enzyme contains two distinct types of subunit (Xia & Matthews, 1990). In subunit 1 both domains are resolved and the FMN is in the fully reduced, hydroquinone state. No electron density attributed to either substrate or product is located in the active site. In subunit 2, electron density attributed to a molecule of pyruvate is seen at the active site. The flavin in this subunit is in the semiquinone state. Another feature of subunit two is the unresolved electron density for the cytochrome b_2 domain which is attributed to positional disorder. The recombinant enzyme is essentially isostructural with the wild-type, it too contains two crystallographically distinct types of subunit (Tegoni & Cambillau, 1994). Only a few differences between the structures have been noted. There are larger disordered regions in the recombinant structure, residues 300-320. In the recombinant structure, arginine 289 may adopt two different conformations, one similar to the wild-type enzyme and one totally different.

4.2.4. The catalytic cycle

Dehydrogenation of L-lactate at the active site generates two electron eqivalents. These electrons are then passed singly to two molecules of ferricytochrome *c* via the b_2 haem. The three oxidation states of the flavin (oxidised, semiquinone and hydroquinone) enable flavocytochrome b_2 to act as a "molecular transformer". This refers to its use of a two electron donor and a single electron acceptor. There is negligible direct transfer of electrons from FMN to cytochrome *c* (Balme *et al.*, 1995). The mechanism of L-lactate dehydrogenation has been extensively studied (Lederer, 1991 & references therein). The microscopic rate constants for the entire catalytic cycle have now been determined (Daff *et al.*, 1996).

Figure 4.6. illustrates the electron-transfer steps involved in a single turnover of the enzyme. Firstly, a molecule of L-lactate binds at the active site to form a Michaelis complex. Lactate then undergoes a two-electron oxidation to pyruvate. The two electrons generate a fully reduced flavin. The second step involves an intramolecular electron transfer from FMN to the b_2 haem. The next step involves binding of a cytochrome *c* molecule and an intermolecular electron transfer from the b_2 haem to cytochrome *c* haem. The flavin semiquinone is then able to transfer its remaining electron to the b_2 haem. This constitutes the rate determining step for the whole cycle, as the rates in Figure 4.6. indicate. The final step in the cycle is reduction of another molecule of ferricytochrome *c* which returns the enzyme to the start of the cycle.

4.2.5. Interdomain electron transfer

One turnover of the catalytic cycle of flavocytochrome b_2 involves two intramolecular electron-transfer steps. The first (following Figure 4.6) is from the flavin hydroquinone to b_2 haem, with a rate estimated to be greater than 1500 s^{-1} (Daff *et al.*, 1996). The second intramolecular electron-transfer is from the stable flavin semiquinone to haem with a rate of 120 s^{-1}. The shortest distance from FMN to haem in the crystal structure of flavocytochrome b_2 is approximately 9.8 Å. An optimised, activationless system would be expected to have a rate of ~10^9 s^{-1} over a distance of 10 Å. The observed rates for flavocytochrome b_2 indicate it is obviously nowhere near

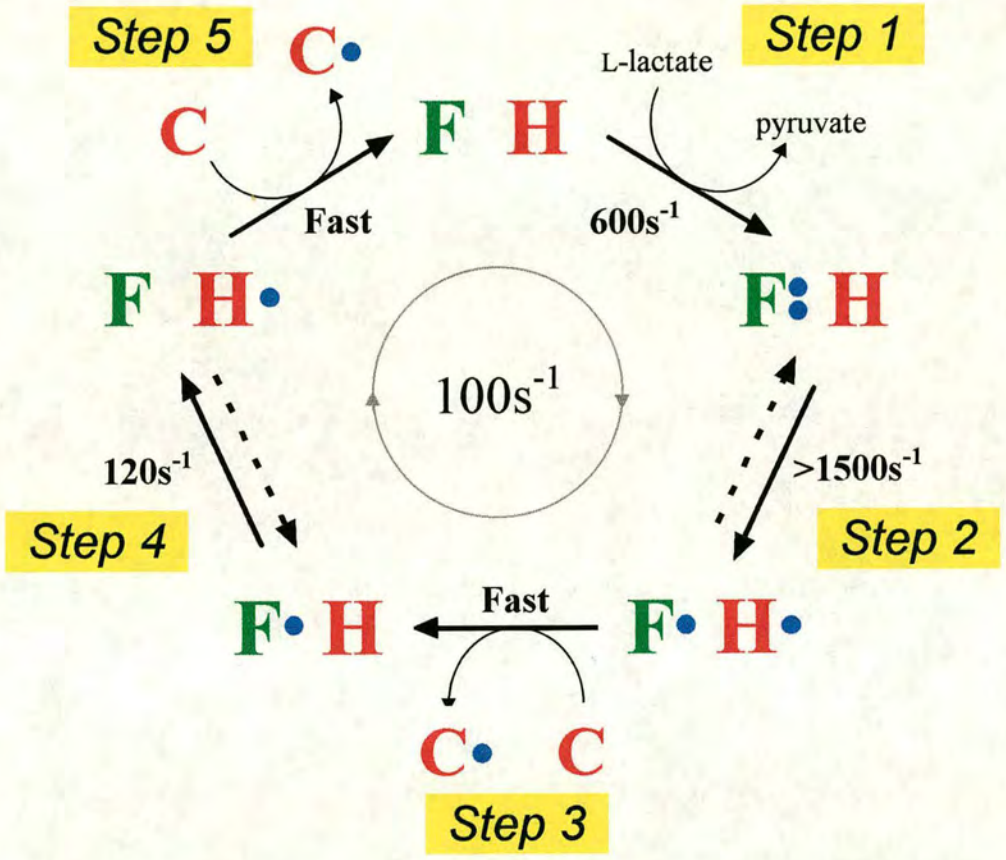

Figure 4.5 : The catalytic cycle of flavocytochrome b_2 based on individual electron-transfer steps. The symbols F and H denote the flavin and haem of flavocytochrome b_2 respectively, C represents cytochrome *c* haem. Blue dots denote electrons. *Step 1*: Reduction of FMN to its hydroquinone form, and oxidation of L-lactate to pyruvate. *Step 2*: Inter-domain electron-transfer from fully reduced FMN to b_2-haem, generating reduced haem and FMN semiquinone. *Step 3 & 5*: Binding and reduction of ferricytochrome *c* by b_2-haem. *Step 4*: Inter-domain electron-transfer from FMN semiquinone to b_2-haem. (From Daff *et al.*, 1996)

an optimised system. Even making alterations for the driving force and reorganisation energies do not lower predictions as far as the observed rate. Hence, another explanation is required.

A number of structural elements have been identified which affect the rate of flavin to haem electron transfer. The two domains of flavocytochrome b_2 are joined by a hinge polypeptide of approximately 10 residues in length, which allows them to move relative to each other. Both lengthening and shortening the hinge decrease the rate of interdomain electron transfer (Sharp *et al.*, 1994; 1996a & 1996b). The maximum electron transfer rate is found in the wild-type enzyme suggesting the hinge length has been optimised. The dependence of rate on hinge length is probably a combination of distance and orientation effects. It was suggested that the rate is limited by the frequency of productive encounters between the two domains. A further study used mutagenesis to construct an enzyme containing the flavin and haem domains from *S. cerevisiae*, joined by the hinge from *Hansenula anomala* flavocytochrome b_2 (White *et al.*, 1993). The two enzymes are homologous but the two hinges differ in length and sequence. The decrease in rate observed for the 'hinge-swap' enzyme suggest that optimal hinge compositions have evolved for both enzymes.

Strong interaction between the two domains has been ruled out by the evidence for mobility and the lack of interaction between the separate domains on mixing (Brunt *et al.*, 1992). Examination of the crystal structure reveals a network of hydrogen bonds between the two domains. The residue, Tyr-143 forms significant hydrogen bonding interactions between the two cofactors. In subunit 1 of the crystal structure, it is hydrogen bonded to a haem propionate and a water molecule. In subunit 2, the haem domain is disordered and Tyr-143 forms a hydrogen bond with a molecule of pyruvate in the active site. Removal of this interaction, in the Y143F mutant enzyme significantly reduces the rate of flavin to haem electron transfer (Miles *et al.*, 1992), from >1500 s^{-1} to 20 s^{-1}. The lowering of electron transfer rate was attributed to a reduction in the number of productive encounters between the two domains. If a pathway model for electron transfer were correct, this hydrogen bond

could play a significant part in facilitating flavin to haem electron transfer (Daff, 1996).

A recent study used NMR to probe the mobility of the haem domain (Bell *et al.*, 1996; Bell, 1997) in the wild-type enzyme, two hinge extension mutants and a disulphide bridged mutant. The results obtained for the wild-type enzyme somewhat contradict NMR results for *Hansenula anomala* flavocytochrome b_2 (Labeyrie *et al.*, 1988). The *H. anomala* study focused on the linewidths of paramagnetically shifted haem peaks which were narrower than expected for the large tetrameric enzyme. The narrow linewidths were explained in terms of intrinsic mobility of the haem domain. The results obtained by Bell, had linewidths close to those expected for a protein the size of the flavocytochrome b_2 tetramer. However, the two mutant enzymes containing longer hinge peptides had shorter correlation times, supporting the theory of increased haem domain mobilty.

The burden of experimental evidence suggests that the haem domain of flavocytochrome b_2 is mobile. The data from the point mutant Y143F indicates that interactions in the region between the two domains can have major effects on interdomain electron transfer. In the crystal structure, a number of residues lie between the domains and form interdomain contacts. The purpose of this study was to investigate the effect of two point mutations in this region, on interdomain electron transfer. The mutations made were, Arg289→Lys and Lys296→Met.

Part 2-Flavocytochrome b_2

Chapter 5 : *MATERIALS AND METHODS*

5.1. GROWTH AND MAINTENANCE OF STRAINS

5.1.1. Bacterial strains

Name	Genotype
E. coli TG1	*supE, hsdΔ5, thi, Δ(lac-pro), F', trad36, proAB$^+$, laqI^q, lacZΔM15*
E. coli AR120	*λM99, (F', galK2, LAM', prsL200),* derivative *(cI, Δ-gal, nadA::Tn10)*

5.1.2. Growth of bacterial cultures

Liquid cultures of bacteria were grown by inoculating a given volume of broth containing appropriate antibiotic, with a single colony using a sterile loop. The cultures of *E. coli* were all grown at 37°C. Bacteria were stored for up to 1 month at 4°C on LB agar plates containing antibiotic.

5.1.3. Growth media

Luria-Bertani Broth (per litre)	
Bacto-tryptone	10g
Bacto-yeast	5g
NaCl	5g

5.1.4. Antibiotics

	[stock] mg mL^{-1}	[working] μg mL^{-1}
Ampicillin	100	100
Carbenicillin	50	50

Stock solutions were sterilised with 0.22 μm filters and stored at -20°C. Antibiotics were added to growth media once it had been autoclaved and cooled.

5.2. BUFFERS

5.2.1. Protein purification buffer

305 mL of 200 mM Na_2HPO_4

195 mL of 200 mM NaH_2PO_4

500 mL dH_2O

0.96 g L-lactate (lithium salt)

0.37 g EDTA (disodium salt)

5.2.2. 10 mM Tris/HCl buffer, pH 7.5, (I=1.0)

NaCl	5.265g
1 M HCl	10 mL
dH_2O	to 1 L

pH adjusted to 7.5 with tris base

5.3. PURIFICATION OF FLAVOCYTOCHROME b_2

5.3.1. Cell Growth

A starter culture containing about 50 mL of LB medium and 50 μg mL^{-1} of the antibiotic carbenicillin, was inoculated with a single bacterial colony. The culture was grown overnight at 37°C in an orbital incubator. Carbenicillin is used in preference to ampicillin because it gives a stronger selection for the plasmid pDSb_2 and results in greater over-production of flavocytochrome b_2.

A small aliquot (typically 5 mL) of the overnight culture was added to flasks containing 500 mL of LB and carbenicillin, typically 5 L was grown. The flasks were incubated overnight at 37°C. The cells were pelleted by centrifugation at 10000g for 15 minutes. The resulting pellet was frozen at -20°C until it was required.

5.3.2. Cell Lysis

The pellet of cells were thawed and then 'snap-frozen' in liquid nitrogen to facilitate cell lysis. The cells were allowed to thaw and then resuspended in about 200 mL of purification buffer (100 mM phosphate pH 7, 1 mM EDTA, 10 mM L-lactate). EDTA assists cell lysis by removing calcium ions which stabilise the cell walls, the lactate helps to maintain flavocytochrome b_2 in it's stable reduced form. Lysozyme (~0.2 mg mL^{-1}) was added to the cell suspension and the mixture was stirred at 4°C for 90 minutes. The suspension was spun at 39000g for 20 minutes to remove cell debris and unlysed cells and the red / pink supernatant containing flavocytochrome b_2 was retained. If the cell pellet was still very red, it was subjected to another round of lysis. All supernatant was pooled for the next purification step.

5.3.3. Ammonium sulphate precipitation

This stage of the purification procedure removes bulk contaminants from the supernatant containing flavocytochrome b_2. It is based upon the different solubilities which proteins exhibit. As the salt concentration of a protein solution is increased, proteins begin to "salt out".

The volume of supernatant from the previous step was measured and ammonium sulphate was added, to give a 40% saturated solution. The solution was spun at 39000g for 15 minutes. The pellet containing impurities was discarded and the supernatant was retained. The ammonium sulphate concentration of the supernatant was increased to 70% saturation. The 70% saturated solution was spun at 39000g for 15 minutes. A pink pellet, containing flavocytochrome b_2 was obtained, the supernatant was discarded.

5.3.4. Dialysis

The protein pellets were dissolved in a small volume of protein purification buffer and added to seamless dialysis tubing (typically 12-14000 molecular weight cut off). The dialysis tubing is soaked in dH_2O for around 30 minutes before use. The dialysis bag was sealed and placed in 5 L of half-strength dialysis buffer (50 mM phosphate). Nitrogen was bubbled through the buffer and the dialysis was left overnight. The protein was removed from the dialysis membrane and spun at 39000g for 10 minutes to remove any insoluble material.

5.3.5. Ion-exchange chromatography

The first chromatography step uses DE-52 anion exchange resin to remove impurities. Flavocytochrome b_2 itself does not stick to the column but a number of the other proteins present do.

The column matrix was swollen by addition of 100 mM phosphate buffer and fines were decanted from the slurry. A typical column would be poured to give dimensions of 2.5 x 15 cm. The pH of buffer eluted from the column was checked to ensure proper equilibration of the resin. The dialysed protein solution was loaded onto the column, washed through with buffer and collected as soon as it eluted.

5.3.6. Hydroxyapatite column chromatography

Flavocytochrome b_2 binds tightly to hydroxyapatite allowing removal of the remaining impurities. A column of approximate dimensions 2.5 x 10 cm was poured and equilibrated with two volumes of purification buffer. Flavocytochrome b_2 bound

onto the column giving a tight pink / red band near to the top. The protein was eluted with a 0 to 10% ammonium sulphate gradient. Fractions of flavocytochrome b_2 were collected and their purity was assessed spectrophotometrically. The ratio UV / visible peaks (A_{279nm} / $A_{423\ nm}$) give a useful measure of flavocytochrome b_2 purity. For totally pure protein a ratio of 0.5 is expected. Fractions with a ratio below 1 were generally pooled. Protein for stopped flow kinetics was purified with greater stringency.

5.3.7 Protein concentration and storage

The pooled protein fractions were precipitated by the addition of ammonium sulphate to 70% saturation and spun at 39000g for 10 minutes. The pellets obtained were resuspended in a very small volume of tris buffer, keeping it as concentrated as possible. The protein solution was run down a G-25 (gel filtration) column of dimensions 1.5 x 15 cm in tris buffer. The G-25 column removes the salt and lactate from the protein. As the lactate is removed, flavocytochrome b_2 becomes oxidised and changes colour from pink to orange. The oxidised protein is eluted and then frozen into small balls by dripping it into liquid nitrogen. In this state, protein is stored long term, without appreciable loss activity.

5.4. STEADY-STATE KINETICS

5.4.1. Introduction

The concept of the steady-state is widely applied to enzyme kinetics. It refers to the situation when, the quantity of a particular species is constant "in steady-state". The concept is generally applied to the concentration of enzyme bound intermediates. Steady-state applies to dynamic process where the rate of depletion of the species is balanced with the rate of formation. The steady state is an approximation, as substrate is being depleted over time. If activity is measured over short periods the change is negligible and the approximation is a good one.

The initial rate, V, of an enzyme catalysed reaction tends towards a maximum, saturation value, V_{max} as the substrate concentration is increased. This type of behaviour is described well by the Michaelis-Menten equation:

$$V/[E_{total}]=(k_{cat} [S]) / (K_M + [S])$$

The experimentally determined parameters are; k_{cat}, the catalytic turnover number- representing the maximum number of substrate molecules converted to product per active site per unit time (units s^{-1}), and K_M, the Michaelis constant which in some cases is equal to K_s, the dissociation constant, for the enzyme-substrate complex (units M).

5.4.2. Kinetic parameter determination

Flavocytochrome b_2 obeys Michaelis-Menten kinetics, making its reactions relatively easy to study. For the turnover of lactate to pyruvate under steady state conditions, flavocytochrome b_2 needs to pass the resulting electrons to an external acceptor. Either its physiological partner, cytochrome *c*, or the artificial electron acceptor ferricyanide, can be used. Reduction of either acceptor can be followed under saturating conditions, to obtain steady state turnover data for the enzyme.

All experiments were performed on a Shimadzu 2101PC spectrometer. Kinetics were performed in 10 mM Tris-HCl buffer, pH 7.5, ionic strength adjusted to

100 mM with NaCl. Assays were performed in quartz cuvettes of path length 0.1, 0.2, or 1 cm.

The parameters, k_{cat} and K_M were determined by carrying out assays at a range of substrate concentrations. All assays were done under conditions of saturating substrate concentration. Saturation values for the acceptors were determined by fixing the substrate concentration whilst varying the acceptor concentration. The data was manipulated using the Microcal Origin package.

5.4.2.1. Ferricyanide

Assays were carried out at 1 mM ferricyanide for the R289K mutant and at 5 mM for the K296M mutant. The use of higher ferricyanide concentrations necessitates changing the path length of the cuvette to 0.1 or 0.2 cm. The activity was recorded as a rate of decrease in absorbance at 420 nm as the ferricyanide becomes reduced. The ferricyanide extinction coefficient $\Delta\varepsilon_{ox\text{-}red} = 1010\ M^{-1}\ cm^{-1}$ was used.

5.4.2.2. Cytochrome c

Horse heart cytochrome *c* (type IV Sigma) was used at a saturating concentration of around 50 μM. The cytochrome *c* was made up freshly before use and its concentration was determined from the reduced spectrum. The extinction coefficient at 550 nm for reduced cytochrome *c* is 30900 $M^{-1}cm^{-1}$. Assays were monitored at 550 nm using the extinction coefficient $\Delta\varepsilon_{ox\text{-}red} = 22640\ M^{-1}cm^{-1}$ (Hazzard *et al.*,1986) .

5.4.2.3. Flavocytochrome b_2

The enzyme concentrations were determined using the absorbance spectrum of the reduced enzyme. The Soret peak extinction coefficient at 423 nm is $\varepsilon_{red} = 183000\ M^{-1}cm^{-1}$. Enzyme was thawed on ice and only diluted to working concentration immediately before use.

5.5. STOPPED-FLOW KINETICS

5.5.1 Introduction

Steady-state kinetic data is useful for providing overall turnover rates. These may be a combination of rates for many individual steps. The stopped-flow technique allows analysis of some of these microscopic rates in a pre-steady-state situation. The basic experiment involves rapid mixing of a small, equal volume of enzyme and substrate which is monitored spectrophotometrically. The small lag time between mixing of the solutions and monitoring of the experiment, is referred to as the lag time (typically <1 ms). After the rapid mixing and a single turnover, the system will of course, go into steady state. For flavocytochrome b_2, a number of electron transfer steps can be monitored; substrate to flavin (monitoring FMN reduction by lactate), interdomain electron transfer from FMN to haem (monitoring haem reduction by lactate).

5.5.2. Experimental details

All experiments were performed on an Applied Photophysics SF.17 micro volume stopped-flow spectrofluorimeter. Data were collected and analysed using the SF.17MV software package. All experiments were performed in 10 mM Tris-HCl buffer, pH 7.5 (I=0.1 M) at 25±1°C.

5.5.3. Pre-steady-state oxidation of L-lactate

Several traces were obtained using a suitable timebase and averaged before analysis. Reduction of the FMN prosthetic group was monitored at 438.3 nm which is a haem isosbestic point. Haem reduction was monitored at 557 nm.

5.5.4. 'Super-steady-state' reduction of cytochrome *c*

This experiment makes use of the fact that once reduced flavocytochrome b_2 and cytochrome *c* have undergone one turnover in the machine, they are effectively under steady state conditions. By monitoring the cytochrome *c* reduction rate as the

oxidised cytochrome *c* concentration falls, one has another method for determining k_{cat} and K_M.

A 2-3 mL solution of oxidised cytochrome *c* was made up to approximately 30 μM. Flavocytochrome b_2 was made up to about 0.1μM in tris buffer containing 10 mM L-lactate. After mixing, this gives rise to a cytochrome *c* concentration of around 15 μM which when reduced, reaches the practical limit for absorbance measurements on the equipment. The reaction is monitored at 550 nm. The two solutions were rapidly mixed and 1000 data points were collected over 5 seconds. A number of traces were obtained and then averaged. The data was analysed using Microcal Origin. A quick ferricyanide assay was performed to check the activity of the enzyme. The raw data was analysed as described by Short, 1996.

Part 2-Flavocytochrome b_2

Chapter 6 : *RESULTS AND DISCUSSION*

6.1. INTRODUCTION

As has been mentioned previously, the two domains of flavocytochrome b_2 are joined by a short length of polypeptide which is termed the hinge. It has been postulated that the hinge is flexible and allows movement of the haem domain relative to the flavin domain. This is supported by evidence from NMR data of the intact *Hansenula anomala* enzyme (Labeyrie *et al.*, 1988). The linewidth of haem resonances in the intact enzyme were compared with those from the cytochrome b_2 core (the independently produced haem domain). It was concluded that the linewidths observed in the intact enzyme were too narrow unless the haem domain had intrinsic mobility. However, a recent NMR study suggested lower mobility for the haem domain in the *S. cerevisiae* enzyme (Bell, 1997). Other evidence for haem domain mobility comes from the crystal structure of flavocytochrome b_2 (Xia & Matthews, 1990). In subunit 2 the haem domain was disordered in the electron density map, this was attributed to mobility.

In the X-ray crystal structure of the enzyme, a network of interactions can be seen between the two domains. These include several hydrogen bonds and an interdomain salt bridge (Figure 6.1.). The salt bridge is formed between lysine 296 on the flavin domain and a propionate on the haem domain. In order to probe the importance of this residue, the mutation Lys296→Met was made. This retains most of the steric bulk of lysine but removes the charge. If this salt bridge is an important interdomain interaction, its removal may affect mobility of the two domains and hence the intraprotein electron transfer rate.

This study is also concerned with residue Arg-289 which lies between the two domains, hydrogen bonded to the haem propionate via a water molecule. Arg-289 is also notable because it displays two different conformations in the crystal structure of recombinant flavocytochrome b_2 (Tegoni & Cambillau, 1994). This suggests it may have some conformational flexibility. An explanation for the two conformations observed for Arg-289 is an electrostatic attraction to the sulphite molecule bound at the active site in this particular structure.

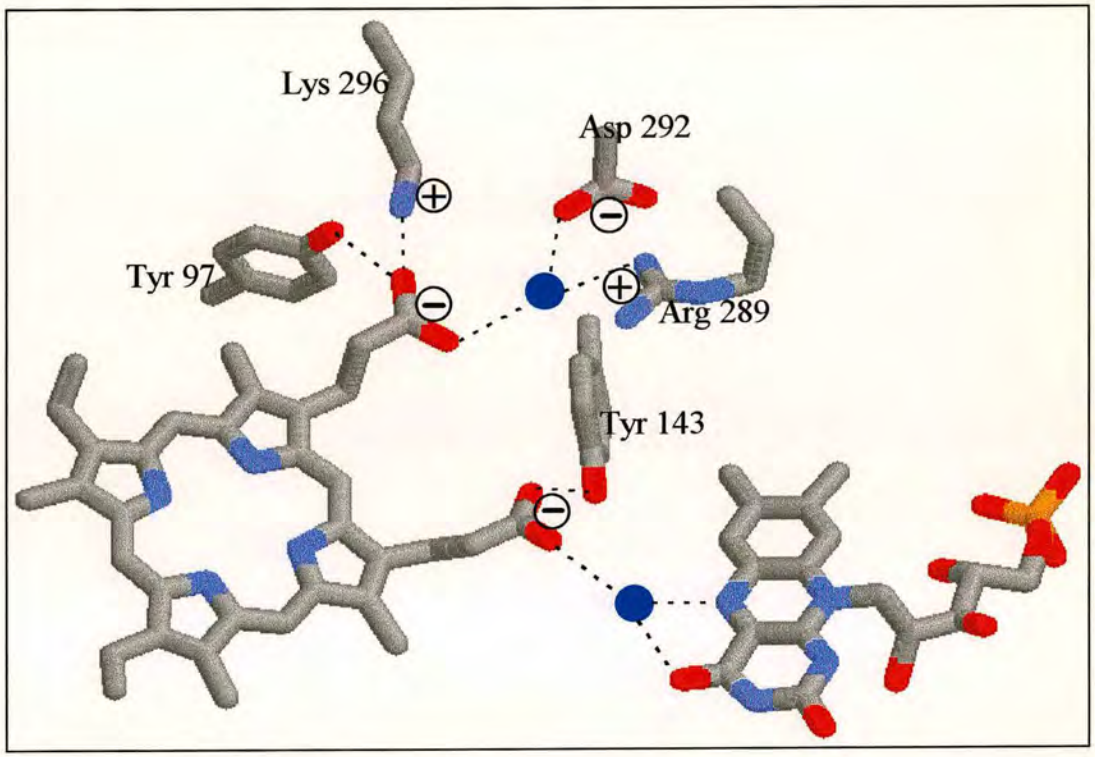

Figure 6.1. : Some of the hydrogen bonding interactions observed in the crystal structure of flavocytochrome b_2 . The blue circles indicate water molecules. The hinge peptide lies above the diagram in its present orientation. Arg-289 hydrogen bonds with a haem propionate via a water molecule, Lys-296 lies in the flavin domain and forms a salt bridge with a haem propionate-the only interdomain salt bridge.

In the wild-type crystal structure, a molecule of product, pyruvate is bound at the active site. The residue also stacks closely with Arg-376, which is known to bind and orientate the carboxylate group of lactate in the enzyme active site (Black *et al.*, 1989). Arg-376 is strictly conserved in the sequence of a number of flavin containing dehydrogenases and oxidases, as is Arg-289 which is shown in Figure 6.2. (e.g. *Hansenula anomala* flavocytochrome b_2, spinach glycolate oxidase, *Pseudomonas putida* mandelate dehydrogenase & rat kidney hydroxy-acid oxidase (Daff, 1996).

6.2. THE LYSINE296→METHIONINE MUTANT

6.2.1. Steady-state kinetic data

The steady-state assay for flavocytochrome b_2, L-lactate dehydrogenase activity involves spectroscopic monitoring of electron acceptor reduction (ferricyanide or ferricytochrome *c*). Kinetic data were recorded over a range of lactate concentrations and fitted to a Michaelis function to yield values of k_{cat} and K_M. In order to ensure saturating conditions, electron acceptor concentrations were also varied. One effect of the mutation was an increase in the ferricyanide K_M from 0.1 mM in the wild-type, to 0.6 mM. The effect might be explained by the decrease in the overall positive charge of the enzyme due to the removal of a lysine. As the acceptor is negatively charged, there will be a reduced electrostatic attraction between the two. The K_M for cytochrome *c* did not appear to be affected, but this is not unexpected. The interaction between flavocytochrome b_2 and cytochrome *c* is complex and thought to take place primarily on the haem domain, at a site remote from the mutation.

As can be seen from the data in Table 6.1., the steady-state characteristics of K296M for L-lactate oxidation are essentially unaltered from the wild type.

Table 6.1. : Steady-state kinetic parameters determined for L-lactate oxidation with saturating potassium ferricyanide as the electron acceptor. (Tris/ HCl buffer, pH 7.5, 25°C, I=0.1 M.)

	Lactate k_{cat} (s^{-1})	Lactate K_M (mM)
Wild-Type	407 ± 10	0.49 ±0.05
K296M	375 ± 50	0.5 ± 0.2

6.2.2. Stopped-flow kinetic data

Kinetic parameters were obtained for the reduction of the flavin and haem in the mutant flavocytochrome b_2.. As with the steady-state data, the kinetic characteristics were equal to the values obtained for wild-type, within experimental error. It seems apparent that the salt bridge seen in the crystal structure has little influence on the catalytic competence of the enzyme. It also indicates that Lys-296 and the salt bridge it forms have no influence on the flow of electrons from flavin to haem.

Table 6.2. : Stopped-flow kinetic parameters for reduction of the haem and flavin in flavocytochrome b_2 observed upon mixing the enzyme with L-lactate (Wild-type values from Miles *et al.*, 1992). (Tris/ HCl buffer, pH 7.5, 25°C, I=0.1 M.)

	Haem Reduction rate (s^{-1})	Flavin Reduction Rate (s^{-1})
Wild-Type	445 ± 10	604 ± 60
K296M	392 ± 50	524 ± 70

6.3. THE ARGININE289→LYSINE MUTANT

The location of Arg-289, close to Arg-376 and the active site of flavocytochrome b_2 is illustrated in Figure 6.2. It is possible that in the Michaelis complex the negative carboxylate of lactate could be neutralised by a combination of the charges on Arg-376 and Arg-289.

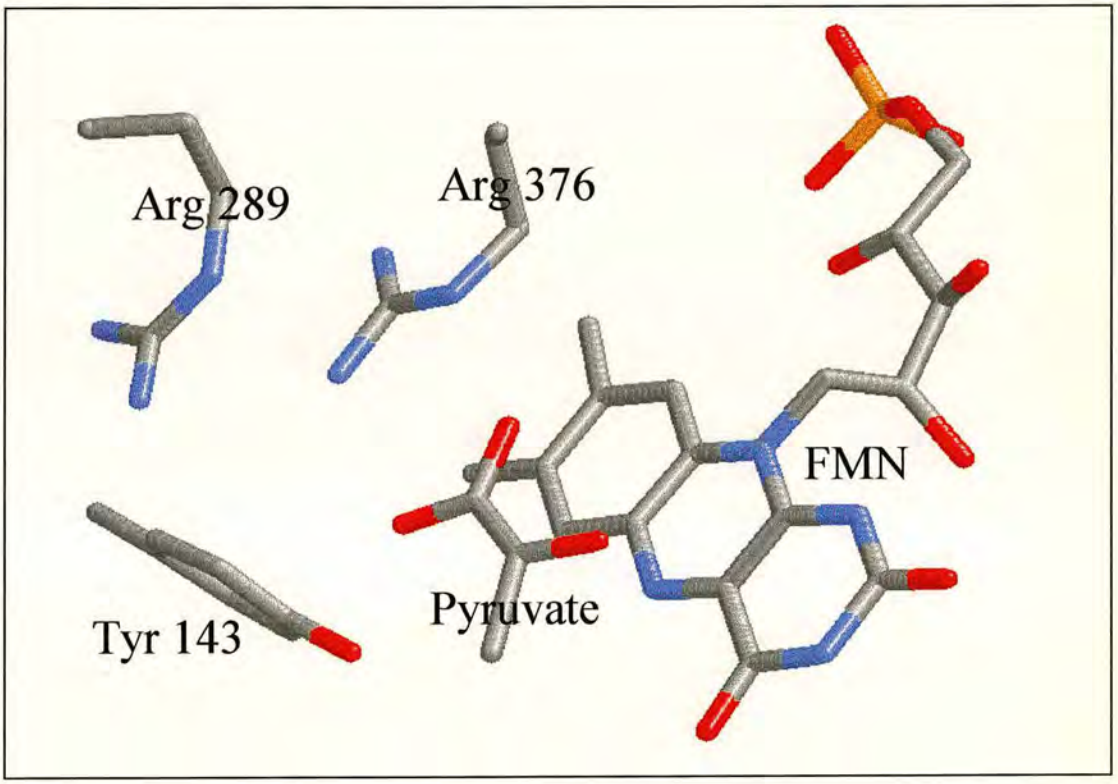

Figure 6.2. : The location of arginine 289 relative to the active site of flavocytochrome b_2. The residue stacks against arginine 376, responsible for binding the carboxylate of the substrate, L-lactate (here a molecule of the product, pyruvate is shown at the active site). Also shown is residue tyrosine 143 which known to influence interdomain electron transfer rates (Miles *et al.*, 1992).

6.3.1. Steady-state kinetic data

Sample data shown in Appendix 1.

It is obvious from the data in Table 6.3. that the major effect of the mutation has been to increase the K_M for L-lactate relative to wild-type. The altered K_M, which corresponds to decreased substrate binding strength, might be explained by an altered interaction with the substrate. However, a local structural alteration cannot be ruled out. The mutant enzyme has approximately tenfold lower activity than wild-type with either ferricyanide or cytochrome *c* as the terminal acceptor. Although ferricyanide has no physiological relevance, it is a useful acceptor because it can accept electrons from both the flavin and haem domains. This is in contrast to the physiological acceptor, cytochrome *c* which can only accept electrons from the haem domain of flavocytochrome b_2. Information about the rate of electron flow through the enzyme can be inferred from the ratio of k_{cat} using the two acceptors. The ratio is the same for R289K as for wild-type (within experimental error) implying no major perturbation of the flavin to haem electron transfer rate. It is most likely that the change in the kinetic parameters are due to effects at the enzyme active site.

A kinetic isotope effect (KIE) was also determined for the mutant enzyme, using L-[2-^{2}H]lactate as a substrate and ferricyanide as the acceptor. The KIE determined for steady state turnover was 4.4 ± 1.5 which is the same as wild-type (4.7 ± 0.4), implying a similar transition state in both enzymes.

Table 6.3. : Steady-state kinetic parameters for L-lactate oxidation by wild-type and the R289K mutant enzyme using two different terminal electron acceptors. K_M and k_{cat} refer to lactate. (Tris/ HCl buffer, pH 7.5, 25°C, I=0.1 M.)

	Ferricyanide		**Cytochrome *c***	
	k_{cat} (s^{-1})	K_M (mM)	k_{cat} (s^{-1})	K_M (mM)
Wild-Type	400 ± 10	0.49 ± 0.05	207 ± 10	0.24 ± 0.04
R289K	33 ± 3.9	3.2 ± 0.4	17.7 ± 0.2	0.95 ± 0.03

6.3.2. Stopped-flow kinetic data

Sample data shown in Appendix 1.

The stopped flow kinetic data obtained for the R289K mutant are summarised in Table 6.4. The traces were fitted to double exponential curves to allow for rearrangement of electrons between protomers (Chapman et al., 1994, Capelliere-Blandin, 1975). This electron rearrangement occurs after the initial reduction of the flavin and haem when no external electron acceptor is present. The rate of flavin reduction has fallen quite dramatically from that obtained for the wild type. The decrease can be attributed to transition state destabilisation. The rate observed for haem reduction is limited by flavin reduction. From Figure 4.5. it is apparent that the observed rate is influenced by step 1 and step 2 of the catalytic cycle.

Table 6.4. : Stopped-flow kinetic parameters obtained for L-lactate oxidation by the R289K mutant compared with those for wild-type. No K_M was determined for the mutant. (Tris/ HCl buffer, pH 7.5, 25°C, I=0.1 M.)

	Flavin reduction		**Haem reduction**
	k (s^{-1})	K (mM)	k (s^{-1})
Wild-type	604 ± 60	0.84 ± 0.2	445 ± 50
R289K	20 ± 2	1.7 ± 0.5	15 ± 2

In order to obtain an estimate of the true rate for step 2 alone, the method of Daff *et al.* (1996) was used. The method involves mixing fully reduced flavocytochrome b_2 with oxidised cytochrome *c*, this facilitates selective oxidation of the b_2 haem. Monitoring the flavocytochrome b_2 haem re-reduction by the flavin allows estimation of the electron transfer rate. It was clear from experiments that the rate was still very rapid as haem reduction all occurred during the dead time of the spectrophotometer. This supports the steady-state data which show no significant effect on interdomain electron transfer.

Kinetic isotope effects were determined for R289K using L-[2-^{2}H]lactate and are shown in Table 6.5. The value obtained for flavin reduction indicates that cleavage of the carbon-α-hydrogen bond in lactate is the major rate limiting step in flavin reduction. Kinetic isotope effects measured for haem are unaltered, again supporting the view that flavin to haem electron transport is unaffected.

Table 6.5. : Isotope effects obtained using L-[2-^{2}H]lactate(Tris/ HCl buffer, pH 7.5, 25°C, I=0.1M.)

	KIE for flavin reduction	**KIE for haem reduction**
R289K	6.8 ± 1.1	6.2 ± 0.9
Wild-type	8.1 ± 1.4	6.3 ± 1.2

6.3.3. The R289K crystal structure

The R289K mutant provided by us, has been crystallised in the lab of Professor Scott Matthews in St. Louis, preliminary data have allowed determination of a low resolution structure. Figure 6.3. shows the active site region from the R289K mutant structure overlaid on the wild-type structure. Due to uncertainty in the data, it is only possible to draw tentative conclusions.

The main difference between the two structures is the position of the Arg-376 side-chain. The side-chain of Lys-289 lies in essentially the same position as Arg-289. The movement in Arg-376 residue is probably responsible for the alteration observed in the kinetic characteristics of the enzyme, especially the increased K_M. Refinement of the crystal structure will allow distances to be assigned for the conformational shift of active site side-chains.

6.4. CONCLUSIONS

A number of previous studies have investigated the domain structure of flavocytochrome b_2 and the electron transfer from flavin to haem. It has been established that the interface between the flavin and haem domains contains residues which play a role in catalysis and interdomain electron transfer. Single mutations (*i.e.*Tyr-143→Phe, Miles *et al.*, 1992) have been shown to have substantial effects on the flavin to haem electron-transfer rate. In the case of the Tyr-143 mutation, a critical hydrogen bond between the two domains is removed. The Tyr-143 sidechain actually lies between the flavin and haem in the crystal structure and is thought to participate in the electron transfer between the two cofactors. Work which introduced mutations into the hinge region of the enzyme (Sharp *et al.*, 1996a & b), also affected the rate of flavin to haem electron transfer. These results implied that the mobility of the two domains had been affected. The mobility is thought to be a factor governing the rate of flavin to haem electron transfer. In terms of Marcus theory, mobility of the two domains would affect the donor to acceptor distance. This also affects the nature of the intervening medium for through space electron transfer. The distance of 9.8 Å between flavin and haem, observed in the crystal structure may be due to one of many conformations actually achieved in solution. NMR solution studies on flavocytochrome b_2 probed the domain mobility but the results were ambiguous (Bell, 1997). Bell also linked the two domains of the enzyme with a disulphide bridge to try and limit mobility. The result was an active enzyme which had lowered flavin to haem electron transfer rate. The position of the disulphide was decided on the basis of the crystal structure. The disulphide may thus lock the enzyme into a conformation which does not allow an optimal tunnelling pathway to the haem.

Clearly much evidence exists to suggest some degree of domain mobility. The role of the two residues Arg-289 and Lys-296 is of interest in conjunction with mobility. It could be expected that interdomain interactions would limit the mobility of the two domains. In order for a separation of the domains these interactions would have to be broken. Furthermore the interactions may favour productive collisions

between the two domains and affect the electron transfer rate. The lysine residue was particularly interesting because it forms the only salt bridge between the two domains although it is not conserved in the closely related enzyme from *Hansenula anomola*.

From the results obtained it is clear that changing Arg-289 or Lys-296 has no significant effect on the rate of flavin to haem electron transfer. Removal of the salt bridge between Lys-296 and the haem propionate (Figure 6.1.) has no detectable effect on the catalytic competence of the enzyme. It can be concluded that this Lys-296 is not a critical residue or else its contribution is too small to be detected. It may be interesting to introduce further salt bridges between the two domains to reduce their mobility. However introduction of a disulphide bond (Bell, 1997) showed that trying to close the 'gap' between domains will not necessarily enhance the rate of flavin to haem electron transfer.

Alteration of Arg-289 significantly affects the catalytic efficiency of flavocytochrome b_2. The steady-state results indicate a ten-fold fall in the rate of L-lactate oxidation by K296M (compared to the wild-type). An increase in the K_M for lactate indicates weaker substrate binding in the mutant. This was also observed in the R376K mutant (Reid et al 1988) though to a greater extent. The stopped flow rate of flavin reduction is decreased and this appears to limit the haem reduction rate which is also lowered. The stopped flow KIE for flavin indicates that cleavage of the α-hydrogen bond of lactate is rate limiting, as for wild-type. The stopped flow KIE for haem reduction indicates no significant effect on flavin to haem electron transfer. This was confirmed by haem re-reduction in fully reduced flavocytochrome b_2, after abstraction of a single electron by cytochrome *c*.

The observed effects are attributed to an alteration of the Arg-376 conformation, indicated by preliminary crystal structure data for K296M (Figure 6.3.). It is known that Arg-376 plays significant role in binding and orientating L-lactate in the active site of the enzyme. The alteration of Arg-289 results in movement of the

Arg-376. The conformation change probably results in binding of L-lactate at the active site, in a position which is not optimised for efficient catalysis.

Mobility of the two domains of flavocytochrome b_2 still provides a sound explanation for all experimental observations. There may still be critical residues lying in the interface of the two domains which promote their interaction. It is more likely that it is a compound effect of the hydrophobic and hydrogen bonding residues lying in the region. Studies of the separate domains indicate weak interactions between the two domains when their tether is removed. The enzyme is essentially a chimera, evolved from two convenient motifs (one to bind FMN and one to bind haem). The interface has probably evolved to remove repulsions rather than to maximise electron transfer. Hence single residues are likely to have minor or secondary effects as this study has shown.

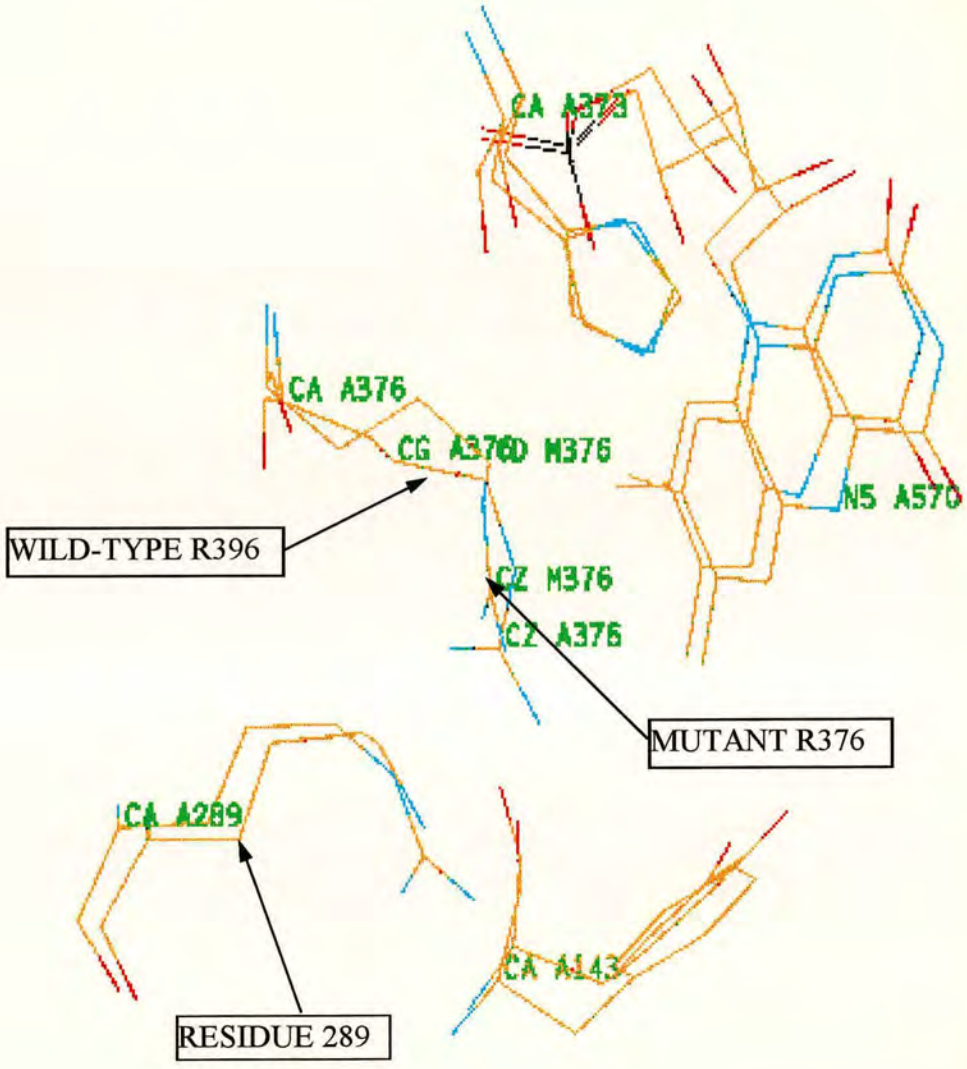

Figure 6.3. : The active-site residues from preliminary crystal structure data of the R289K mutant. The lysine at position 289 appears to adopt a conformation similar to that of the original arginine. The most striking difference from the wild type structure is the shift of residue Arg-376 which is responsible for binding and orientating the carboxylate group of lactate

Part 2-Flavocytochrome b_2

REFERENCES

Axup A. W., Albin M., Mayo S. L., Crutchley R. J., Gray H. B., (1988) Distance dependence of photoinduced long-range electron transfer in zinc / ruthenium-modified myoglobins, *J. Am. Chem. Soc.*, **110**, 435-439.

Balme A., Brunt C. E., Pallister R. L., Chapman S. K., Reid G. A., (1995) Isolation and characterisation of the flavin binding domain of flavocytochrome b_2 expressed independantly in *Escherichia coli*, *Biochem. J.*, **309**, 601-605.

Bell C., Uhrinova S., Barlow P. N., Chapman S. K., Reid G. A., (1996) Domain Mobility in flavocytochrome b_2 : fact or fiction, Flavins and Flavoproteins, University of Calgary Press.

Bell C., (1997) Probing the role of haem domain mobility in flavocytochrome b_2, Ph.D. Thesis, University of Edinburgh.

Beratan D. N., Onuchic J. N., Hopfield J. J., (1987) Electron tunneling through covalent and noncovalent pathways in proteins, *J. Chem. Phys.*, **86**, 4488-4498.

Beratan D. N., Betts J. N., Onuchic J. N., (1991) Protein electron transfer rates set by the bridging secondary and tertiary structure, *Science*, **258**, 1740-1741.

Beratan D. N., Onuchic J. N., (1996) The protein bridge between redox centres, In "Protein Electron Transfer", pp 23-42, D. S. Bendall (ed.) Bios scientific publishers, Oxford

Bernheim F., (1928) The specificity of the dehydrases. The separation of the citric acid from liver and the lactic acid dehydrase from yeast, *Biochem. J.*, **22**, 1178.

Bjerrum M. J., Casimiro D. R., Chang I. J., Dibilio A. J., Gray H. B., Hill M. G., Langen R., Mines G. A., Skor L. K., Winkler J. R., Wuttke D. S., (1995) Electron transfer in ruthenium modified proteins, *J. Bioenerg. Biomem.*, **27**, 295-302.

Black M. T., White S. A., Reid G. A., Chapman S. K., (1989) High level expression of fully active yeast flavocytochrome b_2 in *Escherichia coli*, *Biochem. J.*, **258**, 255-259.

Brunt C. E., Cox M. C., Thurgood A. G. P., Moore G. R., Reid G. A., Chapman S. K., (1992) Isolation and characterization of the cytochrome domain of flavocytochrome b_2 expressed independently in *Escherichia coli*, *Biochem. J.*, **283**, 87-90.

Capeillere-Blandin C., Bray, R. C., Iwatsubo M., Labeyrie F., (1975) Flavocytochrome b_2 : Kinetic studies by absorbance and electron paramagnetic resonance spectroscopy of electron distribution among prosthetic groups, *J. Biochem.*, **54**, 549-566.

Chapman S. K., White S. A., Reid G. A., Flavocytochrome b_2 (1991) *Advances in Inorganic Chemistry*, **36**, 257-301.

Chapman S. K., Reid G. A., Daff S. N., Sharp R. E., White P., Manson F. D. C., Lederer F., (1994) Flavin to haem electron transfer in flavocytochrome b_2, *Biochem Soc. Trans.*, **22**, 713-718

Chapman S. K., Mount A. R., (1995) Electron transfer in proteins, *Nat. Prod. Rep.*, **12**, 93-100.

Closs G. L., Calcaterra L. T., Green N. J., Miller J. R., Penfield K. W., (1986) Distance, spectroelectronic effects, and the Marcus inverted region in intramolecular electron-transfer in organic radical-anions, *J. Phys. Chem.*, **90**, 3673-3683.

Daff S. N., (1996) Analysis of the catalytic cycle & manipulation of the substrate specificity in flavocytochrome b_2, PhD. Thesis, University of Edinburgh.

Daff S., Ingledew W. J., Reid G. A., Chapman S. K., (1996) New insights into the catalytic cycle of flavocytochrome b_2, *Biochemistry*, 35, 6345-6350.

Deisenhofer J., Epp O., Miki K., Huber R., Michel H., (1985) Structure of the protein subunits in the photosynthetic reaction center of *Rhodopseudomonas viridis* at 3 Å resolution, *Nature*, **318**, 618-624.

DeVault D., (1984) Quantum mechanical tunneling in biological systems, 2nd edn., Cambridge University Press, New York.

Guiard B., Lederer F., (1979) The "cytochrome b_5 fold": structure of a novel protein superfamily, *J. Mol. Biol.*, **135**, 639-650.

Guiard B., (1985) Structure, expression and regulation of a nuclear gene encoding a mitochondrial protein- the yeast L-lactate cytochrome *c* oxidoreductase (cytochrome b_2), *EMBO. J.*, **4**, 3265-3272.

Hazzard J. T., Cusanovich M. A., Tainer J. A., Getzoff E. D., Tollin G., (1986) Kinetic-studies of reduction of a 1-1 cytochrome *c* flavodoxin complex by free flavn semiquinones and rubredoxin, *Biochemistry*, **25**, 3318-3328.

Ho P. S., Sutoris C., Liang N., Margoliash E., Hoffman B. M., (1985) Species specificity of long-range electron transfer within the complex between zinc-substituted cytochrome *c* peroxidase and cytochrome *c*, *J. Am. Chem. Soc.*, **107**, 1070-1071.

Labeyrie F., Beloeil J. C., Thomas M. A., (1988) Evidence by NMR for mobility of the cytochrome domain within flavocytochrome b_2, *Biochim. Biophys. Acta*, **953**, 134-141.

Lederer F., (1991) Review, *Chem. Biochem. Flavoenz.*, (Franz Miller, ed., CRC Press) Vol. II, Chapter 7, 153-242.

Lindqvist Y., Bränden C., Matthews F. S., Lederer F., (1991) Spinach glycolate oxidase and yeast flavocytochrome b_2 are structurally homologous and evolutionarily related enzymes with distinctly different flavin mononucleotide binding motifs, *J. Biol. Chem*, **266**, 3198-3207.

Marcus R. A., (1968) Electron transfer at electrodes and in solution: comparison of theory and experiment, *Electrochim. Acta*, **13**, 95.

Marcus R. A., (1996) Electron transfer reactions in chemistry. Theory and experiment. In "Protein Electron Transfer", pp 249-272, D. S. Bendall (ed.) Bios scientific publishers, Oxford.

Miles C S., Rouviere-Fourmy N., Lederer F., Matthews F. S., Reid G. A., Black M. T., Chapman S. K., (1992) Tyr-143 facilitates interdomain electron transfer in flavocytochrome b_2, *Biochem. J.*, **285**, 187-192.

Miller J. R., Beitz J. V., Huddleston R. K., (1984) Effect of free energy on rates of electron transfer between molecules, *J. Am. Chem. Soc.*, **106**, 5057-5068.

Moser C. C., Dutton P. L., (1992) Engineering protein structure for electron transfer function in photosynthetic reaction centers, *Biochim. Biophys. Acta*, **1101**, 171-176.

Moser C. C., Keske J. M., Warncke K, Farid R. S., Dutton P. L., (1992) The nature of biological electron transfer, *Nature*, **355**, 796-802.

Moser C. C., Page C. C., Farid R., Dutton P. L., (1995) Biological electron transfer, *J. Bioenerg. Biomemb.*, **27**, 263-274.

Moser C. C., Dutton P. L., (1996) Outline of theory of electron transfer reactions In "Protein Electron Transfer", pp 1-21, D. S. Bendall (ed.) Bios scientific publishers, Oxford.

Pajot P., Claisse M., (1974) *Eur. J. Biochem.*, **49**, 275-285.

Reid G. A., White S.A., Black M. T., Lederer F., Matthews F. S., Chapman S. K., (1988) Probing the active site of flavocytochrome b_2 by site-directed mutagenesis, *Eur. J. Biochem.*, **178**, 329-333.

Scrutton N. S., (1994) α / β Barrel evolution and the modular assembly of enzymes: emerging trends in the flavin oxidase / dehydrogenase family, *Bioessays*, **16**, 115-122.

Sharp R. E., White P. W., Chapman S. K., Reid G. A., (1994) Role of the interdomain hinge of flavocytochrome b_2 in intra- and inter-protein electron transfer, *Biochemistry*, **33**, 5115-5120.

Sharp R. E., Chapman S. K., Reid G. A., (1996a) Deletions in the interdomain hinge region of flavocytochrome b_2 -effects on intraprotein electron-transfer, *Biochemistry*, **35**, 891-899.

Sharp R. E., Chapman S. K., Reid G. A., (1996b) Modulation of flavocytochrome b_2 intraprotein electron-transfer, *Biochem. J.*, **316**, 507-513.

Short D., (1996) The location of the cytochrome *c* binding site on flavocytochrome b_2, Ph.D. Thesis, University of Edinburgh.

Taube H., (1984) Electron-transfer between metal complexes-retrospective, *Science*, **226**, 1028-1036.

Tegoni M., Cambillau C., (1994) The 2.6-Å refined structure of the *Escherichia coli* recombinant *Saccharomyces cerevisiae* flavocytochrome b_2-sulfite complex, *Prot. Sci.*, **3**, 303-313.

Tollin G., Meyer T. E., Cusanovich M. A., (1986) Elucidation of the factors which dtermine reaction-rate constants and biological specificity for electron-transfer proteins, *Biochim. Biophys. Acta*, **853**, 29-41.

Wherland S., Gray H. B., (1977) in Biological aspects of inorganic chemistry (Addison A. W., Cullin, W. R., Dolphin D., James B. R., eds.) 289-368, John Wiley, New York.

White P., Manson F. D. C., Brunt C. E., Chapman S. K., Reid G. A., (1993) The importance of the interdomain hinge in intramolecular electron transfer in flavocytochrome b_2, *Biochem. J.*, **291**, 89-94.

Winkler J. R., Nocera D. G., Yocom K. M., Bordignon E., Gray H. B., (1982) Electron transfer kinetics of pentaammineruthenium (III) (His-33) ferricytochrome *c*, *J. Am. Chem. Soc.*, **104**, 5798-5800.

Winkler J. R., Gray H. B., (1992) Electron transfer in ruthenium-modified proteins, *Chem. Rev.*, **92**, 369-379.

Xia Z., Matthews F. S., (1990) Molecular structure of Flavocytochrome b_2 at 2.4 Å resolution, *J. Mol. Biol.*, **212**, 837-863.

APPENDIX

APPENDIX 1- SAMPLE DATA FROM STOPPED-FLOW AND STEADY STATE EXPERIMENTS

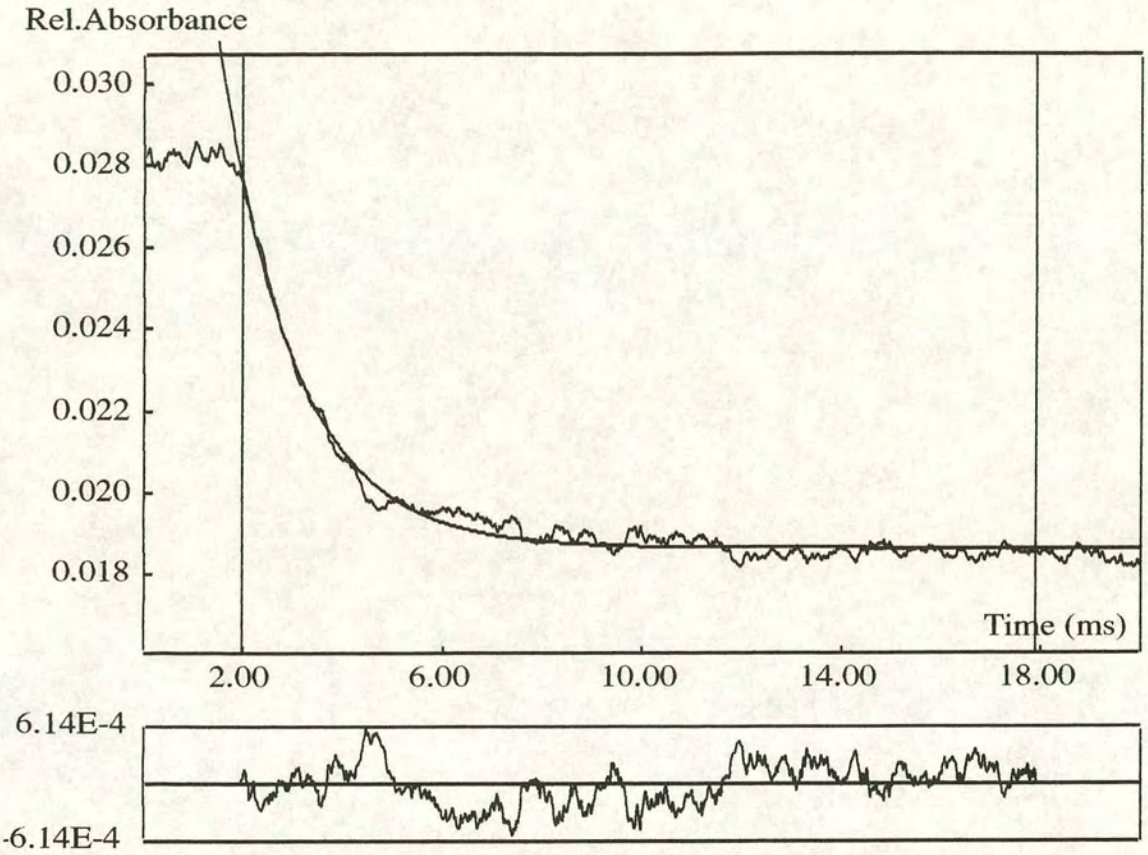

FILE: Avge_15 DATE: Tue,17 Mar 1998.17:48
Disc Group: F302FL10 Origin: Fri,04 Mar 1994.15:20:01
[3 trace av]
Timebase=0.020s Ch:#1 Temp=25.3°C
Wlength=438.3nm PM volts=594v Offset=4v Filter=Direct
REGRESSION RESULTS:
Library: Standard Software: SX18MV v4.34
Function name: Single exponential, floating end point
Formula: P(1)*EXP(-P(2)*X)+P(3)

Parameter:		Value:	Std.Error:
P(1)	Amp	3.36E-2	5.32E-4
P(2)	Rate	6.63E2	6.00E0
P(3)	Endpt	1.86E-2	9.96E-6
Norm. Variance:		4.92E-8	Fit range: 99-895

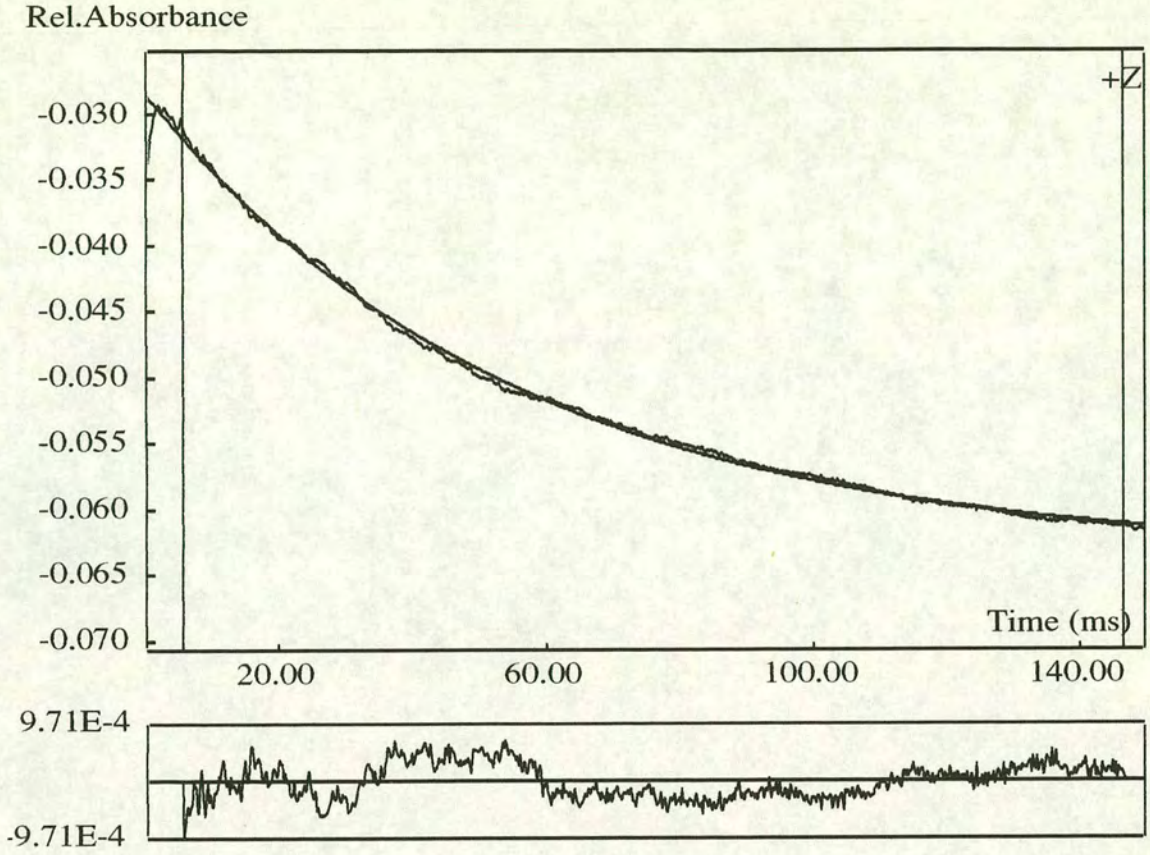

FILE: Avge_02 DATE: Tue,17 Mar 1998.17:13
Disc Group: 289F20 Origin: Mon,23 Oct 1995.13:27:53
[3 trace av]
Timebase=0.20s Ch:#1 Temp=25.1°C
Wlength=438.3nm PM volts=630v Offset=4v Filter=Direct
REGRESSION RESULTS:
Library: Standard Software: SX18MV v4.34
Function name: Single exponential, floating end point
Formula: P(1)*EXP(-P(2)*X)+P(3)

Parameter:		Value:	Std.Error:
P(1)	Amp	3.51E-2	4.85E-5
P(2)	Rate	1.81E1	8.68E-2
P(3)	Endpt	-6.37E-2	5.39E-5
Norm. Variance:		8.67E-8	Fit range: 28-733

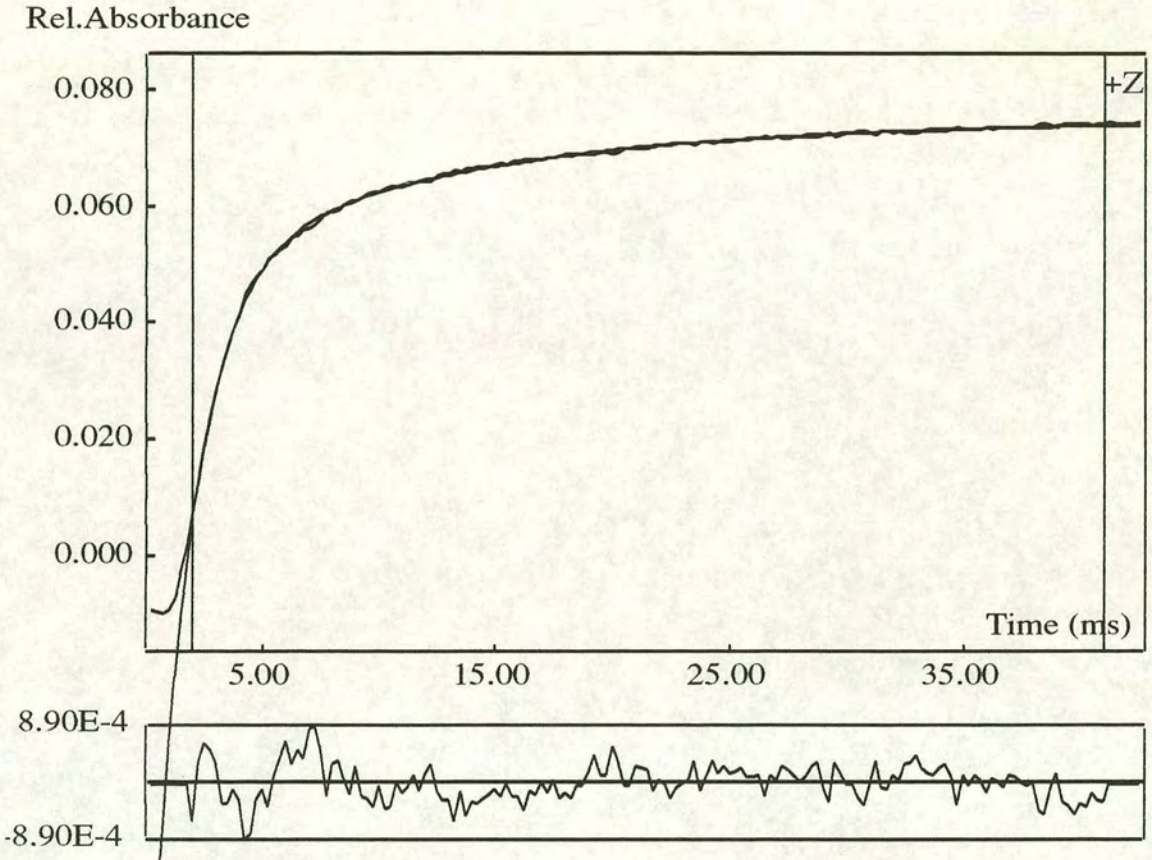

FILE: Avge_02 DATE: Tue,17 Mar 1998.17:23
Disc Group: I100WT Origin: Thu,28 Sep 1995.15:55:45
[4 trace av]
Timebase=0.10s Ch:#1 Temp=24.8°C
Wlength=557nm PM volts=676v Offset=4v Filter=Direct
REGRESSION RESULTS:
Library: Standard Software: SX18MV v4.34
Function name: Double exponential, floating end point
Formula: P(1)*EXP(-P(2)*X)+P(3)*EXP(-P(4)*X)+P(5)

Parameter:		Value:	Std.Error:
P(1)	Amp 1	-1.48E-1	2.14E-3
P(2)	Rate 1	6.03E2	8.83E0
P(3)	Amp 2	-2.80E-2	4.80E-4
P(4)	Rate 2	8.43E1	2.04E0
P(5)	Endpt	7.47E-2	1.09E-4
Norm. Variance:		8.41E-8	Fit range: 8-164

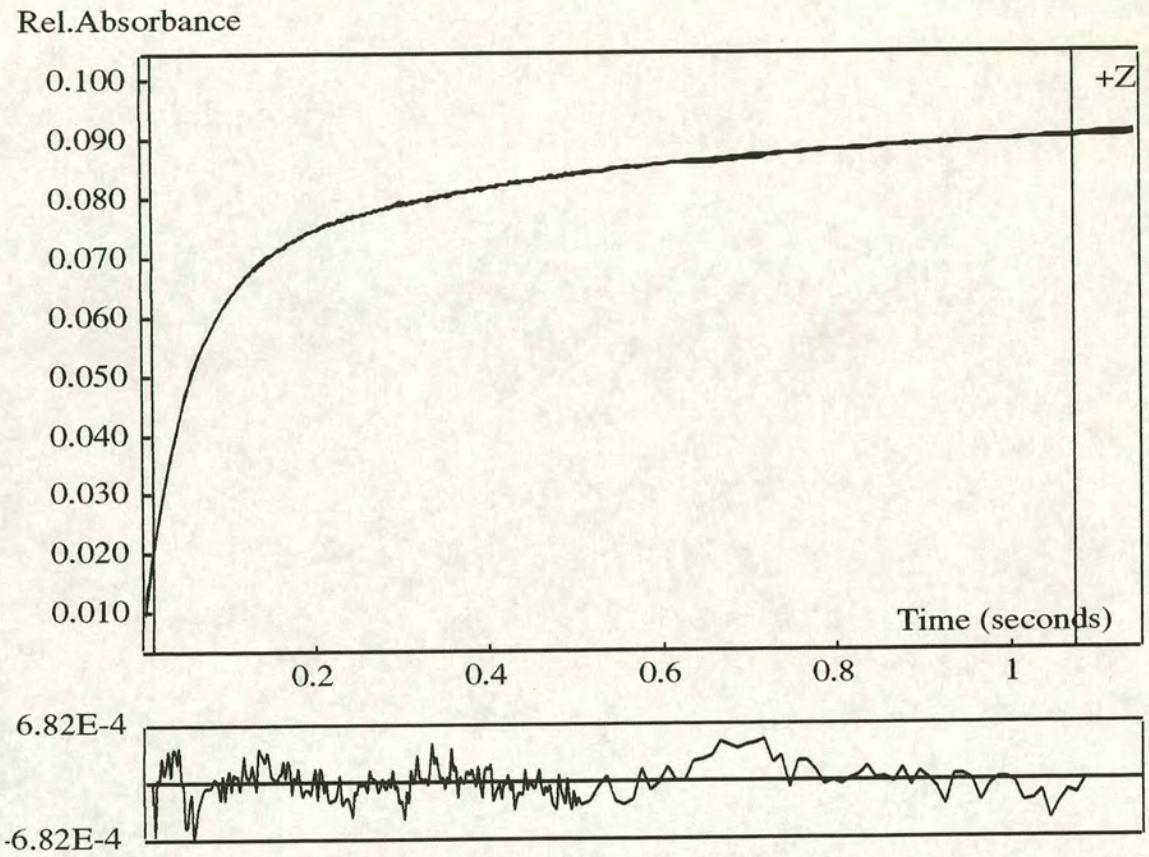

FILE: Avge_05 DATE: Tue,17 Mar 1998.17:19
Disc Group: 289H4-1 Origin: Mon,16 Oct 1995.16:41:22
[4 trace av]
Split Timebase=0.50s / 2.00s Ch:#1 Temp=25.1°C
Wlength=557nm PM volts=661v Offset=4v Filter=Direct
REGRESSION RESULTS:
Library: Standard Software: SX18MV v4.34
Function name: Double exponential, floating end point
Formula: P(1)*EXP(-P(2)*X)+P(3)*EXP(-P(4)*X)+P(5)

Parameter:		Value:	Std.Error:
P(1)	Amp 1	-5.99E-2	1.87E-4
P(2)	Rate 1	1.92E1	1.25E-1
P(3)	Amp 2	-2.58E-2	1.25E-4
P(4)	Rate 2	2.25E0	3.99E-2
P(5)	Endpt	9.21E-2	1.34E-4
Norm. Variance:		4.15E-8	Fit range: 5-258

R289K Lactate Dependance, 1mM ferricyanide (18-08-95)

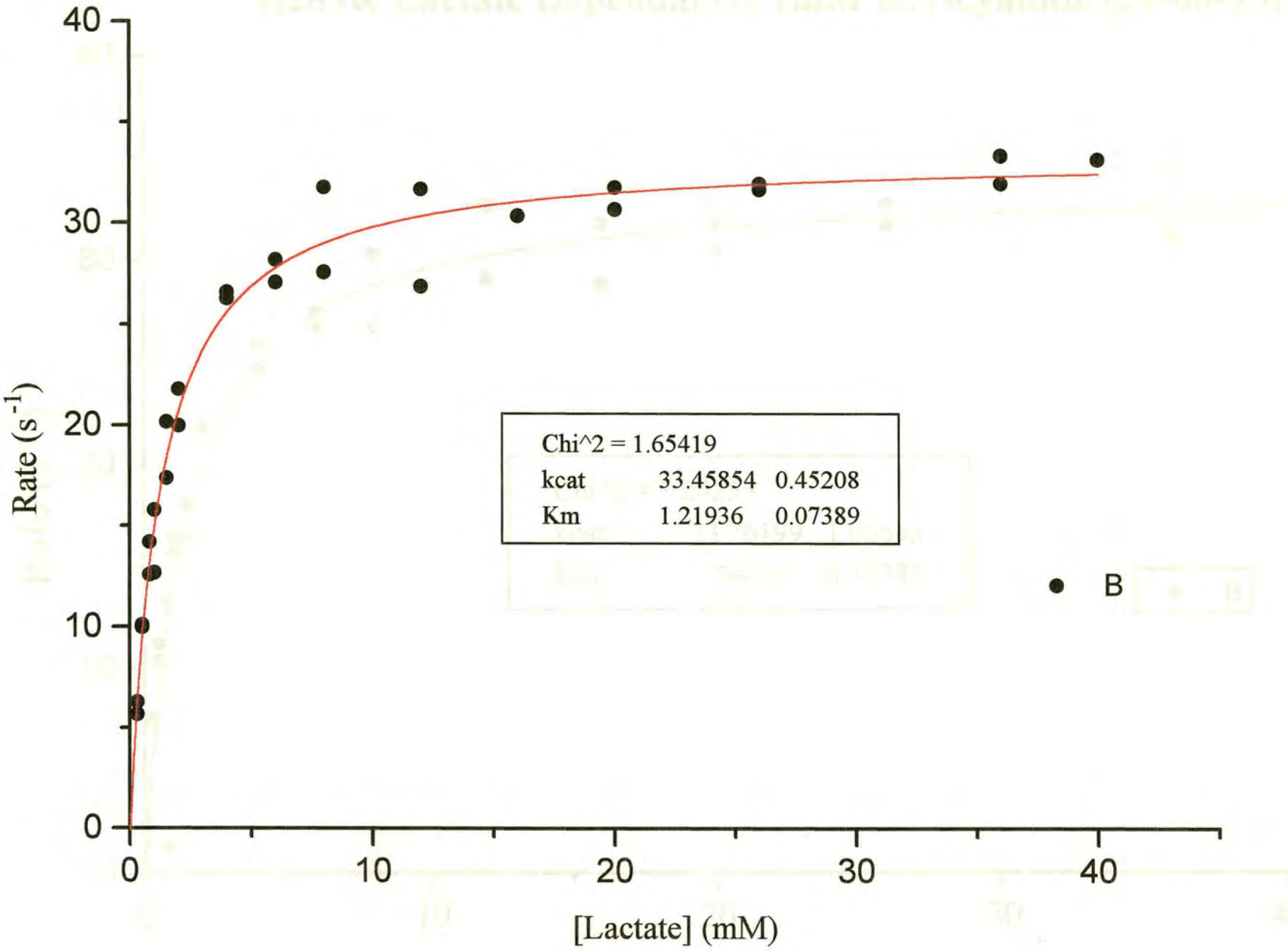

APPENDIX 2- COURSES AND CONFERENCES ATTENDED

Flavins and Flavoproteins Network (FLAPS),
Wageningen, The Netherlands (1994).

Scottish Protein Structure Group,
Aberdeen, Scotland (1994).

Six Week Exchange To Work in The Lab
Of Dr. F. Lederer, Paris (1995).

International Conference on Bioinorganic Chemistry (ICBIC 5),
Lübeck, Germany (1995) - Poster presented.

Biochemical Society Meeting,
Dublin, Ireland, (1995) - Poster presented.

12th International Symposium on Flavins and Flavoproteins,
Calgary, Canada, (1996) - Poster presented.

Departmental Colloquia.

APPENDIX 3- PUBLICATIONS

Investigating the importance of an interface residue in interdomain eletron transfer, (1996), Pike A. D., Chapman S. K., Manson F. D. C., Reid G. A., Gondry M., Lederer F., in Flavins and Flavoproteins, University of Calgary Press.

A reprint is located at the back of this thesis.

Investigating the Importance of an Interface Residue in Interdomain Electron Transfer

Andrew D. Pike[†], Stephen K. Chapman[†], Forbes D. C. Manson[‡], Graeme A. Reid[‡].
[†]Department of Chemistry, [‡]Institute of Cell and Molecular Biology, University of Edinburgh, Scotland EH9 3JJ

Muriel Gondry, Florence Lederer
CNRS, 91198 Gif-Sur-Yvette, Cedex, France

INTRODUCTION

Flavocytochrome b_2 is a soluble dehydrogenase which catalyses the oxidation of L-lactate to pyruvate in yeast mitochondria and subsequently reduces cytochrome *c*. Crystal structures have been obtained for both the wild-type and recombinant enzymes from *S. cerevisiae* and *E. coli* respectively (1, 2). The enzyme is homotetrameric, with two distinct domains per monomer (Fig. 1.). The largest domain binds FMN and the smaller binds protohaem IX.

Fig. 1. The structure of flavocytochrome b_2 showing the hinge (black) between the flavin and haem domains.

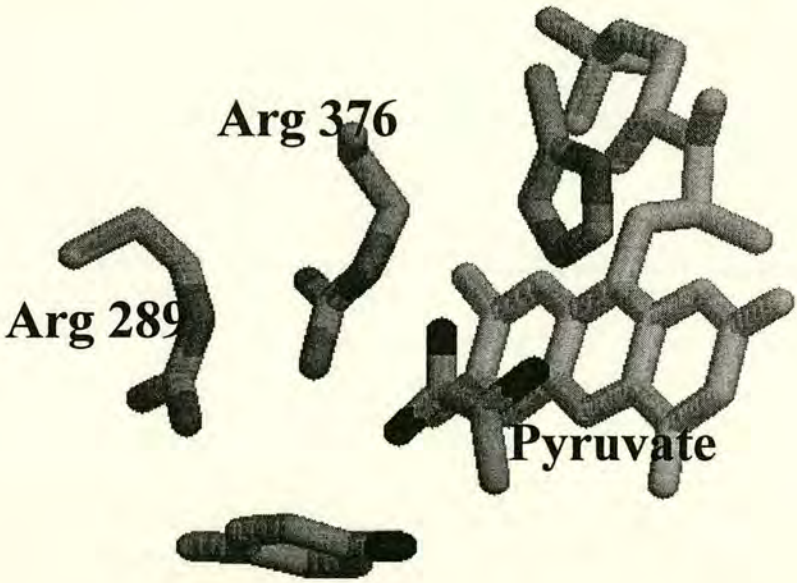

Fig. 2. The location of Arg-289 relative to the active site

During turnover lactate binds in the active site of the flavin domain and transfers a pair of electrons to flavin. The flavin group passes electrons singly to the b_2 haem. The presence of the haem domain allows the enzyme to efficiently reduce cytochrome *c*, which the flavin domain alone is incapable of doing.

The domains of flavocytochrome b_2 are joined by a short flexible region of peptide referred to as the hinge. This was thought to allow mobility of the haem domain relative to the flavin domain. Previous work (3) has shown the hinge peptide length and sequence is optimised for efficient catalysis. As a consequence of domain mobility, several favourable interactions in the interface need to be constantly broken and reformed. A single salt bridge exists between domains; removal of this interaction by mutagenesis shows no effect on enzyme activity. The remaining majority of interdomain interactions are hydrogen bonding in nature.

In the crystal structure Arg-289 forms several hydrogen bonds, including one to the haem propionate via a water molecule. The residue is conserved in a family of similar oxidases and dehydrogenases (4). In flavocytochrome b_2 the residue lies between the two domains, close to the active site allowing a stacking interaction with

Arg-376 (Fig. 2.). This interaction is important because Arg-376 binds and orientates the carboxylate of lactate. Indeed, it is possible that in the michaelis complex the negatively charged carboxylate of the substrate may be neutralised by a combination of Arg-289 and Arg-376. An interesting observation in the crystal structure of recombinant flavocytochrome b_2 (2) was that Arg-289 could adopt two different conformations. This was accounted for by a strong affinity for sulphite, which was bound in place of pyruvate at the active site. Nonetheless this would appear to indicate some mobility in the residue. The point mutant, Arg-289→Lys, R289K was used to probe the importance of these interactions in catalysis and interdomain electron transfer.

RESULTS

Steady-state kinetics(25°C, pH7.5, Tris buffer I=0.10M.)

TABLE I: **R289K and (wild-type) steady-state parameters for lactate oxidation.**

Electron acceptor	k_{cat} (s^{-1})	Lactate K_M (mM)
Ferricyanide	33±3.9 (400±10)	3.2±0.4 (0.49±0.05)
Cytochrome c	17.7±0.2(207±2)	0. 95±0.03(0.24±0.04)

Saturating acceptor concentrations were; 1mM [ferricyanide], 10μM [cytochrome *c*].
k_{cat} values are expressed in terms of electrons transferred.

The mutant enzyme R289K is well expressed in *E. coli* and was purified using standard procedures(5). Steady-state and stopped-flow kinetic parameters were determined at 25°C in 10mM Tris buffer pH7.5, I=0.1M.

Table 1 shows the results of steady-state analysis of the R289K enzyme compared with wild-type flavocytochrome b_2. The mutant enzyme has a k_{cat} approximately ten fold lower than wild-type with ferricyanide or cytochrome *c* as the terminal electron acceptor. Ferricyanide, although not physiologically relevant, is useful because it can accept electrons from both flavin and haem. Cytochrome *c*, however, can only accept electrons from the haem domain. The ratio of rates obtained for the mutant is unchanged (within experimental error) from that seen for the wild type enzyme. The increase in lactate K_M value, corresponding to decreased substrate binding strength, might be explained by an altered interaction with the substrate, but a local structural alteration cannot be ruled out. A steady-state kinetic isotope effect of 4.4±1.5 was determined using L-[2-^{2}H]Lactate, the same within error as for wild type enzyme implying a similar transition state in the mutant enzyme.

Stopped-flow kinetics(25°C, pH7.5, Tris buffer I=0.10M.)

TABLE II: **Microscopic rate constants for flavin and haem reduction**

	k, K_M for FMN reduction (s^{-1}, mM)	k for haem reduction (s^{-1})
Wild-type	604±60, 1.7±0.5	445±50
R289K	20±2, 0.84±0.2	15±2

All values at saturating [substrate]

Flavin and haem reduction rates were determined using stopped-flow spectrometry (Table II). The decrease in the R289K flavin reduction rate can be attributed to transition state destabilisation. The haem reduction rate is limited by the flavin reduction rate, hence the value obtained does not give a true measure of flavin to haem electron transfer. An estimate of the true flavin to haem electron transfer rate can be obtained by measuring re-reduction of b_2 haem following oxidation by cytochrome *c*, as recently determined for wild-type enzyme(6). It was clear from experiments that the rate was still very rapid as the reduction all occurred during the dead time of the spectrophotometer. This supports the results obtained by steady-state methods which indicate no effect on interdomain electron transfer.

CONCLUSION

The mutation R289K, although conservative, has a major impact on catalytic efficiency and substrate binding in flavocytochrome b_2. The interdomain contacts observed in the crystal structure seem to have little or no role in the enzymes ability to transfer electrons from flavin to haem.

REFERENCES

1. Matthews, F. S., Xia, Z. 1990. J. Mol. Biol. **212**, 837.
2. Tegoni, M., Cambillau, C. 1994. Protein Science **3**, 303.
3. Sharp, R. E., White, P., Chapman, S. K., Reid, G., 1994. Biochemistry **33**, 5115.
4. Scrutton, N. S. 1994. BioEssays **16**, 115.
5. Black, M. T., White, S. A., Reid G. A., Chapman, S. K. 1989. Biochem. J. **258**, 255.
6. Daff, S., Ingledew, W. J., Reid, G. A., Chapman S. K. 1996. Biochemistry **35**, 6347.